Review

Pitfalls and caveats in applying immunostaining to histopathological diagnosis

Yutaka Tsutsumi, M.D.[1,2)]

[1.] Diagnostic Clinic, Pathos Tsutsumi, clinic director, 1551-1 Sankichi-ato, Yawase-cho, Inazawa, Aichi 492-8342, Japan. Phone: +81-587-96-7088, Fax: +81-587-96-7098
[2.] Specially-Appointed Professor, Department of Medical Technology, Yokkaichi Nursing and Medical Care University, 1200 Kayou-cho. Yokkaichi, Mie 512-8045, Japan.
Email: pathos223@kind.ocn.ne.jp
ORCID ID: https://orcid.org/0000-0002-4136-9678

Abstract

Immunostaining is an essential histochemical technique for analyzing pathogenesis and making a histopathological diagnosis. The needs are prompted by technical development and refinement, commercial availability of a variety of antibodies, deepened knowledge of immunohistochemical markers, accelerated analysis of morphofunctional correlations, progress in molecular target therapy, and the expectation of advanced histopathological diagnosis. However, immunostaining does have various pitfalls and caveats. We should learn from mistakes and failures, as well as from false positivity and false negativity. The present review article describes various devices, technical hints and trouble-shooting guides to keep in mind in performing immunostaining.

Keywords: Epitope retrieval, Fixation, Histopathological diagnosis, Immunostaining, Sensitivity, Specificity, Trouble-shooting

1. Introduction

Techniques of immunohistochemistry or immunostaining have already been established.[1-8)] We now need measures against technical artifacts and appropriate trouble-shooting tips. The present review article overviews technical aspects, knowhows, pitfalls and trouble-shooting guides in routinely performing immunostaining.

2. The needs for immunostaining

In daily diagnostic pathology services, immunostaining using formalin-fixed, paraffin-embedded (FFPE) sections is indispensable to help the histopathological diagnosis fundamentally based on hematoxylin and eosin (H&E) staining. Differential diagnoses are listed up first, and appropriate immunohistochemical markers for the diagnosis are then chosen. The expression of lymphocyte surface markers, hormones and tumor markers is evaluated for morphofunctional diagnosis. The degree of malignancy can be analyzed by immunostaining for p53 and cell proliferation markers, including Ki-67 (MIB-1). We now have a variety of cell-specific markers to clarify the origin and nature of neoplasms. For example, cytokeratins are useful to show the epithelial nature of the cells (**Figure 1**). For determining molecular target therapy of breast cancer, for example, such markers as estrogen receptor (ER), progesterone receptor (PgR), human epidermal growth factor receptor-2 (HER2) and Ki-67 are consistently immunostained.

Appropriate applications of immunostaining to diagnostic pathology are dependent upon the following three points: a) how to stain, b) how to select immunohistochemical markers, and c) how to evaluate the immunostained findings.

3. Choice of methodology for immunostaining

A variety of primary antibodies and immunostaining kits are commercially available, and autostaining apparati have become popular. Now, the immunostaining is sensitive enough and technically reliable. As the secondary reagent with high sensitivity, horseradish peroxidase (HRP)-labeled polymers such as Envision Flex, Simple Stain Max and Novolink are widely used. When necessary, the catalyzed signal amplification (CSA)-II using fluorescein isothiocyanate (FITC)-labeled tyramide (Agilent/Dako, San Jose, CA, USA) can be applied (**Figure 2**). We now abandon biotin-labeled techniques such as avidin biotinylated peroxidase complex (ABC) method and labeled streptavidin biotinylated peroxidase (LSAB) method. The reasons are as follows: a) endogenous biotin activity in mitochondria is retrieved by the pretreatment with heat-induced epitope retrieval (HIER),[9)] b) staining steps are a little bit complicated, and c) the sensitivity of detection is not enough when compared with the polymer technique. The original version of the CSA employing biotinylated tyramide should thus be avoided.

Antigen detection with ultra-high sensitivity techniques is not necessarily requested, because of the agitation of background staining and difficulty in stably keeping the highly diluted antibodies in refrigerators or freezers. The method should be

Preprints (www.preprints.org) | NOT PEER-REVIEWED | Posted: 28 April 2021 doi:10.20944/preprints202104.0750.v1

chosen based on the ease of handling, stability and reproducibility. The antibodies must be diluted with 0.01 M phosphate-buffered saline (PBS), pH 7.4, containing 1% bovine serum albumin (BSA) to avoid inactivation of antibody reactivity. Repeated freezing and thawing damages the diluted antibodies. Suppose you have a 100 μL aliquot of an antibody working at a 1:1,000 dilution. A recommended management of the antibody is as follows. A half volume is kept in an undiluted form, and the remaining part (50 μL) is diluted at 1:10 with BSA-PBS to keep 10 plastic tubes containing 50 μL 1:10-diluted antibody in a freezer after appropriate labeling. One must realize that the avoidance of repeated freezing and thawing of diluted antibodies is of critical importance for stable and reproducible immunostaining.

FFPE sections are the common target of immunostaining in diagnostic pathology, so that the antibodies chosen must be applicable to the FFPE sections. Diaminobenzidine (DAB) solution, containing 20 mg DAB and 3 μg hydrogen peroxide in 100 mL of 50 mM Tris-HCl buffer, pH 7.6, is routinely utilized for the final coloring reaction in brown. The nuclei are briefly counterstained with Mayer's hematoxylin in purple (usually dipping for 10 seconds).

4. Application of double staining

Double staining is the method simultaneously localizing two different antigenic substances in a single section. Two different colors are used for the differential localization. For example, Antigen A is visualized in brown with a mouse monoclonal antibody and the HRP-labeled anti-mouse IgG polymer reagent, while Antigen B is localized in blue with a rabbit polyclonal antibody and the alkaline phosphatase (ALP)-labeled anti-rabbit IgG polymer reagent. Representative examples are displayed in **Figure 3**. Endogenous ALP activity is totally quenched during the preparation of FFPE sections. To inhibit endogenous ALP activity in cytology specimens or fresh-frozen sections, 5 mM levamisole hydrochloride should be added to the reaction mixture for the final coloring with azo dyes. The sensitivity and beauty of immunostaining are inferior to immunofluorescence techniques, but the cellular localization of the antigen is much clearer and more distinct than the immunofluorescence. The double immunostaining with enzyme-labeled probes should be applied particularly when the intracellular localization of the antigens is separated (e.g., the nucleus in one and the plasma membrane in another).

One can immunolocalize two different neuropeptides in single nerve fibers with the following meticulous technique.[10] Serial sectioning is not suitable in this situation. Antibodies raised in rabbit are used here. The first neuropeptide is immunostained with 4-chloro, 1-naphthol for HRP coloration or with azo dyes for ALP coloration in blue. After photographing, the sections are soaked in glycine-hydrochloric acid buffer, pH 2.2, to dissociate the primary antibody. Then, the dyes can be removed by dipping sections in 100% ethanol. The second neuropeptide is visualized with the DAB coloration in brown, and the same area should be photographed again to compare the localization of the two neuropeptides.

Here, the author wants to emphasize the usefulness of double staining for immunostain and routine special stains, such as periodic acid-Schiff (PAS), alcian blue, Congo red and Berlin blue (**Figure 4**). In case of PAS reaction, periodic acid oxidation functions as a quencher of endogenous peroxidase activity. Therefore, the section is first oxidized with 0.5% periodic acid solution for 10 minutes and then immunostaining with DAB coloration should follow. Finally, the Schiff reagent is reacted to complete double staining. It is of note that the periodate oxidation destroys sugar molecules so that carbohydrate antigens such as CA19-9, CA15-3, CA125, blood group substances and some lymphocyte surface antigens including CD4 become undetectable. In such an occasion, periodic acid oxidation should be done after the completion of immunostaining with DAB coloration.

5. Effect of formalin fixation

1) Antigenic alterations by formalin fixation

The target sections for immunostaining are routinely fixed in 10% or 20% formalin (3.5% or 7% formaldehyde aqueous solution). The formalin solution naturally contains formic acid as a result of auto-oxidation of formaldehyde, so that the formalin solution shows a low pH value. The damage to the antigenicity or the destruction of genomic information on DNA or RNA can be mitigated when we use buffered or neutralized formalin, but the morphological preservation for H&E preparations is not good enough for diagnostic purpose when compared with sections fixed in the acidic formalin solution, the author believes so. Genomic DNA or total RNA extracted from FFPE sections can be amplified stably by polymerase chain reaction (PCR) for DNA analysis and reverse transcription-PCR (RT-PCR) for RNA analysis, when the primer pairs are designed to yield a target genomic sequence as short as 100 base-pair length.[11,12]

The antigenicity of certain antigens may be weakened or even lost when the specimen is fixed in formalin and embedded in paraffin. Representative examples are shown in **Figure 5**. However, we can now choose commercially available antibodies applicable to FFPE sections. When combined with high-sensitivity detection kits and epitope retrieval techniques described below, a considerable number of antigens are able to be reproducibly visualized in FFPE sections.

2) Choice of fixatives

Preprints (www.preprints.org) | NOT PEER-REVIEWED | Posted: 28 April 2021 doi:10.20944/preprints202104.0750.v1

Formaldehyde provokes a cross-linkage between tissue protein components, so that the epitope retrieval step is often needed. In contrast, dehydration-induced protein aggregation is the main mechanism of fixation in such organic solvents as ethanol and acetone. In general, the antigenicity and DNA/RNA structure are well preserved in organic solvent-fixed paraffin sections. Sato, *et al*. invented cold acetone-based tissue processing nicknamed as the AMeX method, that can preserve not only antigenicity but also high molecular-weight DNA sequence in paraffin blocks.[13] A disadvantage of this method includes that significant tissue shrinkage results in difficulty of cutting and mild alteration of H&E histology.

It is of note that antigenic substances packaged in small granules in the cytoplasm are lost after fixation in ethanol and acetone. This is particular true if the granules are ultrastructurally electron-dense. Presumably, the osmiophilic (lipid-rich) granule content is easily extracted by the organic solvent. **Figure 6** represents false negativity of platelet factor 4 and insulin caused by fixation in acetone and ethanol. In contrast, somatostatin can be visualized in ethanol-fixed paraffin sections. It is well known that somatostatin granules show low electron density in ultrastructural appearance.

3) Use of archival pathology material

Some antigens and RNA signals are stably detectable in archival pathology specimens fixed in acidic formalin for a considerably long period of time. In other words, fixation in acidic formalin can keep the antigenic and genomic signals to the evaluable level of histochemical detection.

As shown in **Figure 7**, we detected HBs antigen of hepatitis B virus (HBV) and the genome of hepatitis C virus (HCV) in liver cirrhosis specimens soaked in the fixative for up to 110 years, by applying immunostaining using a monoclonal antibody against HBs antigen and nested RT-PCR against the core region of HCV, respectively.[14]

Once the author visited the Gordon Museum of Pathology at Guy's Hospital in London, UK, he had a chance to get unstained glass slides of autopsy specimens of Hodgkin's lymphoma sampled by Dr. Thomas Hodgkin himself 170 years before. The specimens were fixed in ethanol for 80 years and then in formalin for 90 years. The unstained sections were then kept at room temperature for months. By applying the cell transfer technique described below, immunostaining for CD15 and *in situ* hybridization for Epstein-Barr virus-encoded small nuclear RNA (EBER) were performed. CD15 was immunoreactive on the plasma membrane of Reed Sternberg (RS) cells and Hodgkin's cells, and EBER signals were detected in the nuclei of RS cells and Hodgkin's cells (**Figure 8**).[15]

Empirically, the antigenicity of amyloid A protein in secondary amyloidosis, *Bacillus* Calmette Guérin (BCG) antigens in tuberculous and leprosy mycobacteria, as well as bacterial antigens such as streptococcal and pneumococcal antigens are stable and reproducibly immunolocalized in specimens fixed in formalin for more than 70 years (**Figure 9**). HCV antigens are also immunohistochemically detectable with monoclonal antibodies in archival FFPE specimens (**Figure 10**).

6. Artifacts by formalin fixation

1) Penetration of plasma proteins into the cytoplasm of certain cells: A diffusion artifact

During formalin fixation, plasma proteins rich in the plasma and tissue fluid are penetrated into the cytoplasm of certain cells in FFPE sections. The nuclei remain completely negative. This represents a nonspecific diffusion artifact.[1] The phenomenon is often seen in giant cells. The plasma proteins such as albumin, fibrinogen, IgG, Ig A, IgM, and kappa/lambda chains of immunoglobulins permeate through a damaged plasma membrane into the cytoplasm of unfixed cells, and the cells are then fixed by formaldehyde. The immunoreactivity is specific, but the positivity represents a fixation artifact. Typical examples include RS cells and Hodgkin's cells in Hodgkin's lymphoma (**Figure 11**).[16] The cytoplasm of RS cells and Hodgkin's cells is polyclonally positive for both kappa and lambda chains. Such diffusion artifacts are observed in a variety of cells, including hepatocytes and hepatocellular carcinoma cells, normal and neoplastic thyroid epithelial cells, epidermal keratinocytes and non-Hodgkin's lymphoma cells (**Figure 12**). Since cells immunoreactive for IgG and albumin are surrounded by completely negative cells, it seems the positive signals mean something, but nothing is significant at all. **Figure 13** illustrates albumin immunostaining in autopsied normal pancreas. The cytoplasm of ductular cells, acinar cells or islet cells/peripheral nerve appear positive in different part of the tissue. Accordingly, when we try to immunostain IgG or alpha-1 antitrypsin in FFPE sections, albumin should be chosen for an indifferent control.

2) False positive and false negative results due to uneven formalin fixation

Uneven formalin fixation may lead to both false positivity and false negativity.[1] Not only cells improperly fixed by formalin but also cells overfixed by formalin show false negativity. Since vimentin in lymphocytes, macrophages, fibroblasts and vascular endothelial cells often turns to be negative in poorly fixed tissues, vimentin serves as an internal control for judging whether the fixation is proper or not.[17] Lymphocyte surface markers such as CD20 may be positive at the peripheral part of B-cell lymphoma tissue, while lymphoma cells in the poorly fixed (vimentin-negative) central part are false-negative (**Figure 14**). **Figure 15** illustrates glutathione peroxidase immunoreactivity seen at the outermost part of the paraformaldehyde-fixed frozen rat liver tissue. Occasionally, a reversed pattern of the antigen localization is also experienced. The peripheral area is overfixed to show

Preprints (www.preprints.org) | NOT PEER-REVIEWED | Posted: 28 April 2021 doi:10.20944/preprints202104.0750.v1

false negativity for leukocyte common antigen (LCA, CD45), while the antigenicity is preserved in the central part. Vimentin is negative in CD45-positive central zone. In this case, vimentin does not function as an internal control. **Figure 16** illustrates such paradoxical immunostained findings.

7. Tips and pitfalls in immunostaining

1) To get low background staining

The signal/noise ratio should be high. We must aim for immunostaining with distinct positive signals with minimal background staining. The recent development of epitope retrieval techniques and the availability of a wide variety of monoclonal antibodies have significantly contributed to the art of immunostaining: the staining must be artistic, the author believes.

When you encounter immunostaining with high background noise, the following three possibilities should be checked.

a) The concentration of the primary or secondary antibodies is too high.
b) The antibody titer is too low.
c) Rinsing in PBS is insufficient.

As a prerequisite for artistic immunostaining with a high signal/noise ratio, the appropriate antibody dilution should be predetermined (**Figure 17**). Generally speaking, monoclonal antibodies provide low background staining, when compared with polyclonal antibodies. However, monoclonal antibodies of IgM type may be aggregated during repeated freezing and thawing to result in high background staining.

In order to lower the background noise, the following tips should be tried.

a) The primary antibody should further be diluted 10 times to incubate overnight, instead of short incubation time for 30–60 minutes.
b) The PBS rinse should be prolonged to overnight.
c) High concentration (1 M) sodium chloride should be added to PBS for rinsing.
d) Non-ionic detergents such as Tween 20 or Triton X-100 (0.05–0.1%) should be added to PBS for rinsing.
e) Skim milk (5–10%) or bovine serum albumin (1–5%) should be added to the diluted primary antibody.

2) The removal of endogenous confounding reactivities

a) Endogenous peroxidase activity

Peroxidase activity in FFPE sections can be quenched by the following methods. Eosinophils and neutrophils have a strong peroxidase activity, and hemoglobin in red cells reveal pseudoperoxidase activity. Peroxidase activity in macrophages, platelets and epithelial cells (salivary gland, mammary gland, thyroid, and renal tubules) is completely inactivated during FFPE preparations. The most common method to inactivate endogenous peroxidase activity is dipping in 0.3% hydrogen peroxide-methanol solution or 3% hydrogen peroxide aqueous solution for 15–30 minutes. Oxidation in 0.5% periodic acid for 10 minutes is also effective, but never suitable for carbohydrate antigens. The hydrogen peroxide-mediated method is also harmful to the carbohydrate antigens when the treatment is too long up to 2 hours. Addition of 10 mM sodium azide to the DAB solution also assists at inhibiting endogenous peroxidase activity.

When a lymphocyte surface marker study is performed with ethanol-fixed fresh-frozen sections, the endogenous peroxidase quenching should be performed after the incubation of primary antibodies. The epitopes of lymphocytes surface markers frequently belong to sugar moieties, and the sugar molecules in fresh-frozen sections are easily destroyed by the oxidation step, as illustrated in **Figure 18**.

b) Endogenous biotin activity

Biotin (vitamin H), a coenzyme of the decarboxylation reaction, is mainly distributed in mitochondria. Cells rich in mitochondria, such as proximal renal tubules, hepatocytes and striated muscle cells, have a strong endogenous biotin activity, particularly in fresh frozen sections or cytology preparations. When one utilizes biotin-based detection systems such as ABC or LSAB method, quenching of endogenous biotin activity should be performed by preincubating with avidin solution.[18] Binding between biotin and avidin is quite strong, and once bound, they never dissociate any longer.

The endogenous biotin activity is inactivated by formalin fixation. Exceptions include “opaque nuclei” seen in endometrial gland cells, endometrioid carcinoma cells and embryonal-type lung adenocarcinoma cells.[19] The opaque nuclei reveal strong endogenous biotin activity in FFPE sections. It should be noted that the endogenous biotin activity in mitochondria-rich cells in FFPE sections is retrieved by the heat-induced epitope retrieval step.[9] This is especially evident when 10 mM citrate buffer, pH 7.0 or 1 mM ethylenediamine tetraacetic acid (EDTA), pH 8.0 is employed as a dipping aqueous solution (**Figure 19**).[20]

This is the reason why biotin-based detection methods should be avoided, and instead, the HRP-labeled polymer technique has become the mainstream.

Preprints (www.preprints.org) | NOT PEER-REVIEWED | Posted: 28 April 2021 doi:10.20944/preprints202104.0750.v1

c) Endogenous protein A and protein G activity

Staphylococcus aureus and *Streptococcus pyogenes* have protein A and protein G on the cell wall, respectively. These proteins strongly bind the Fc portion of IgG molecules. Their IgG-binding activity is lost by formalin fixation, but HIER to FFPE sections retrieves IgG Fc-binding activity of the cocci. This may cause a pitfall in immunohistochemical identification of the coccal pathogen seen in FFPE sections (**Figure 20**).[21] For the epitope retrieval of the coccal antigens, proteinase digestion should be employed, instead of the heating pretreatment. When the heating pretreatment is employed, preincubation with diluted normal human or animal serum is indispensable.

d) Endogenous pigments

Brown or black-colored endogenous pigments may hamper the observation of the DAB coloring reaction of target. Melanin shows metachromasia, so that Giemsa or methylgreen should be chosen for counterstaining, instead of hematoxylin. The greenish-colored metachromatic melanin is clearly distinguishable from the brown DAB deposit. Hemosiderin pigments can be distinguished from the DAB product by counterstaining with Berlin blue. **Figure 21** illustrates representative examples. Black-colored formalin pigments are often dispersed in and around the lesion with hemorrhage. Formalin pigment is particularly troublesome in autopsy cases. For the removal of the formalin pigment, unstained slides should be treated with alcoholic solutions containing picric acid, sodium hydroxide or ammonium hydroxide.[22] In the liver, aggregated bilirubin pigments may be confused with the specific DAB products (**Figure 22**). A trouble-shooting tip is as follows. ALP-labeled probe should be chosen as the secondary reagent, instead of HRP-labeled probe. The specific reaction products of azo dyes can be visualized in red or blue.

3) Staining artifacts: effects of dewatering, contamination of cytokeratin-positive squams and insufficient deparaffinization

When sections happen to be dried during antibody incubation, DAB coloring reaction is seen in the area of drying, mainly located at the periphery of the sections. This is because the antibody molecules are dry-fixed onto the glass slide in the area of dewatering. Sections are occasionally contaminated with cytokeratin-positive squams of skin origin, which may cause false-positive judgment. Fine adjustment of the microscopic focus reveals that the positivity is seen on the section but not in the section. If deparaffinization is incomplete or when air bubbles are formed on the glass slide, round-shaped negative zones are observed because of the lack of antibody penetration. Representative features are demonstrated in **Figure 23**.

4) Antigenic deterioration due to prolonged conservation of unstained sections

As positive control sections, it is convenient for us to conserve unstained glass slides in diagnostic pathology divisions. Importantly, the detection of certain antigens is not suitable for the storage at room temperature for a long period of time. Particularly susceptible are nuclear antigens, such as Ki-67 (MIB-1), p53, ER and PgR (**Figure 24**). Positive control sections should thus be cut from the control paraffin block just before immunostaining. Another method of convenience is to keep unstained glass slides in a freezer at -20C or lower.[23]

5) Effects of section-stretching temperature on a hot plate and drying period after cutting sections

Some antigens are quite susceptible to high section-stretching temperature on a hot plate (**Figure 25**). In our experience, immunoreactivities of glutathione-S-transferase (GST)-π, an isozyme of cytoplasmic peroxide-reducing enzyme, and orotate phosphoribosyltransferase (OPRT), a cytoplasmic enzyme phosphorylating 5-fluorouracil (5-FU), an anti-cancer drug, are markedly reduced after stretching on a hot plate at 70C for 2–3 seconds.[24] CD8 antigen is also susceptible to the high temperature stretching. The antigenicities of human epidermal growth factor receptor-2 (HER2), epidermal growth factor receptor (EGFR), Ki-67, cytokeratins and CD20 are mildly weakened. The temperature and period for the stretching should be set at 40C for 20 seconds or at 50C for 10 seconds for the safety purpose.

Regarding the drying period after cutting sections, HER2 immunoreactivity is significantly weakened after leaving unstained sections in an incubator at 40C for 3 days (**Figure 26**).[25] A milder effect for HER2 immunostaining is observed after incubation at 40C for 1 day. When sections are kept in the incubator at 60C for 3 days, immunoreactivities of cytokeratins and pepsinogen 2 are apparently weakened.

6) Effect of decalcification

Formalin-fixed bone or calcified tissue should be decalcified before preparing FFPE tissue. Four kinds of solution are commonly used for decalcification, including 10% formic acid in formalin, Plank-Rychlo solution (containing 8.5% hydrochloric acid, 5% formic acid and 7% aluminum chloride), 5% trichloroacetic acid, and 10% EDTA disodium solution, pH 7. EDTA-mediated decalcification, requiring a longer time to complete, has little effect on the expression of lymphocyte surface markers and Ki-67, while significant damages to the antigenicity are observed after decalcification by formic acid solution and particularly Plank-

Preprints (www.preprints.org) | NOT PEER-REVIEWED | Posted: 28 April 2021 doi:10.20944/preprints202104.0750.v1

Rychlo solution and trichloroacetic acid. Therefore, Plank-Rychlo solution and trichloroacetic acid should be avoided for immunohistochemical analysis for lymphocyte surface markers.[26] In contrast, Mukai, *et al*. described that routinely decalcified tissues can be used for immunostaining without significant loss of immunoreactivity.[27]

When necessary, the surface decalcification procedure is performed on paraffin blocks to prepare higher quality FFPE sections without chattering. The surface of paraffin blocks is exposed to the decalcification solution for 30 minutes to 24 hours. Ki-67 immunoreactivity is especially susceptible to the surface decalcification procedure (**Figure 27**). Surface decalcification with formic acid for less than 1 hour does show a negligible effect on the marker expression.[28]

7) Pitfalls and caveats in high-sensitivity immunostaining

HRP-labeled polymer techniques such as Envision Flex, Simple Stain Max and Novolink have enabled us to visualize various tissue antigens in FFPE sections. The CSA employing fluorescein isothiocyanate (FITC)-labeled tyramide (CSA-II, available from Agilent Co./Dako) is an ultrasensitive detection system to visualize hidden antigens, which have been never detectable in FFPE sections. However, the higher the sensitivity of detection, the higher the background staining. Intracellular localization of antigens becomes blurred: i.e., the membrane antigen may diffuse into the cytoplasm.

PharmDx™ is an immunostaining kit available from Agilent/Dako for the detection of EGFR in colonic adenocarcinoma. The problem is that positive signals are commonly weak not only in cancer cells but also in the normal colonic mucosa. The kit employs the EnVision as the secondary reagent. However, the use of the CSA-II system available from the same company significantly enhances the positive signals (**Figure 28**).[29]

When the concentration of the primary antibody is too high, false-negative results may happen paradoxically when one uses the CSA-II system.[30] We evaluated the localization of CD4, interleukin-6 (IL-6) and interferon-gamma (IFN-γ) in heat-retrieved FFPE sections of the pharyngeal tonsil with the CSA-II system. When the antibodies were diluted at 1:5,000, clear positivity was observed in immunocytes in FFPE sections. False negative findings were seen with anti-IFN-γ polyclonal antibody at a 1:500 dilution. In case of CD4 (monoclonal) and IL-6 (polyclonal), the antibodies at 1:50 dilution gave false-negative results (**Figure 29**). The background staining was increased. False negativity was partially recovered by 10-times dilution of the HRP-labeled secondary reagent and the FITC-labeled tyramide.

The autostainers are usually programmed for detecting the antigen with ultrahigh sensitivity. For example, HER2 immunostaining for breast and gastric cancer using a Ventana's Benchmark ULTRA (Roche Diagnostics, Rotkreuz, Switzerland) gives very strong positivity in HER2-overexpressed lesions. and normal mammary ducts and normal gastric foveolar cells also tend to be stained fairly strongly. When pathologists are unfamiliar with the result of this system, false positive judgment may happen in cancerous lesions not overexpressing HER2.

8) Pitfalls and caveats in antigen retrieval sequences

FFPE sections often require an antigen retrieval step before immunostaining. Cross-linkage of cellular proteins formed during formalin fixation may mask antigenic sites (epitopes). Epitope retrieval sequences, pretreatments before antibody incubation, can expose antigenic sites to allow antibodies to bind by breaking or loosening the formaldehyde-mediated methylene bridges. Two methods are mainly utilized for the epitope retrieval: enzymatic digestion and heat-induced epitope retrieval (HIER). To prevent detachment of sections during the pretreatments, the use of coated glass slides is inevitable: (3-aminopropyl)trimethoxysilane-coated glass slides are most commonly utilized.

a) Proteinase pretreatment

A variety of proteinases have been employed for the digestion of FFPE sections for the epitope retrieval. These include proteinase K, protease-1, pronase, actinase, trypsin, pepsin and ficin. The proteinase pretreatment is effective for retrieving the antigenicity of type 4 collagen (**Figure 30**) and laminin. Cytokeratins and lymphocyte surface markers may be retrieved with this pretreatment.

Glomerular immune deposits consisting of immunoglobulins and complements can be detected reproducibly by thoroughly digesting sections (**Figure 31**).[31] Prolongation of the digesting period is required. In case of trypsin digestion, the immune deposits are visible after 2 hour treatment (4 times longer than the usual use). We detected IgM deposits in glomeruli of IgM nephropathy in the FFPE autopsy kidney.[32] IgG deposition on the plasma membrane was proven in the skin, gut and bronchus in lethal paraneoplastic pemphigus.[33]

Of note is that the antigenicity may be lost by the proteinase pretreatment. Representative examples include peptide hormones (substance P and gastrin-releasing peptide), IgD and J-chain of IgA and IgM (**Figure 32**). The epitopes detected by certain monoclonal antibodies, such as anti-vimentin V9 and anti-cytokeratin KL-1, are lost by the pretreatment. Of note is that cytokeratin immunoreactivity detected with monoclonal antibody KL-1 is lost after trypsin treatment but enhanced by pepsin digestion. The protease pretreatment should also be avoided for localizing CD20 (L26), CD45 (LCA) (2B11+PD7/26), CD45RO

Preprints (www.preprints.org) | NOT PEER-REVIEWED | Posted: 28 April 2021 doi:10.20944/preprints202104.0750.v1

(UCHL1), desmin (D33), Ki-67 (MIB-1), neutrophil elastase (NP57), neuron-specific enolase (NSE) (BBS/NC/VI-H14), p53 (DO-7) and proliferating cell nuclear antigen (PCNA) (PC-1).

b) Heat-induced epitope retrieval (HIER)

Hydrated heating is quite effective for retrieving hidden antigenicities in FFPE sections.[3,6] Typically, deparaffinized sections are heated at 60–121C in 10 mM citrate buffer, pH 6.0 or pH 7.0 or in 1 mM EDTA solution, pH 8.0. The devices used for heating include the incubator (at 60C, overnight), water bath (at 95C), microwave oven (at 100C), steamer (at >100C), pressure pan (at 121C) and autoclave oven (at 121C). The author strongly recommends pressure pan cooking, because of its stability, reproducibility and ease of handling (**Figure 33**).

A variety of antigens (epitopes) can be retrieved, such as intranuclear antigens (p53, Ki-67, ER, PgR, thyroid transcription factor-1 [TTF1], caudal-type homeobox-2 [CDX2], etc.), plasma membrane antigens (lymphocyte surface markers, epithelial membrane antigen [EMA], etc.), cytoskeletal proteins (cytokeratins, vimentin, desmin, actin, etc.), and secretory proteins (parathyroid hormone, α-fetoprotein, fibrinogen, etc.). Typical examples are displayed in **Figures 34 and 35**. Peptide hormone immunoreactivity may also be retrieved by the heating pretreatment. Choice of the solution is important for appropriate HIER of the respective antigens (**Figure 36**). Supposedly, chelation of calcium iron by citric acid and EDTA is a key factor for HIER. It is of note that nuclear antigens such as ER and p53 show an HIER effect in ethanol-fixed cytology preparations (**Figure 37**).[34]

The heating treatment changes double-stranded DNA into single-stranded to allow nuclear antigens hidden within the DNA stretches to bind antibodies. Occasionally, we happen to experience false-negativity of nuclear antigens such as p53, ER and PgR when monoclonal antibodies are incubated overnight at 4C or at room temperature. Nuclear reactivity is evident when the same antibodies at the same dilution are incubated for 60 minutes (**Figure 38**). This paradoxical phenomenon can be explained as follows. During the prolonged incubation period, heat-provoked single-stranded DNA naturally returns to double-stranded, so that the nuclear antigens are hidden again to become inaccessible to the antibodies.

Hematoxylin is suitable for nuclear counterstaining in heat-treated sections. Methylgreen stains the nuclei only faintly in the heat-treated sections. This is explained by the fact that the methylgreen dye has an affinity to double-stranded DNA. Nuclear affinity to hematoxylin is evidently decreased after heating in 1 mM EDTA solution, pH 8.0, so that prolongation of hematoxylin staining time is needed (**Figure 39**).[35] It should also be noted that, during heating in 10 mM citrate buffer, pH 7.0, sections tend to be detached off.

Ironically, the antigenicity of some antigens is markedly weakened or lost after the heating pretreatment (**Figure 40**). These include BM-1 (a marker of the myeloid precursors), neutrophil elastase (NP57), von Willebrand factor, NSE and GST (α, μ and π).

One must know that the nuclear localization of Ki-67 is dependent upon how to cool down sections after heating.[36] When sections are rapidly cooled down in tap water after heating, Ki-67 often reveals a false negative finding. In contrast, clear nuclear positivity is observed in sections cooled down gradually by leaving sections in the heating solution at room temperature for more than 30 minutes (**Figure 41**). When one employs a high molecular weight polymer reagent (EnVision, Agilent/Dako Co) as the secondary probe, the cytoplasm of the mitotic cells is stained for Ki-67 while the nuclei of proliferative cells remain unstained (**Figure 42**). Such a strange phenomenon is not experienced when the secondary polymer reagent of smaller molecular size such as EnVision Plus or EnVision Flex is employed.

c) Other methods for epitope retrieval

Immunoreactivity of β-amyloid protein in the brain is retrieved by soaking in 100% formic acid solution for 5 minutes (**Figure 43**),[37] while protease treatment and HIER are ineffective. Bromodeoxyuridine (BrdU) experimentally incorporated in the nuclei of proliferative cells can be detected in FFPE sections after the exposure in 2-4 N hydrochloric acid solution for 20–90 minutes.[38] DNase I from the bovine pancreas can also be utilized for the same purpose.[39] Actin immunoreactivity of intracytoplasmic eosinophilic inclusion bodies in infantile digital fibromatosis is retrieved by treating sections in 1 N potassium hydroxide in 70% alcohol for 60 minutes followed by trypsin digestion.[40]

8. How to judge the immunostained results

1) False positivity or equivocal negativity

When the target cells appear to be immunostained faintly, it is critically important how to judge the result: whether they are weakly positive or equivocally negative. The author once experienced a regrettable misjudgment for a mediastinal small round tumor of a middle-aged man. Placental alkaline phosphatase (PALP) was judged as weakly positive, so that the author's final diagnosis was germinoma (seminoma). However, it was actually small cell carcinoma of the lung with false-positive (or equivocally negative) PALP immunoreactivity. In general, immunoreactivity of secretory proteins in neoplastic cells tends to be weaker than the normal cells. Examples include chromogranin A, insulin, gastrin, von Willebrand factor and immunoglobulins.

Preprints (www.preprints.org) | NOT PEER-REVIEWED | Posted: 28 April 2021 doi:10.20944/preprints202104.0750.v1

2) Intracellular localization pattern of antigens

The specificity of immunostaining can be judged by the intracellular localization pattern of the antigenic substances, as schematically illustrated in **Figure 44**.[1)] Representative immunohistochemical markers are displayed in one panel (**Figure 45**).

Peptide hormones and chromogranin A are localized as intracytoplasmic fine granules. Lysosomal and mitochondrial proteins are visualized as intracytoplasmic coarse granules. Secretory proteins such as alpha-fetoprotein, human chorionic gonadotropin and immunoglobulins are seen as small vesicles in the cytoplasm, representing the ultrastructural localization in the rough endoplasmic reticulum and Golgi apparatus. Particularly in neoplastic cells, immunoreactivity of secretory proteins may be accentuated and clustered in the Golgi area. Diffuse cytoplasmic reactivity is seen for cytosolic proteins such as myoglobin, NSE and GST. S-100 protein, heat-shock proteins, ubiquitin and β-catenin are distributed diffusely in both the cytoplasm and nucleus. The nuclei are diffusely positive for Ki-67 (MIB-1), p53, CDX2, ER and PgR, but nucleolar staining is frequently accentuated for Ki-67. Plasma membrane proteins reveal distinct membrane staining, and the Golgi area is also frequently positive. Carcinoembryonic antigen (CEA) is expressed along the apical plasma membrane in normal gastric and colonic mucosa, while in adenocarcinomas of the stomach and colon, the plasma membranes are circumferentially positive.[41)] Such intracellular antigen distribution patterns are clearly recognized in PPFE sections, when compared with fresh-frozen sections.

When Ki-67 is localized along the plasma membrane instead of the nucleus, one can easily recognize they are nonspecific (**Figure 46**). Ki-67 antigen is positive along the plasma membrane in certain tumors, and the finding has been utilized as a diagnostic marker.[42)] PgR may be expressed along the plasma membrane of breast cancer cells, and the lymphocyte surface markers happen to be localized in the nucleus (**Figure 47**). When an ultra-sensitive method is employed for immunostaining together with HIER, plasma membrane proteins may appear to be localized diffusely in the cytoplasm. Periodic acid treatment after HIER may suppress such non-physiological (artificial) localization.

3) Specificity of antibodies

The specificity of the antibody should be confirmed before practical use. Information supplied by the manufacturer is valuable, but one must not believe it in blindness. It is of note that rabbit antiserum occasionally contains natural antibodies against intermediate filament proteins.[43)] For example, anti-myoglobin antiserum stains the epidermal keratinocytes, vascular endothelial cells and pancreatic islet cells (**Figure 48**). Monoclonal antibodies supplied as a form of the ascitic fluid may show unexpected cross-reactivity due to mouse ascitic components.[44)]

Small molecules (haptens) such as peptide hormones and thyroxine are immunized with carrier proteins, so that antibodies designated against peptide hormones also contain anti-carrier protein antibodies.[45)] When bovine thyroglobulin is used as a carrier protein, the antiserum reacts with colloid and epithelial cells of the human thyroid gland. Anti-cholecystokinin (CCK) antiserum immunized with *Ascaris* proteins as a carrier protein reveals cross-reactivity to the smooth muscle, cartilage and some epithelial cells in human tissues, as well as to neuroendocrine tumors (**Figure 49**). Since the extract of *Mycobacterium tuberculosis* is commonly used as an adjuvant for immunization,[46)] many antisera may stain tuberculous bacilli and other mycobacteria in FFPE sections (**Figure 50**).

4) Specificity of the specific markers

The poorer the degree of cancer differentiation, the more infrequent the expression of specific markers. The lack of marker expression does not necessarily exclude the possibility of specific differentiation of neoplastic cells. The epithelial cells may express vimentin, while a variety of non-epithelial tumor cells are immunoreactive for cytokeratins. Spindle cell carcinoma of the skin co-expresses cytokeratin and vimentin.[47)] Anaplastic large cell lymphoma may express cytokeratins.[48)] Usefulness and pitfalls of cytokeratin immunostaining are displayed in **Figure 51**.

The lack of basal cells is an excellent indicator of prostatic adenocarcinoma. Postatrophic hyperplasia of the prostate histologically resembles adenocarcinoma, causing diagnostic confusion.[49)] The preservation of the cytoleratin 5/6-immunoreactive basal cells around the respective acini is of significant diagnostic value (**Figure 52**).

Neuron-specific enolase (NSE) or gamma-enolase is not necessarily specific to neurons and neuroendocrine cells.[50)] A variety of non-neuroendocrine cells and their tumors may express NSE. Glial fibrillary acidic protein (GFAP) is known to be expressed in some myoepithelial cells and their tumors of the salivary gland.[51)] Antiserum against prostate-specific antigen (PSA) may be cross-reactive to salivary gland duct cells. The reason is that PSA or human kallikrein-3 shares epitopes common to other kallikreins expressed in the salivary gland ducts.[52)] Prostatic acid phosphatase (PAcP) is frequently expressed in neuroendocrine cells and tumors of the rectum.[53)] Representative examples are illustrated in **Figure 53**. Diagnostic pathologists must study and know such unexpected expression of "specific" markers in unrelated cells.

5) Nonspecific adsorption of antibodies by certain cells

Preprints (www.preprints.org) | NOT PEER-REVIEWED | Posted: 28 April 2021 doi:10.20944/preprints202104.0750.v1

Tissue mast cells,[54] neuroendocrine cells (particularly gastrin cells),[55] cerebellar Purkinje cells, parietal cells of the gastric oxyntic mucosa, and HBs antigen-positive groundglass hepatocytes in HBV carriers[56] may adsorb antibodies nonspecifically. Representative examples are demonstrated in **Figure 54**. Stromal collagen fibers also tend to show nonspecific binding with antibodies.[57]

6) Positive and negative controls

Negative controls employing normal animal serum or PBS are important to check the specificity of the immune reaction. When multiple antibodies are evaluated simultaneously, the antibodies mutually function as indifferent antibodies, so that negative control sections may be unnecessary.

Appropriate positive controls are inevitably needed in each run of immunostaining. They function as the evidence to exclude the possibility of inactivation of the antibodies. When positive cells are consistently included in the same sections, for example, cells positive for vimentin, vascular markers and epithelial markers, they act as internal positive controls.[17]

For the diagnostic practice for breast cancer, immunostaining for ER, PgR, HER2 and Ki-67 is consistently requested. When the author looked at borrowed slides sent from an outside hospital as a second opinion consultation for "ER-negative" breast cancer, not only breast cancer cells but also non-neoplastic mammary ductal cells were negative for ER. ER was then immunostained again in our laboratory, and clear nuclear positivity of ER was confirmed in both the normal and cancerous cells. Appropriate judgment for such technical pitfalls is critically important to give precious information for the treatment of the patient.

9. When unexpected results are obtained

It is a chance of particular significance if immunohistochemical results are different from H&E-based expectation. However, pathologists must make a careful judgment by considering the specificity of the markers they immunostained. We may encounter cases of cytokeratin-positive malignant lymphoma, glioma, sarcoma or melanoma. Vimentin is expressed in certain normal and neoplastic epithelial cells. We should know the expression of EMA (as a MUC-1-related molecule) on normal and neoplastic perineurial cells and plasma cells (**Figure 55**).[58] CD138, a marker of normal plasma cells, may not be expressed in neoplastic plasma cells.[59]

Cautions are needed when the clinical and histopathological diagnoses are discrepant. First of all, we must exclude the possibility of tissue contamination or mistake from other patient. The container of the formalin-fixed specimen and the paraffin block should be checked first just to be sure. We can immunostain blood group substances, A, B and H or Lewis a and b, for blood typing. The blood group substances are expressed consistently in vascular endothelial cells and occasionally in epithelial cells, so that we can apply immunohistochemical blood typing to proving the tissue contamination or mistake of FFPE sections, when the blood group of the cases of subject is different.[60] **Figure 56** displays successful immunohistochemical blood typing for contaminated needle biopsy specimens of the prostate, where one specimen contained cancer but not in another.

10. When only one preparation is available

It happens that we have only one unstained or H&E- or Papanicolaou-stained specimen using non-coated glass slide. Particularly, cytology specimens often have a chance of this situation. Can we use the one slide for immunostaining analysis? Yes, two methods can be applied. One is re-staining method and another is the cell transfer technique. See the reference 61 for details.

1) Re-staining method

Suppose you have only one glass slide already stained with H&E or Papanicolaou sequences. We can re-use the specimen.[62] The target cells or areas should be photographed beforehand. The first step is the removal of the cover glass in warm xylene. The stained dyes are bleached in acid alcohol solution (0.5% hydrochloric acid in 70% ethanol) for more than 1 hour. Or, you can leave the specimen in tap water overnight to bleach the dyes. Then the glass slide is ready for immunostaining. One typical example of cervical cytology smear re-stained for a *Chlamydia trachomatis* antigen is illustrated in **Figure 57**.

When the silane-coated glass slide has been used, you can apply HIER to immunostaining. If not, the sections or cells before the bleaching step should be transferred to silane-coated glass slide so as to apply to HIER-assisted immunostaining, as mentioned below. Finally, the same cells or areas of target should be re-photographed. If multiple markers are needed to be immunostained, the antigenic substances should be visualized repeatedly with an ALP-labeled secondary reagent. The azo dyes used for the color reaction for ALP, colored red or blue, can easily be bleached by soaking specimens in ethanol.

When the immunostained (DAB-colored) preparations are re-stained, negative control sections with negative results can be utilized for new immunostaining. If there is focal positivity of the DAB reaction, one can choose the second immunostaining with the ALP-labeled method to have a double-immunostained section.

Preprints (www.preprints.org) | NOT PEER-REVIEWED | Posted: 28 April 2021 doi:10.20944/preprints202104.0750.v1

a) Cell transfer technique

Histological sections or cytology specimens mounted on uncoated glass slides can be transferred to silane-coated glass slides.[63] The cover glasses should be removed by soaking in warm xylene. The sections or cell preparations are covered with mounting resin solution, and, after leaving them for 1–2 days in an incubator at 40C, the solidified resin forming a thick membrane can be peeled off after soaking in warm water for 1 hour. The sections or cells have been detached and transferred to the membrane side. In warm water, the resin membrane is then placed onto silane-coated glass slides. The glass slides with transferred resin membrane should be fully dried in the incubator. The resin can easily be removed by dipping the specimens in xylene. By scissors, you can cut the resin membrane into several pieces to obtain plural silane-coated glass slides for immunostaining (**Figure 58**).

Itoh, *et al*. invented a modified method for rapid cell transfer.[64] The mounting resin solution should be diluted double with xylene, and the resin is solidified on a hot plate at 70–80C. With this modification, the cell transfer can be achieved in one hour.

It should be noted that the cell transfer technique is neither applicable to dry-fixed Giemsa-stained preparations nor to the preparations mounted on silane-coated glass slides, such as cytology specimens of the urine, cerebrospinal fluid or effusions. For these specimens, the re-staining method should be tried. We found miracle coated glass slides supplied for cytology practice termed TACAS (Thinlayer Advanced Cytology Assay System supplied from Medical & Biological Laboratories, Nagoya, Japan), which allow both immunostaining with HIER and cell transfer. The TACAS glass slides prevent detaching off sections during immunostaining with HIER and allow the cell transfer after immunostaining employing the inverted beam capsule method.[65] Both the antigen and genome of severe fever with thrombocytopenia syndrome (SFTS) virus were successfully localized at the ultrastructural level with the pre-embedding technique (**Figure 59**).

11. Immunostaining with low specificity and high sensitivity

Pathogens infected in tissues are proven with antibodies with low or unknown specificity. Two examples are described here. Please refer to the author's previous article (reference 66).

1) Use of antisera against pathogens showing wide cross-reactivity

The antigenicities of pathogens are distinct from those of human cells. Therefore, pathogens can suitably be immunolocalized in FFPE sections. Bacteria or bacterial antigens are visualized with antisera against pathogens showing wide cross-reactivity. These include commercially available rabbit antisera against *Bacillus cereus*, BCG, *Treponema pallidum* and *Escherichia coli*. The immunostaining is useful for screening of bacterial infection in FFPE sections.[66] In other words, the identification of bacteria or bacterial antigens in the infectious lesions is of diagnostic value, even if the specificity is unknown.

A representative example includes *Corynebacterium kroppenstedtii* infected in granulomatous mastitis. The lipophilic bacteria are visualized with the antisera described above mainly in fat vacuoles within the inflammatory breast lesion.[12] Flesh-eating bacteria, *Vibrio vulnificus*, provoking gangrene of the extremity can be localized in the affected skin with antisera against *Bacillus cereus*, BCG and *Treponema pallidum*.[67] *Leptospira interrogans* infected in the liver is immunoreactive with *E. coli* antiserum. The causative bacteria in *Haemophilus pertussis*-provoked pneumonia are clearly shown in FFPE sections with all of the antisera. In colon biopsy specimens of intestinal spirochetosis, the long basophilic spiral-shaped bacteria, *Brachyspira aalborgi*, adhered on the surface of the colonic epithelial cells are strongly immunostained with all of the antisera described above.[66] Representative features are illustrated in **Figures 60 and 61**.

a) Use of patients sera

The sera of patients have high-titer antibodies against the causative pathogen, particularly in cases at the recovery stage or with chronic persistent infection.[66,68] When the host reactions such as abscess or granuloma are observed microscopically, the serum, diluted at 1:500 to 1:1,000, is applicable as a highly sensitive probe to detecting causative pathogens in the infected lesion embedded in paraffin.[66,68] What you need is to make a brief phone call to a laboratorian to save a small aliquot of patient's serum. Indirect immunoperoxidase method using HRP-labeled anti-human IgG or immunoglobulins is suitable in order to obtain low-background immunostaining. The methods with high sensitivity of detection such as LSAB or the polymer method give high background staining due to diffuse distribution of endogenous IgG in tissues. Usually, HIER is unnecessary for the detection, but HIER may occasionally assist at increasing the sensitivity of detection.[66] This low-cost sequence is particularly useful in case of protozoan and helminthic infections, including cryptosporidiosis, isosporiasis, toxoplasmosis, amebiasis, schistosomiasis, ascariasis and gnathostomiasis.[69]

When the clinical diagnosis has been confirmed, we can visualize the causative pathogen in FFPE sections of the infected lesion. Even if the clinical diagnosis is totally unsettled, candidate causative pathogens can be visualized within the lesion. In some cases, the specificity of the patient's serum is totally unknown. The size, shape and localization pattern of la-

belling may suggest certain causative microbes, when considered together with clinical features. Once the specificity of the patient's serum is known, the serum can be used thereafter as a specific probe for immunostaining. In order to avoid biohazard, the serum of the carriers of hepatitis B and C or acquired immunodeficiency virus must not be utilized.

As a representative example, a liver biopsy of visceral leishmaniasis (kala azar) is displayed in **Figure 62.** The patient was a middle-aged Japanese businessman who stayed long in Australia, Thailand and India for business purpose. He complained of fever and malaise, and accompanied anemia, thrombocytopenia and liver dysfunction. The patient's general condition was poor. FFPE liver biopsy preparation showed multifocal small non-caseous granulomas. No positive findings were obtained by immunostaining with a routine panel of anti-microbial antibodies. Immunostaining using 1:500 diluted patient's own serum demonstrated red cell-sized and rounded positive signals in the cytoplasm of epithelioid cells in the granuloma or in Kupffer cells. The size, shape and localization pattern strongly suggested the possibility of visceral leishmaniasis caused by *Leishmania donovanii*, which is endemic in India. Visceral leishmaniasis, never endemic in Japan, was serologically confirmed thereafter, and antimony-based therapy saved patient's life.[66,68)]

Another example is a case of *Balamuthia* encephalitis with a skin nodule. Here, the 1:500 diluted serum of another patient who suffered lethal chronic meningoencephalitis caused by *Balamuthia mandrillaris* was used.[66)] In biopsy samples of both the skin and brain, brown-colored amebic bodies (trophozoites and some cysts) are clearly identified, as shown in **Figure 63**.

The same strategy is applicable to autoimmune disorders. The patient's serum of autoimmune (type A) gastritis can be utilized to detect proton pump molecules on intracytoplasmic secretory canaliculi of parietal cells in the normal oxyntic gastric mucosa in FFPE sections (**Figure 64**).[70)] The dilution at 1:20 was employed in this situation. Autoantibodies against amphiphysin, a 128 kDa presynaptic protein, are seen in a patient of breast cancer who manifested progressive rigidity and painful spasms (an autoimmune encephalitis called Stiff-Man syndrome).[71)] The patient serum at a 1:20 dilution stained the plasma membrane of the breast cancer cells of her own. The serum of another patient with autoimmune limbic encephalitis of non-paraneoplastic type [72)] stains astroglial cells and glial fibers in FFPE basal ganglia of autopsied normal brain. Immunostaining using diluted patient's serum may contribute to clarifying the pathogenesis of autoimmune encephalitis, as illustrated in **Figure 65**.

12. Concluding remarks

Nowadays, it makes sense to have beautiful and specific immunostaining. Biomedical engineers (medical technicians) should know how to select markers and how to judge the result. Pathologists and investigators must understand the pitfalls and caveats of immunostaining procedures. For applying immunostaining to diagnostic pathology services, it is critically important for us how to stain, how to select markers and how to judge the result. The author wants to emphasize the importance of close teamwork and cooperation between the biomedical engineers and pathologists.

Acknowledgments

The author cordially thanks the following four scientists: Kazuya Shiogama, Ph.D., Division of Morphology and Cell Function, Faculty of Medical Technology, Fujita Health University School of Health Sciences, Toyoake, Aichi, Yasuyoshi Mizutani, Ph.D., Department of Molecular Oncology, Fujita Health University School of Medicine, Toyoake, Aichi, Kenji Kawai, M.T., Pathology Analysis Center, Central Institute for Experimental Animals, Kawasaki, Kanagawa, and Shingo Kamoshida, Ph.D., Laboratory of Pathology, Department of Medical Biophysics, Kobe University Faculty of Health Sciences and Graduate School of Medicine Faculty of Health Sciences, Kobe, Hyogo, for their excellent problem-solving ability and skillful technical assistance.

Funding

The authors received no financial support for the research, authorship, and/or publication of the present article.

Competing interests

None declared.

Ethics approval

All the procedures were in accordance with the ethical standards of the responsible institutional committee on human experimentation and with the Helsinki Declaration of 1964 and later versions.

References

1) Nagura H, Osamura RY, Tsutsumi Y (Eds). Watanabe/Nakane's Enzyme-Labeled Antibody Method, 4th Ed. Gakusai-Kikaku, Tokyo, Japan, 2002 (*in Japanese*). ISBN4-906514-43-X.

2) Buchwalow IB, Böcker W. Immunohistochemistry: Basics and Methods. 2010, Springer Publishing, NY, USA. ISBN-13: 978-3642046087.

3) Shi S-R, Taylor CR (Eds). Antigen Retrieval Immunohistochemistry Based Research and Diagnostics. 2010, John Wiley and Sons, Ltd. Hoboken, NJ, USA. ISBN: 978-1-118-06030-8.

4) Chu P, Weiss L. Modern Immunohistochemistry. 2014, Cambridge University Press, Cambridge, UK. ISBN-13: 9781316183748.

5) Lin F, Prichard J (Eds). Handbook of Practical Immunohistochemistry. Frequently Asked Questions. 2015, Springer Science+Business Media, NY, USA. ISBN: 978-1-4939-1577-4

6) Kim SW, Roh J, Park CS. Immunohistochemistry for pathologists: protocols, pitfalls, and tips. *J Pathol Transl Med.* 2016; **50**: 411–418.

7) Renshaw S (Ed). Immunohistochemistry and Immunocytochemistry: Essential Methods, 2nd Ed. 2017, John Wiley and Sons, Ltd. Hoboken, NJ, USA. ISBN:9781118717776.

8) Dabbs DJ (Ed). Diagnostic Immunohistochemistry, Theranostic and Genomic Applications. 5th Ed. 2018, Elsevier Inc., Amsterdam, Netherland. ISBN: 9780323477321.

9) Bussolati G, Gugliotta P, Volante M, Pace M, Papotti M. Retrieved endogenous biotin: a novel marker and a potential pitfall in diagnostic immunohistochemistry. *Histopathology.* 1997; **31**: 400–407.

10) Osamura RY, Watanabe K, Yoshimasa T, *et al*. Immunohistochemical localization of Met-enkephalin, Met-enkephalin-Arg^6-Gly^7-Leu^8, Met-enkephalin-Arg^6-Phe^7 and Leu-enkephalin in human adrenal medulla and pheochromocytomas. *Peptides.* 1984; **5**: 993–1000.

11) Tamakuma K, Mizutani Y, Ito M, Shiogama K, *et al*. Histopathological diagnosis of Japanese spotted fever using formalin-fixed, paraffin-embedded skin biopsy specimens: usefulness of immunohistochemistry and real-time PCR analysis. *Clin Microbiol Infect.* 2012; **18**: 260–267.

12) Fujii M, Mizutani Y, Sakuma T, *et al*. *Corynebacterium kroppenstedtii* in granulomatous mastitis: Analysis of formalin-fixed, paraffin-embedded biopsy specimens by immunostaining using low-specificity bacterial antisera and real-time polymerase chain reaction. *Pathol Int.* 2018; **68**: 409–418.

13) Sato Y, Mukai K, Matsuno Y, *et al*. The AMeX method: a multipurpose tissue-processing and paraffin-embedding method. II. Extraction of spooled DNA and its application to Southern blot hybridization analysis. *Am J Pathol.* 1990; **136**: 267–271.

14) Tsutsumi Y, Shiogama K, Teramoto H, *et al*. Detection of hepatitis virus B and C in archival autopsy specimens of liver. *Biomed J Sci Tech Res.* 2019; 16699–16704. doi: 10.26717/BJSTR.2019.22.003757

15) Tsutsumi Y. Demonstration of Epstein-Barr virus genome in archival paraffin sections of Hodgkin`s lymphoma autopsied by Dr. Thomas Hodgkin nearly 170 years ago. *Acta Histochem Cytochem.* 2003; **36**: 511–514.

16) Chetty R, Biddolph, S, Gatter K. An immunohistochemical analysis of reedsternberg-like cells in posttransplantation lymphoproliferative disorders: The possible pathogenetic relationship to Reed-Sternberg cells in Hodgkin's disease and reedsternberg-like cells in non-Hodgkin's lymphomas and reactive conditions. *Hum Pathol.* 1997; **28**: 493–498.

17) Battifora H. Assessment of antigen damage in immunohistochemistry. The vimentin internal control. *Am J Clin Pathol.* 1991; **96**: 669–671.

18) Wood GS, Warnke R. Suppression of endogenous avidin-binding activity in tissues and its relevance to biotin-avidin detection systems. *J Histochem Cytochem.* 1981; **29**: 1196–1204.

19) Nakatani Y, Kitamura H, Inayama Y, Ogawa N. Pulmonary endodermal tumor resembling fetal lung. The optically clear nucleus is rich in biotin. *Am J Surg Pathol.* 1994; **18**: 637–642.

20) Kamoshida S, Matsuoka H, Matsuyama A, *et al*. Reproducible and reliable immunohistochemical demonstration of thymidylate synthase in formalin-fixed, paraffin-embedded sections: Application of antigen retrieval in EDTA solution. *Acta Histochem Cytochem*. 2003; **36**: 115–118.

21) Shimomura R, Tsutsumi Y. Histochemical identification of methicillin-resistant *Staphylococcus aureus*: contribution to preventing nosocomial infection. *Semin Diagn Pathol.* 2007; **24**: 217–226.

22) Chatzopoulos K, Treeck BV, Venable E, *et al*. Formalin pigment artifact deposition in autopsy tissue: predisposing factors, patterns of distribution and methods for removal. *Forensic Sci Med Pathol*. 2020; **16**: 435–441.

23) Wester K, Wahlung E, Sundstroem C, *et al*. Paraffin section storage and immunohistochemistry. Effect of time, temperature, fixation, and retrieval protochol with emphasis on p53 protein and MIB1 antigen. *Appl Immunohistochem Mol Morphol.* 2000; **8**: 61–70.

24) Kamoshida S, Sakamoto N, Matsuoka H, *et al*. Heat-assisted stretching of paraffin section on hot plate weakens immunoreactivity of orotate phosphoribosyltransferase. *Acta Histochem Cytochem.* 2005; **38**: 69–74.

25) Yamaguchi D, Shiogama K, Takeuchi S, *et al*. Effects of section stretching and drying condition on the immunoreactivity of various antigens. *Kensa-to-Gijutsu.* 2013; **41**: 698–702 (*in Japanese*).

26) Takeshita N, Kuwana S, Shirasuga H, *et al*. The influence of decalcifying solution on immunoperoxidase staining (PAP) in paraffin sections. *Jpn J Oral Biol.* 1983; **25**: 1134–1135.

27) Mukai K, Yoshimura S, Anzai M. Effects of decalcification on immunoperoxidase staining. *Am J Surg Pathol.* 1986; **10**: 413–419.

28) Obana Y, Nemoto N. Effects of surface decalcification on immunostaining (*in Japanese*). 2013. https://www.nichirei.co.jp/bio/tamatebako/pdf/tech_22_dr_obana.pdf

29) Shiogama K, Miyase K, Kamoshida S, *et al*. False negativity in immunostaining with CSA-II under high concentration of antibodies. *Byori-to-Rinsho*. 2010; **28**: 1213–1217 (*in Japanese*).

30) Shiogama K, Wongsiri T, Mizutani Y, *et al*. High-sensitivity epidermal growth factor receptor immunostaining for colorectal carcinomas, compared with EGFR PharmDx™: a study of diagnostic accuracy. *Int J Clin Exp Pathol*. 2013; **6**: 24–30.

31) Singh G, Singh L, Ghosh R, *et al*. Immunofluorescence on paraffin embedded renal biopsies: Experience of a tertiary care center with review of literature. *World J Nephrol.* 2016; **5**: 461–470.

32) Odani K, Tachibana M, Nogaki F, Tsutsumi Y. Late relapse of IgM nephropathy-associated nephrotic syndrome after repeated administration of immune checkpoint inhibitor against pulmonary adenocarcinoma. *Clin Case Rep.* 2021. doi.org/10.1002/ccr3.3903

33) Odani K, Itoh A, Yanagita S, *et al*. Paraneoplastic pemphigus involving the respiratory and gastrointestinal mucosae. *Case Rep Pathol.* 2020, Article ID 7350759 (8 pages). doi.org/10.1155/2020/7350759

34) Cizkova K, Flodrova P, Baranova R, *et al*. Beneficial effect of heat-induced antigen retrieval in immunocytochemical detection of intracellular antigens in alcohol-fixed cell samples. *Appl Immunohistochem Mol Morphol.* 2020; **28**: 166–174.

35) Shiogama K, Tsutsumi Y. Effects of heat-induced epitope retrieval on nuclear staining (*in Japanese*). 2015, http://www.nichirei.co.jp/bio/tamatebako/ /pdf/intro_11_dr_Shiogama.pdf

36) Kawai K, Tsutsumi Y. Pitfalls in MIB-1 immunostaining. *Byori Gijutsu*. 1999; **59**: 20–21 (*in Japanese*).

37) Kitamoto T, Ogomori K, Tateishi J, Prusiner SB. Formic acid pretreatment enhances immunostaining of cerebral and systemic amyloids. *Lab Invest.* 1987; **57**: 230–236.

38) Nagashima T, DeArmond SJ, Murovic J, Hoshino T. Immunocytochemical demonstration of S-phase cells by anti-bromodeoxyuridine monoclonal antibody in human brain tumor tissues. *Acta Neuropathol.* 1985; **67**: 155–159.

39) Gonchoroff NJ, Katzmann JA, Currie RM, *et al*. S-phase detection with an antibody to bromodeoxyuridine. Role of DNase pretreatment. *J Immunol Methods.* 1986; **93**: 97–101.

40) Mukai M, Torikata C, Iri H, *et al*. Immunohistochemical identification of aggregated actin filaments in formalin-fixed, paraffin-embedded sections. I. A study of infantile digital fibromatosis by a new pretreatment. *Am J Surg Pathol.* 1992; **16**: 110–115.

41) Nagura H, Tsutsumi Y, Shioda Y, Watanabe K. Immunohistochemistry of gastric carcinomas and associated diseases: novel distribution of carcinoembryonic antigen and secretory component on the surface of gastric cancer cells. *J Histochem Cytochem.* 1983; **31**(1A_Suppl): 193–198.

42) Leonardo E, Volante M, Barbareschi M, *et al*. Cell membrane reactivity of MIB-1 antibody to Ki67 in human yumors: fact or artifact? *Appl Immunohistochem Mol Morphol*. 2007; **15**: 220–223.

43) Yildiz A, Toh BH, Sotelo J. Smooth muscle autoantibodies reacting with cytoplasmic intermediate filaments in sera from normal, nonimmunized rabbits. *Clin Immunol Immunopathol*. 1980; **16**: 279–286.

44) Bonetti F, Pea M, Martignoni G, *et al*. False-positive immunostaining of normal epithelia and carcinomas with ascites fluid preparations of antimelanoma monoclonal antibody HMB45. *Am J Clin Pathol.* 1991; **95**: 454–459.

45) Skowsky WR, Fisher DA. The use of thyroglobulin to induce antigenicity to small molecules. *J Lab Clin Med.* 1972; **80**: 134–144.

46) Kubota M, Iizasa E, Chuuma Y. Adjuvant activity of *Mycobacteria*-derived mycolic acids. *Heliyon* 2020; **6**: e04064.

47) Smith KJ, Skelton HG 3rd, Morgan AM, et al. Spindle cell neoplasms coexpressing cytokeratin and vimentin (metaplastic squamous cell carcinoma). *J Cutan Pathol.* 1992; **19**: 286–293.

48) Zhang Q, Ming J, Zhang S, et al. Cytokeratin positivity in anaplastic large cell lymphoma: a potential diagnostic pitfall in misdiagnosis of metastatic carcinoma. *Int J Clin Exp Pathol.* 2013; **6**: 798–801.

49) Cheville JC, Bostwick DG. Postatrophic hyperplasia of the prostate. A histologic mimic of prostatic adenocarcinoma. *Am J Surg Pathol.* 1995; **19**: 1068–1076.

50) Påhlman S, Esscher T, Nilsson K. Expression of gamma-subunit of enolase, neuron-specific enolase, in human non-neuroendocrine tumors and derived cell lines. *Lab Invest.* 1986; **54**: 554–560.

51) Huang J, Shrestha P, Takai Y, Mori M. Immunohistochemical evaluation of GFAP in salivary gland tumors. *Acta Histochem Cytochem.* 1996; **29**: 85–92.

52) Tazawa K, Kurihara Y, Kamoshida S, *et al*. Localization of prostate-specific antigen-like immunoreactivity in human salivary gland and salivary gland tumors. *Pathol Int.* 1999; **49**: 500–505.

53) Azumi N, Traweek ST, Battifora H. Prostatic acid phosphatase in carcinoid tumors. Immunohistochemical and immunoblot studies. *Am J Surg Pathol.* 1991; **15**: 785–790.

54) Ruck P, Horny HP, Kaiserling E. Immunoreactivity of human tissue mast cells: nonspecific binding of primary antibodies against regulatory peptides by ionic linkage. *J Histochem Cytochem.* 1990; **38**: 859–867.

55) Grube D. Immunoreactivities of gastrin (G-) cells. II. Non-specific binding of immunoglobulins to G-cells by ionic interactions. *Histochemistry*. 1980; **66**: 149–167.

56) Omata M, Liew C-T, Ashcavai M, Peters RL. Nonimmunologic binding of horseradish peroxidase to hepatitis B surface antigen: a possible source of error in immunohistochemistry. *Am J Clin Pathol.* 1980; **73**: 626–632.

57) Buchwalow I, Samoilova V, Boecker W, Tiemann M. Non-specific binding of antibodies in immunohistochemistry: fallacies and facts. *Sci Rep.* 2011; **1**: 28. doi:10.1038/srep00028

58) Kamoshida S, Tsutsumi Y. Expression of MUC-1 glycoprotein in plasma cells, follicular dendritic cells, myofibroblasts and perineurial cells: immunohistochemical analysis using three monoclonal antibodies. *Pathol Int.* 1998; **48**: 776–785.

59) Setiadi AF, Sheikine Y. CD138-negative plasma cell myeloma: a diagnostic challenge and unique entity. *BMJ Case Reports CP*. 2019; **12**: e232233.

60) Tsutsumi Y. How to evaluate laboratory data? I. *Medicina* 1989; **26**: 692–693 (*in Japanese*).

61) Tsutsumi Y. Cytological diagnosis of infectious diseases: identification of pathogens and recognition of cellular reactions. 2021, IntechOpen: Innate Immunity in Health and Disease, Open access peer-reviewed chapter (60 pages). doi: 10.5772/intechopen.95578

62) Hinton JP, Dvorak K, Robert E. A method to reuse archived H&E stained histology slides for a multiplex protein biomarker analysis. *Methods Protoc.* 2019; **2**: 86. doi:10.3390/mps2040086.

63) Marshall AE, Cramer HM, Wu HH. The usefulness of the cell transfer technique for immunocytochemistry of fine-needle aspirates. *Cancer Cytopathol.* 2014; **122**: 898–902.

64) Itoh H, Miyajima Y, Osamura RY, Tsutsumi Y. A study of quick “cell transfer” technique. *J Jpn Soc Clin Cytol.* 2002; **41**: 302–303 (*in Japanese with English abstract*).

65) Matsui T, Onouchi T, Shiogama K, *et al*. Coated glass slides TACAS are applicable to heat-assisted immunostaining and *in situ* hybridization at the electron microscopy level. *Acta Histochem Cytochem.* 2015; **48**: 153–157.

66) Tsutsumi Y. Low-specificity and high-sensitivity immunostaining for demonstrating pathogens in formalin-fixed, paraffin-embedded sections. 2019, IntechOpen Open access peer-reviewed chapter (46 pages). doi: 10.5772/intechopen.85055

67) Tsutsumi Y. Pathology of gangrene. 2020; IntechOpen access peer-reviewed chapter (52 pages). doi: 10.5772/intechopen.93505

68) Tsutsumi Y. Histopathological diagnosis of infectious diseases using patients' sera. *Semin Diagn Pathol*. 2007; **24**: 243–252.

69) Tsutsumi Y. Histopathological diagnosis of protozoan infection using patients' sera. *In*: Ishikura H (ed), *Host Response to International Parasitic Zoonoses*. Springer-Verlag, Tokyo, 1998; pp. 69–81. ISBN: 978-4-431-68281-3.

70) Tsutsumi Y, Hara M. Application of parietal cell autoantibody to histopathological studies. *Acta Pathol Jpn.* 1985; **35**: 823–829.

71) Folli F, Solimena M, Cofiell R, *et al*. Autoantibodies to a 128-kd synaptic protein in three women with the stiff-man syndrome and breast cancer. *N Engl J Med.* 1993; **328**: 546-551.

72) Shojima Y, Nishioka K, Watanabe M, *et al*. Clinical characterization of definite autoimmune limbic encephalitis: a 30-case series. *Int Med.* 2019; **58**: 3369–3378.

Figure Legends

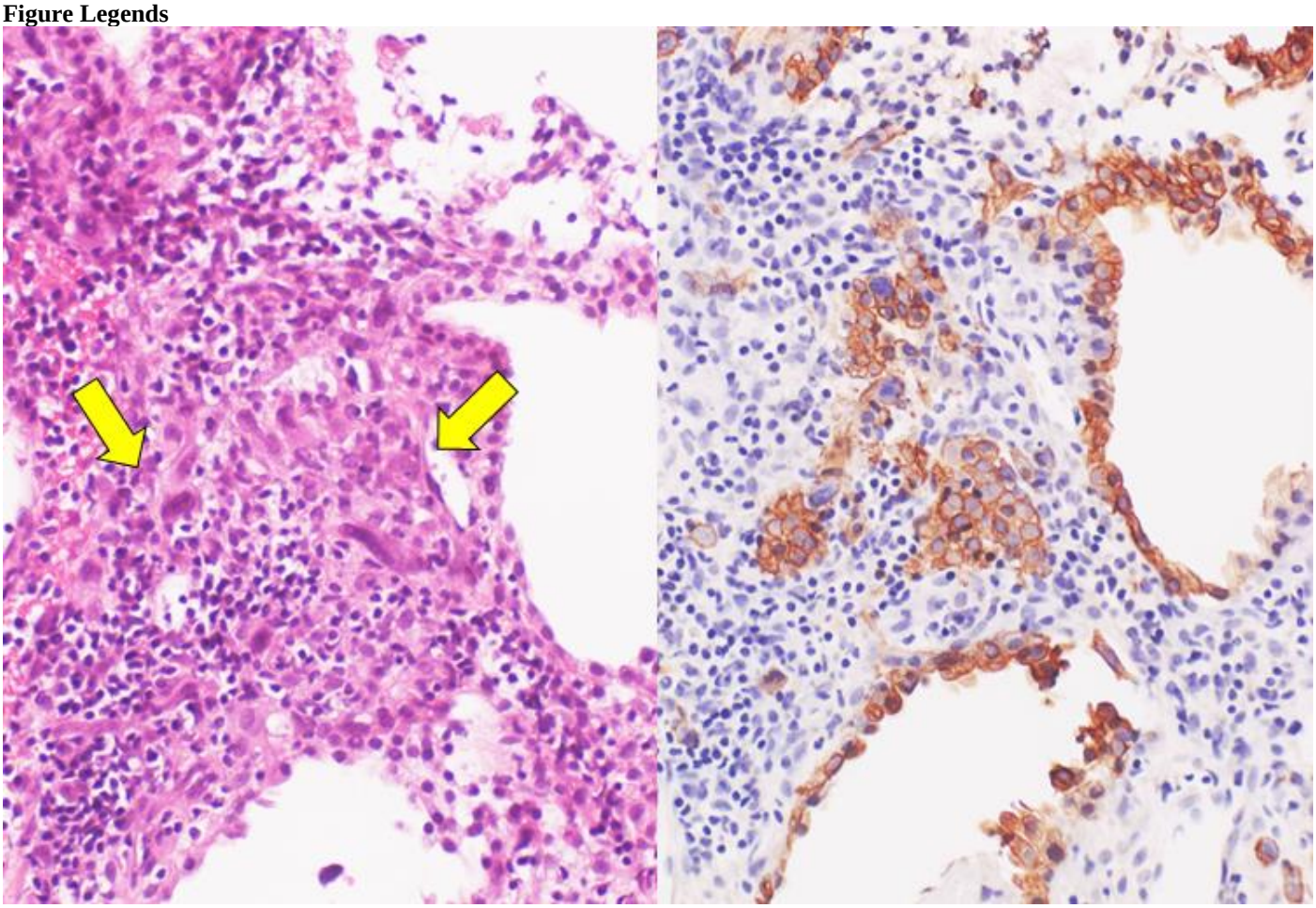

Figure 1. Cytokeratin for identifying intermediate trophoblasts in the placenta. **Left**: H&E, **Right**: cytokeratin immunostaining. Intermediate trophoblasts are observed in the stroma of the placental tissue sampled by curettage. Cytokeratin immunoreactivity with a monoclonal antibody CAM5.2 clearly illustrates their distribution (arrows).

Preprints (www.preprints.org) | NOT PEER-REVIEWED | Posted: 28 April 2021 doi:10.20944/preprints202104.0750.v1

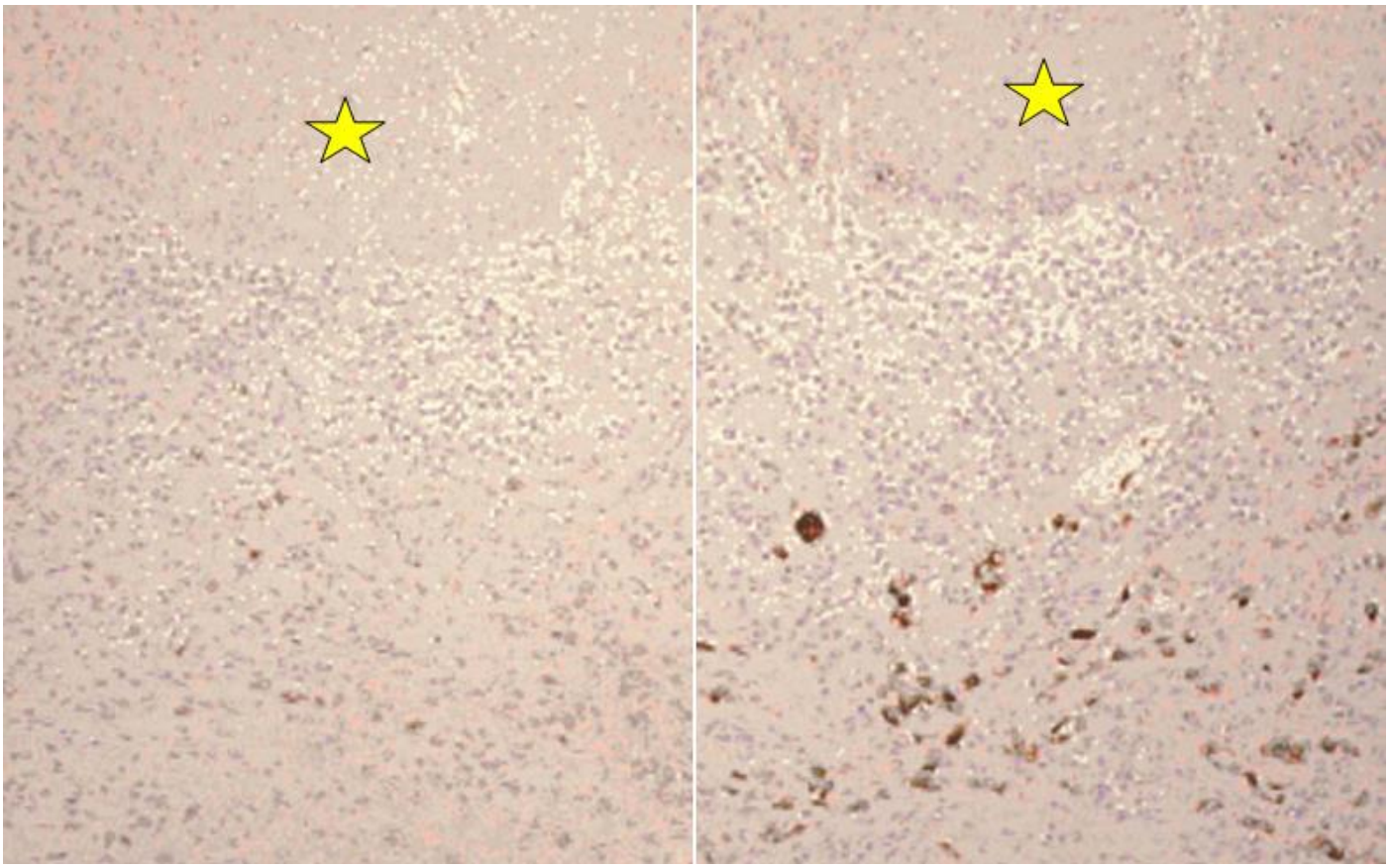

Figure 2. p53 immunostaining without HIER in esophageal squamous cell carcinoma. **Left**: polymer method (EnVision), **Right**: CSA. Submucosally invading cancer cells express p53 in the nuclei. The immunoreactivity is significantly enhanced by the CSA method. Asterisks indicate non-cancerous esophageal squamous mucosa.

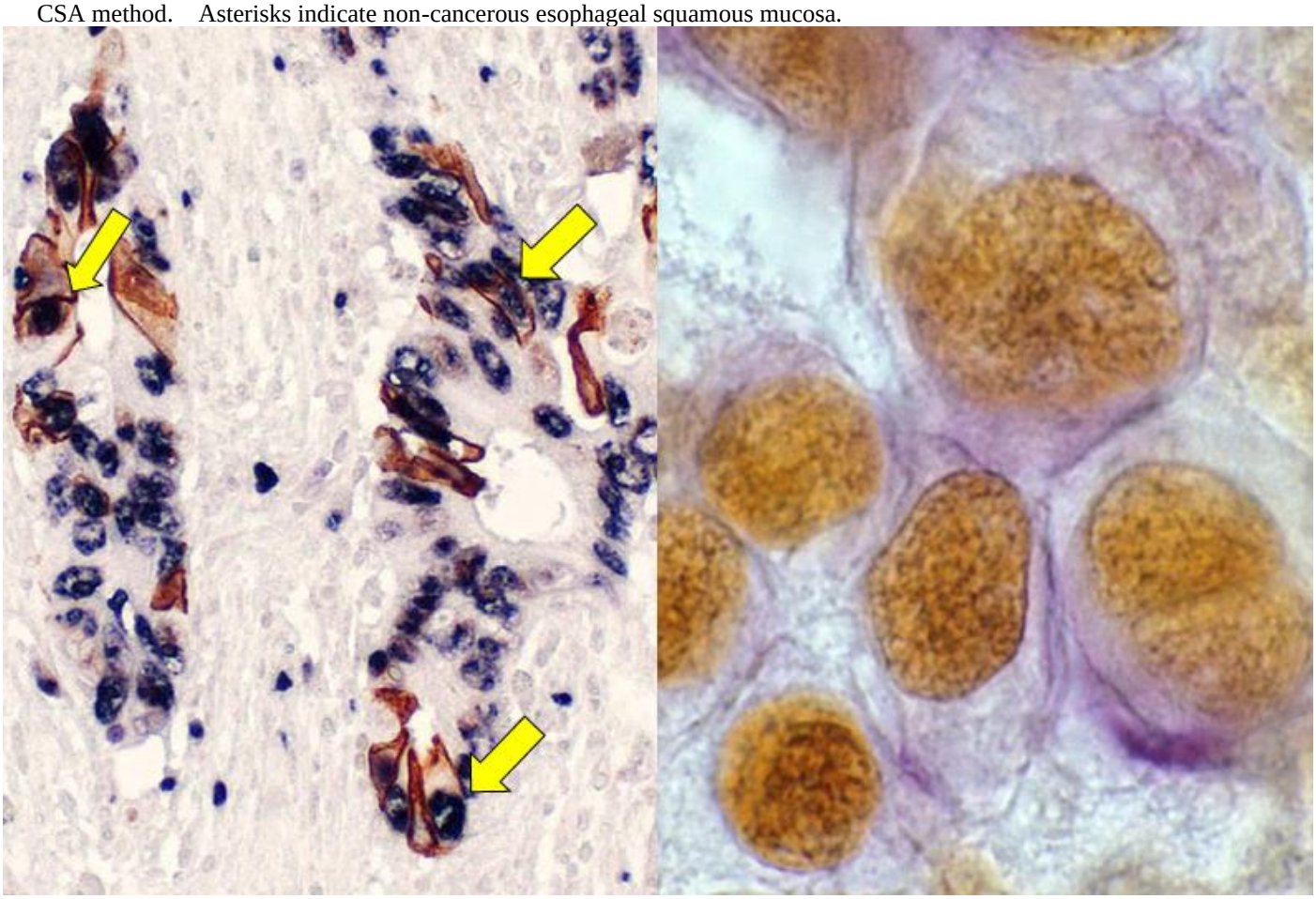

Preprints (www.preprints.org) | NOT PEER-REVIEWED | Posted: 28 April 2021 doi:10.20944/preprints202104.0750.v1

Figure 3. Double immunostaining. **Left**: Ki-67 (proliferative cells in blue) and cleaved cytokeratin 18 (apoptotic columnar cells in brown) in FFPE colonic adenocarcinoma after neoadjuvant chemotherapy. In colon cancer, some proliferative cells are apoptotic, as arrows indicate. Cleaved cytokeratin 18 functions as an excellent marker for apoptotic columnar cells. **Right**: HER2 in blue and p53 in brown in an ethanol-fixed aspiration cytology specimen of breast cancer. In the high-grade breast cancer, the atypical ductal cells express both HER2 and p53.

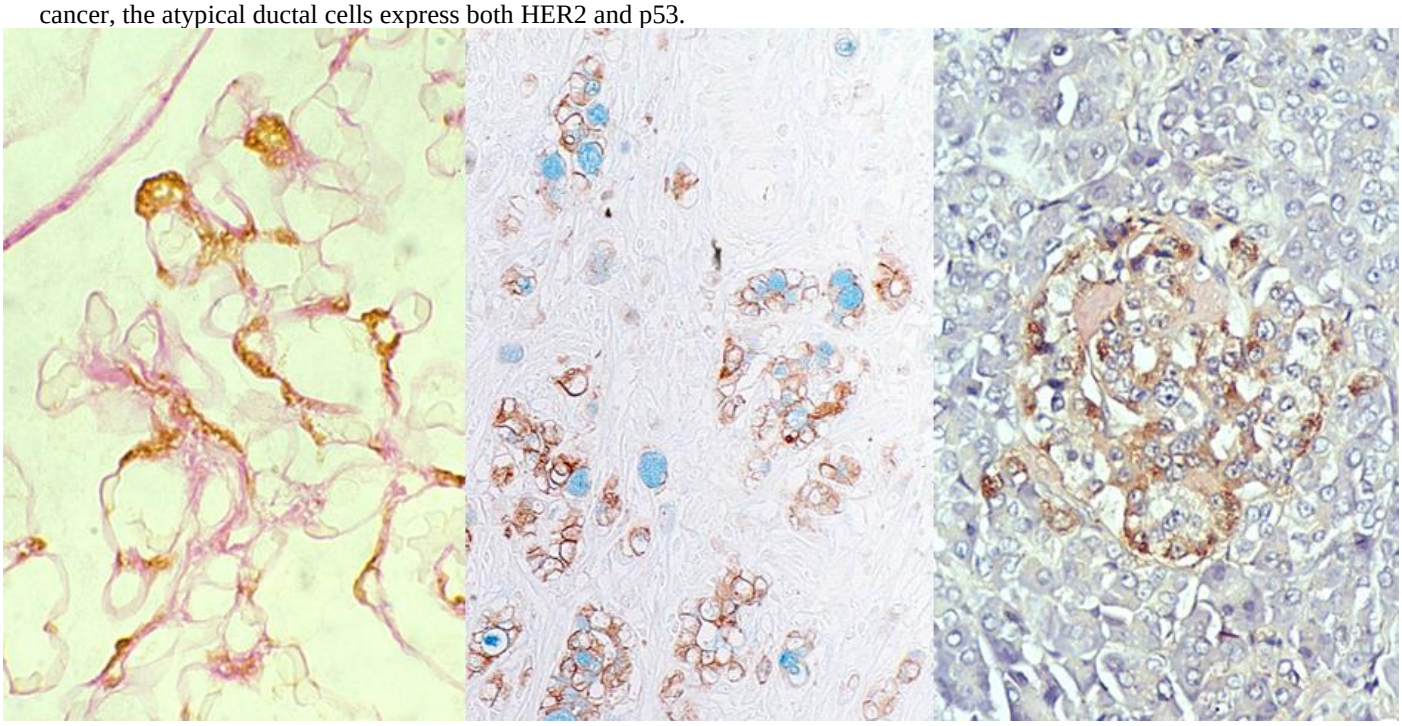

Figure 4. Double labeling of immuno- and conventional staining. **Left**: IgA and PAS in renal biopsy of IgA nephropathy. The PAS-reactive basement membrane surrounds mesangial deposition of IgA seen after prolonged trypsin digestion. **Center**: CEA and alcian blue in gastric signet ring cell carcinoma. CEA expression of mucin-containing cancer cells appears weaker. **Right**: insulin and Congo red in a pancreatic islet in type 2 diabetes mellitus. Orange-colored amyloid deposition is seen among the insulin-positive β-cells.

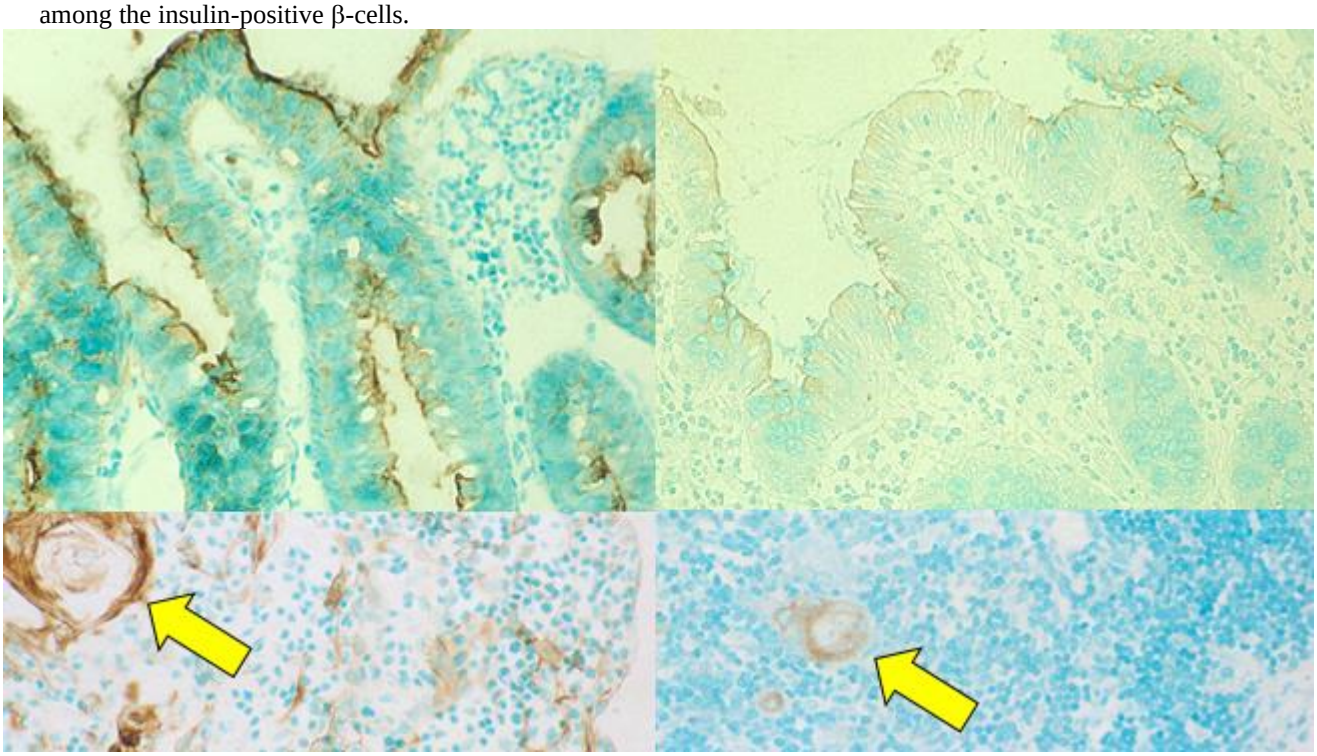

Figure 5. Antigenic deterioration in FFPE sections. **Left**: FFPE sections, **Right**: paraformaldehyde-fixed frozen sections. **Top panels**: CEA in normal gastric mucosa, **Bottom panels**: Cytokeratin in normal infantile thymus. Antigenicities of CEA and cytokeratin detected by polyclonal antibodies are evidently weakened after FFPE. Arrows indicate Hassall's corpuscles in the thymic medulla.

Preprints (www.preprints.org) | NOT PEER-REVIEWED | Posted: 28 April 2021 doi:10.20944/preprints202104.0750.v1

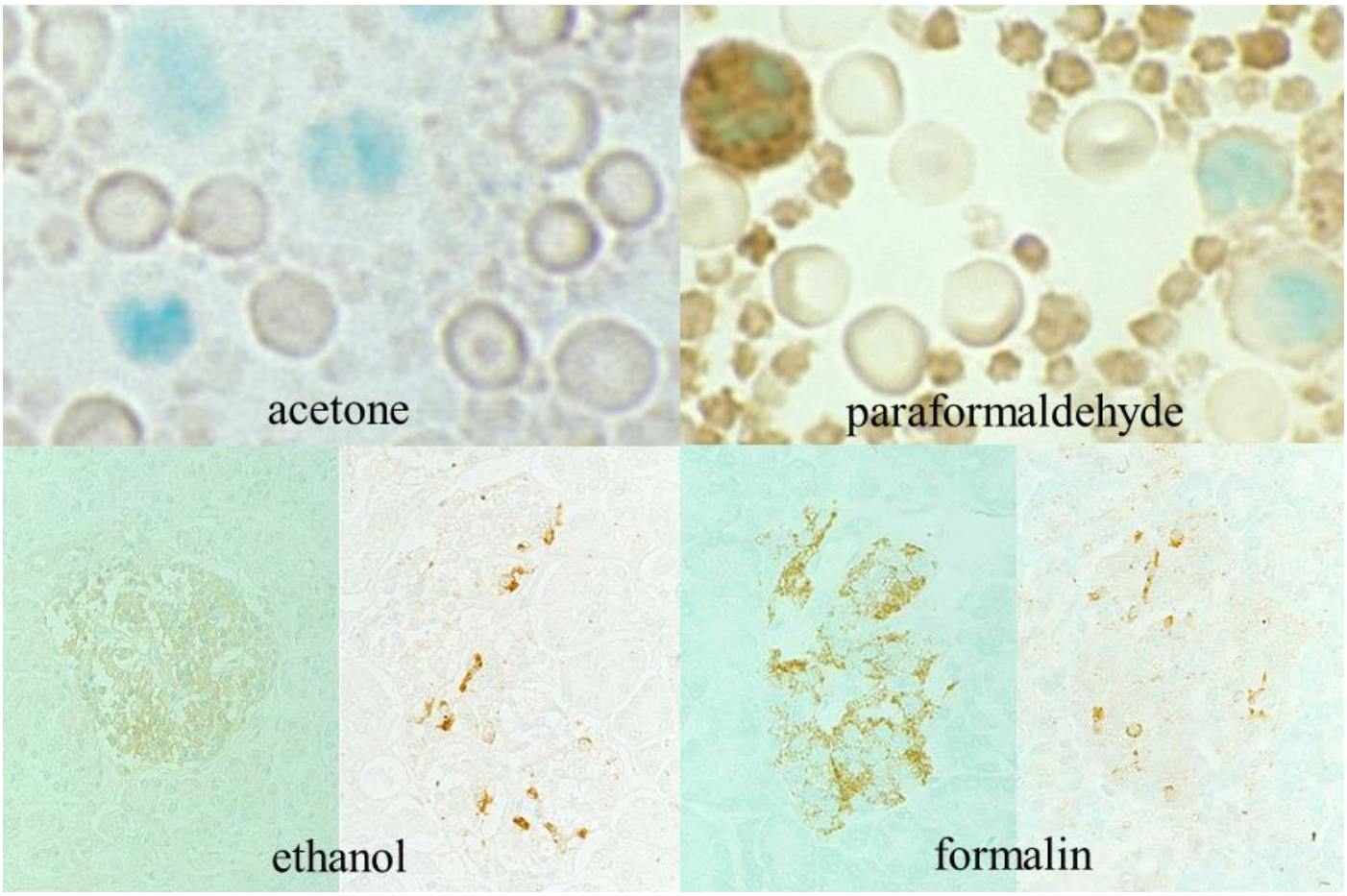

Figure 6. Antigenic loss by fixation in organic solvent. **Left**: Fixation in acetone or ethanol. **Right**: Fixation in 4% paraformaldehyde or in formalin. **Top panels**: Immunostaining for platelet factor 4 in a smeared buffy coat of the peripheral blood. **Bottom panels**: Immunostaining for insulin (left-sided) and somatostatin (right-sided) in paraffin-embedded pancreas. Platelet factor 4 and insulin show false negative findings when fixed in the organic solvent. Somatostatin is resistant to ethanol fixation to be immunolocalized.

Preprints (www.preprints.org) | NOT PEER-REVIEWED | Posted: 28 April 2021 doi:10.20944/preprints202104.0750.v1

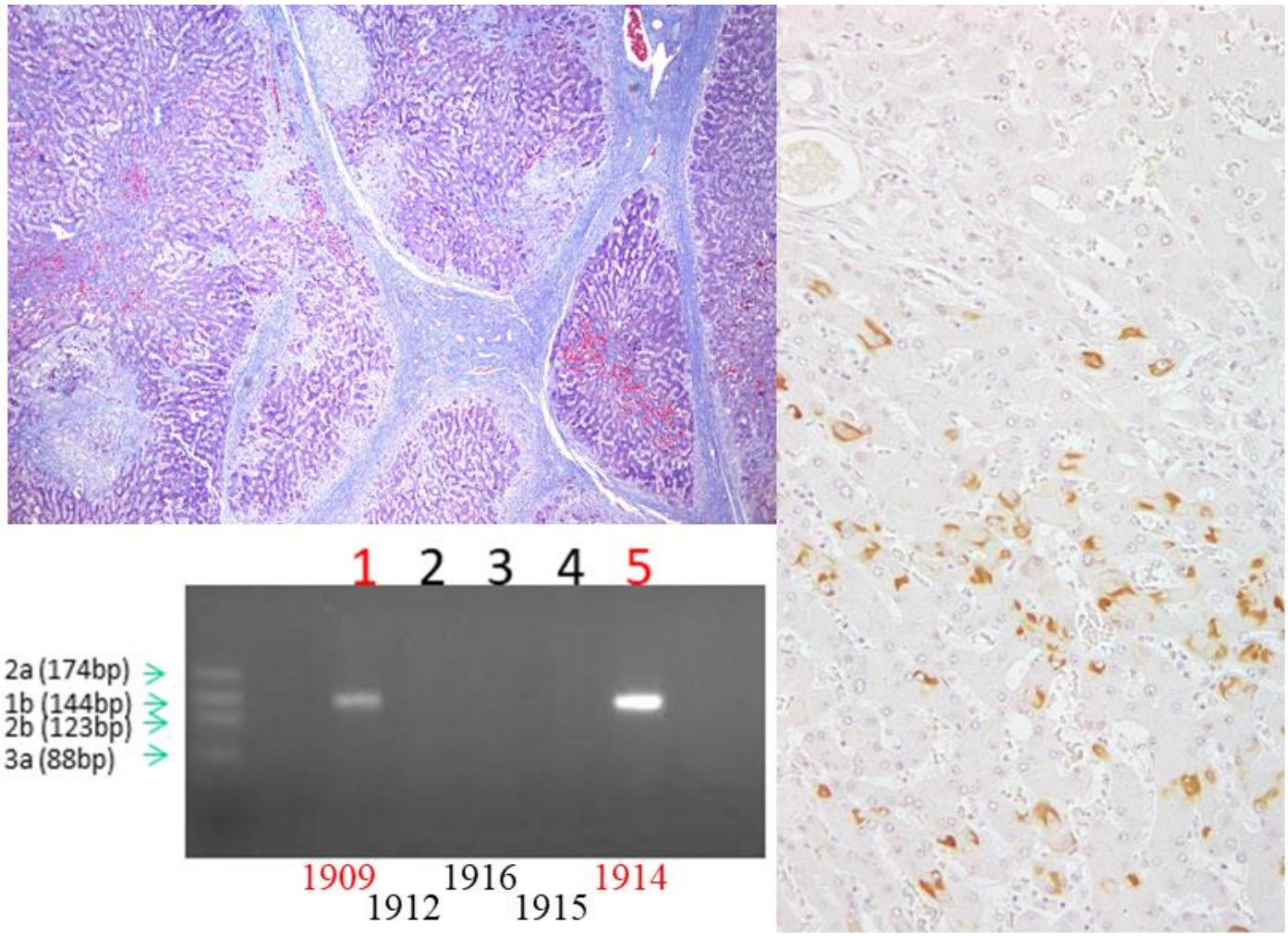

Figure 7. Demonstration of HBs antigen and HCV genome in archival specimens of liver cirrhosis fixed for up to 110 years. **Left top**: Azan stain, **Left bottom**: Nested reverse transcription-PCR for detecting the C-region of the HCV genome, **Right**; Immunostaining for HBs antigen. HCV-RNA subtype 1b was detected with nested RT-PCR (lane 1), and the same cirrhotic specimen in 1909 was immunoreactive for HBs antigen. Double infection of HBV and HCV was proven. Another specimen in 1914 (lane 5) was also double-positive for HCV, 1b-type and HBs antigen.

Preprints (www.preprints.org) | NOT PEER-REVIEWED | Posted: 28 April 2021 doi:10.20944/preprints202104.0750.v1

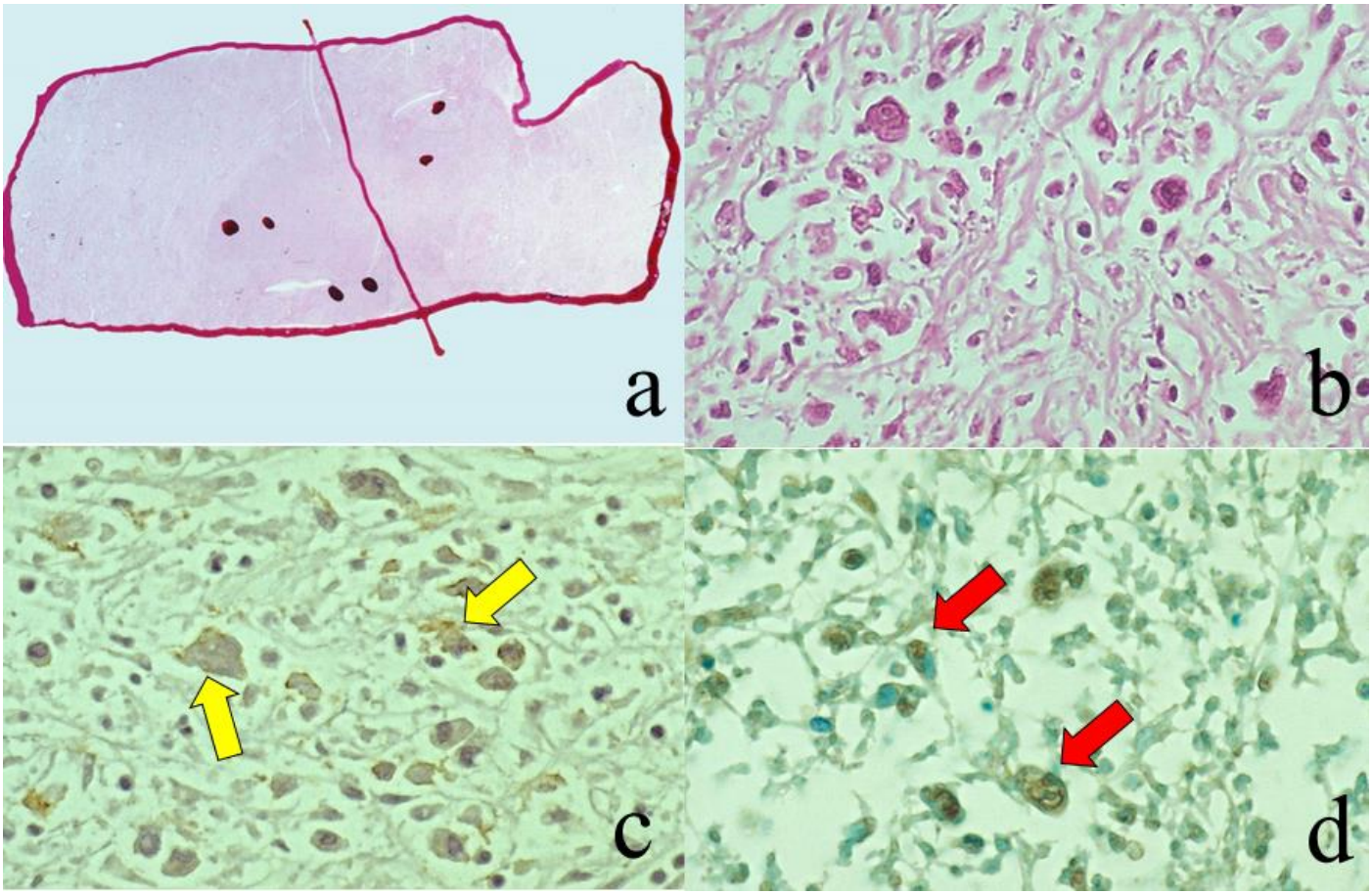

Figure 8. Demonstration of CD15 and EBER in Hodgkin's lymphoma in a male patient aged 50's, autopsied by Dr. Thomas Hodgkin himself 170 years before. **Top panels**: H&E. Only one unstained slide of the liver available was stained with H&E. After photographing, the section was transferred to two silane-coated glass slides (a). Infiltration of Hodgkin's cells is microscopically recognized (b). **Bottom panels**: Immunostaining for CD15 (c) and *in situ* hybridization for EBER (d) gave positive signals on the plasma membrane and in the nucleus, respectively, as indicated by yellow and red arrows.

Preprints (www.preprints.org) | NOT PEER-REVIEWED | Posted: 28 April 2021 doi:10.20944/preprints202104.0750.v1

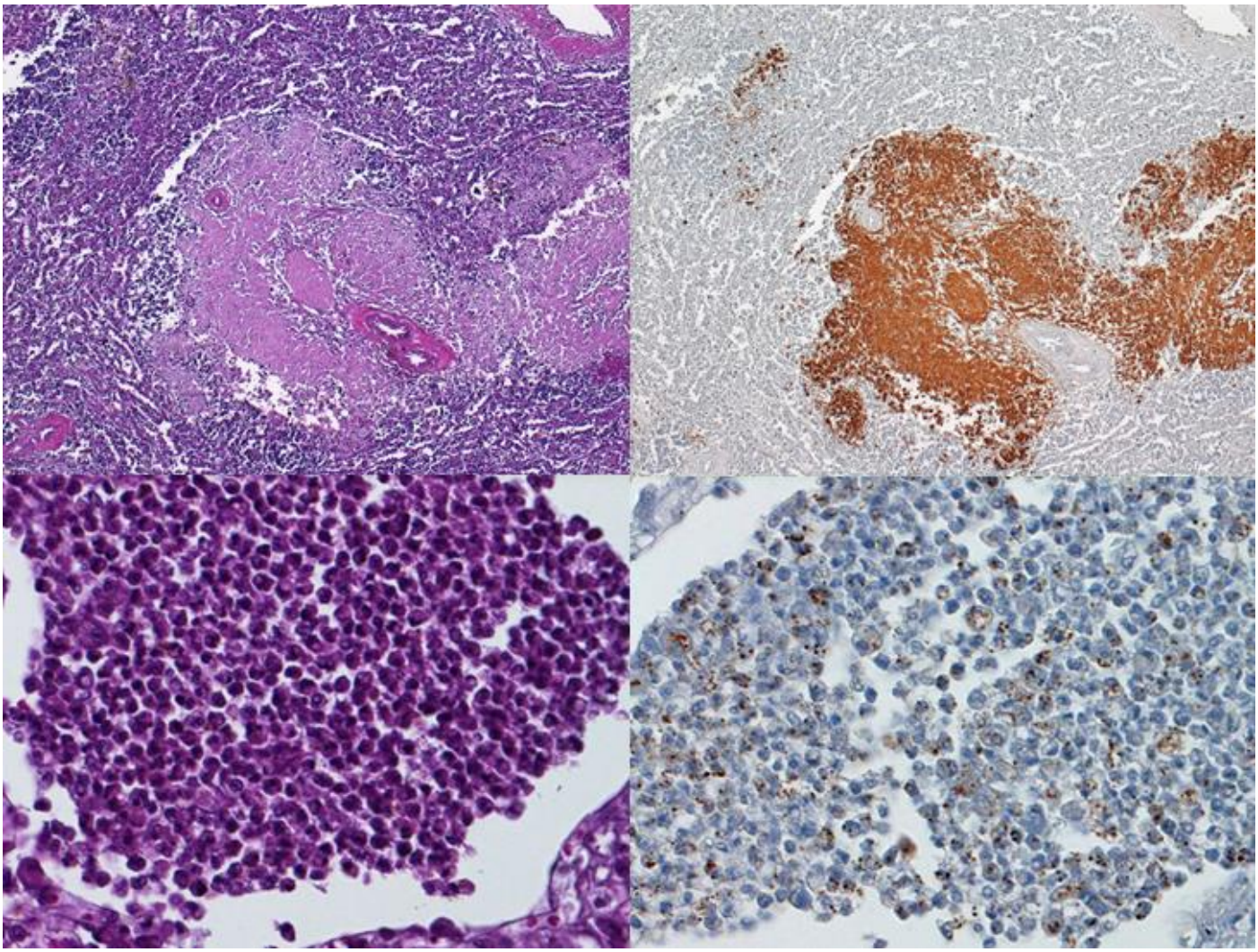

Figure 9. Demonstration of amyloid A in secondary amyloidosis and pneumococcal antigens in lobar pneumonia in archival material. **Left**: H&E, **Right**: immunostaining. **Top panels**: the splenic white pulp with amyloid A deposition, **Bottom panels**: pneumococcal antigens in lobar pneumonia. The specimens were fixed in formalin for 70 years. Deposition of amyloid A protein is evident in the splenic white pulp (no pretreatment needed). Pneumococci phagocytized by neutrophils are visualized immunohistochemically after HIER.

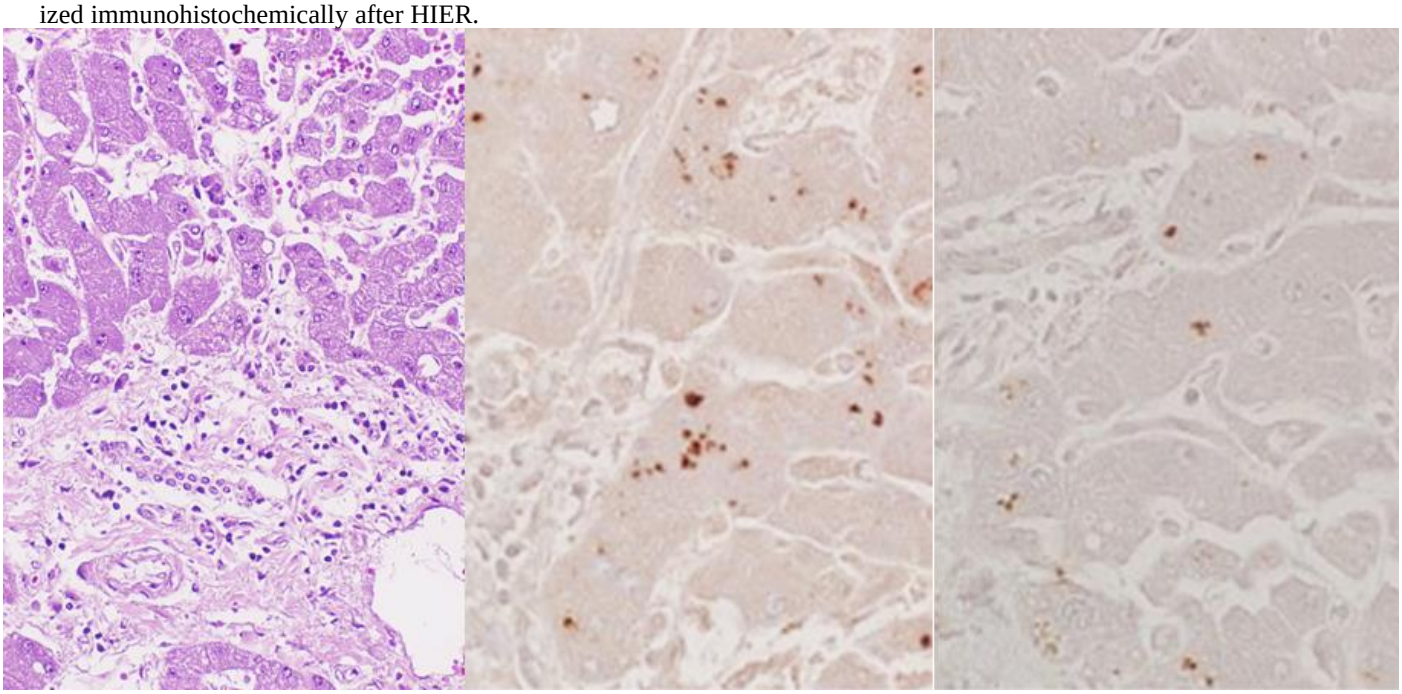

Preprints (www.preprints.org) | NOT PEER-REVIEWED | Posted: 28 April 2021 doi:10.20944/preprints202104.0750.v1

Figure 10. Demonstration of HCV antigens in an archival liver specimen of chronic hepatitis after HIER. **Left**: H&E, **Center**: monoclonal antibody against the NS3 region of HCV, **Right**: monoclonal antibody against the E1). Dot-like immunoreactivity of HCV antigens is seen in the cytoplasm of hepatocytes. The specimen was kept in formalin for 40 years.

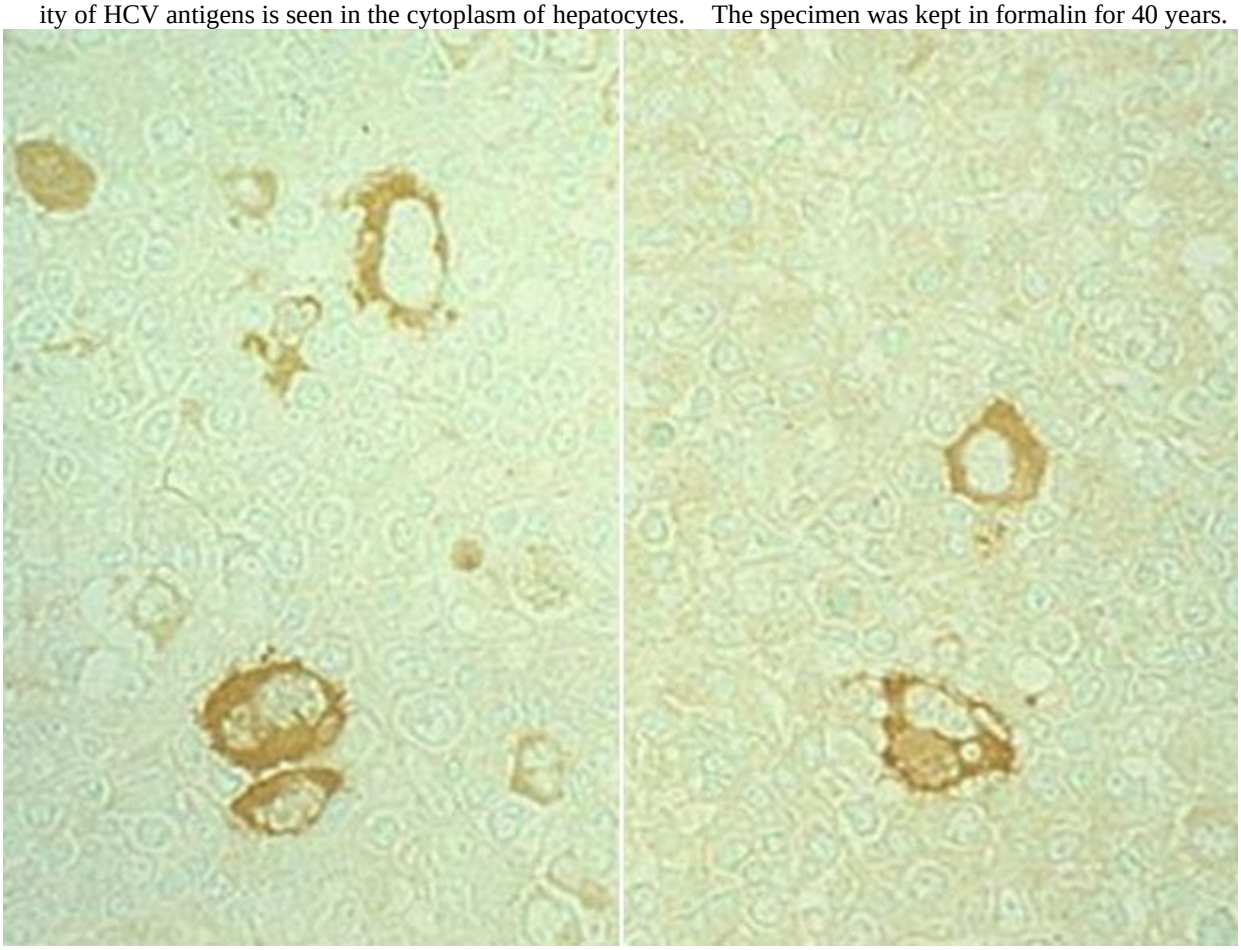

Figure 11. Diffusion artifact (I). Hodgkin's lymphoma. The cytoplasm of Hodgkin's cells is polyclonally positive for both kappa (**left**) and lambda (**right**) chains. The nuclei are negative. This represents an example of diffusion artifact in FFPE preparations.

Preprints (www.preprints.org) | NOT PEER-REVIEWED | Posted: 28 April 2021 doi:10.20944/preprints202104.0750.v1

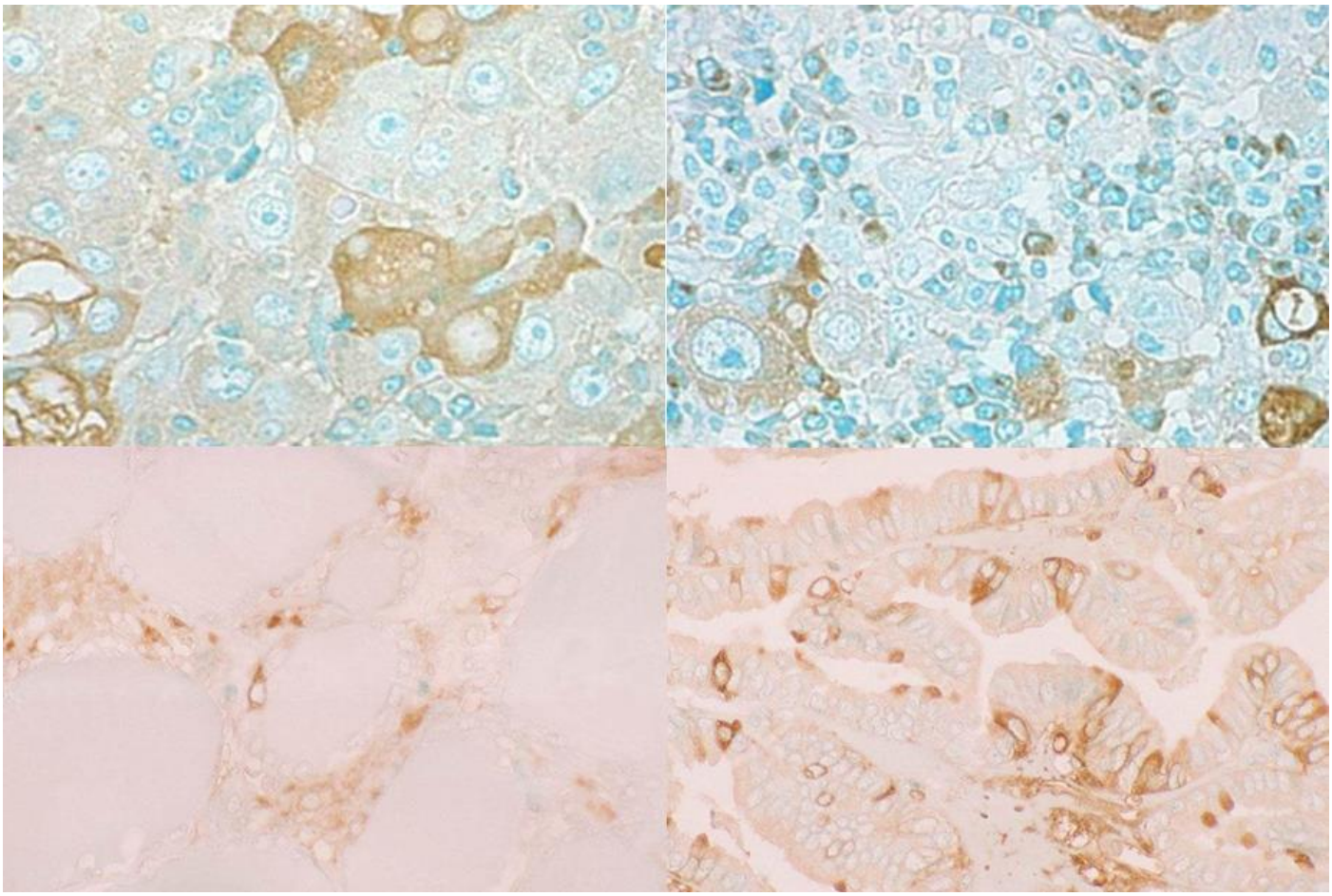

Figure 12. Diffusion artifact (II). **Top panels**: Albumin (**left**) and IgG (**right**) immunoreactivity in hepatocellular carcinoma metastatic to the hepatohilar lymph node. **Bottom panels**: IgA immunostaining in normal (**left**) and neoplastic (**right**) thyroid. Hepatocellular carcinoma cells, normal thyroid follicular cells and papillary thyroid carcinoma cells reveal diffuse cytoplasmic staining for the plasma proteins (albumin, IgG and IgA). The nuclei remain negative. The Golgi area of plasma cells is immunoreactive for IgG in the top right panel.

Preprints (www.preprints.org) | NOT PEER-REVIEWED | Posted: 28 April 2021 doi:10.20944/preprints202104.0750.v1

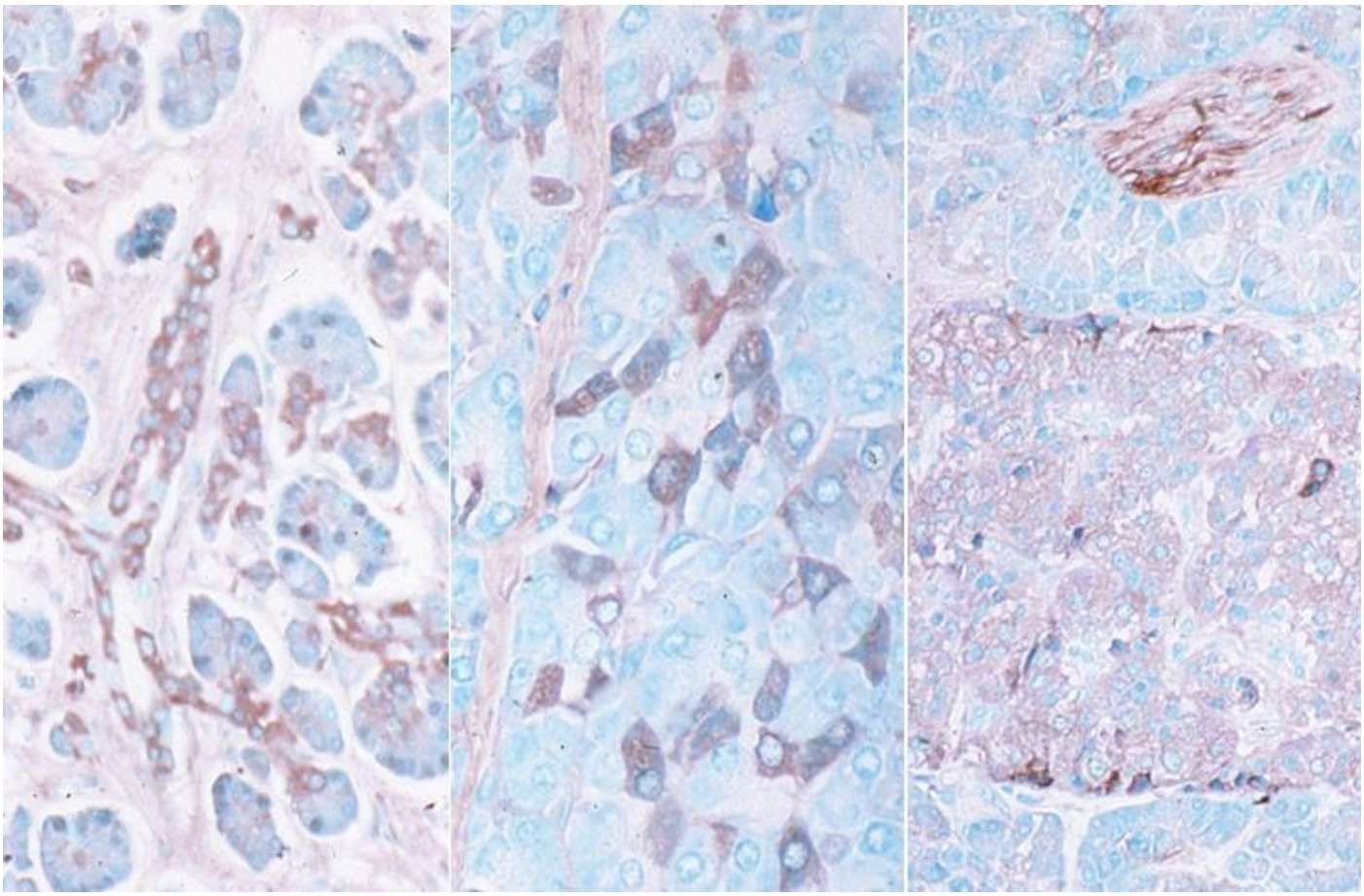

Figure 13. Diffusion artifact (III). Albumin immunoreactivity in FFPE autopsied pancreas. Ductular cells (**left**), acinar cells (**center**) and islet cells and peripheral nerve (**right**) show diffuse cytoplasmic staining. The signals are randomly seen in different cells in different parts of the pancreas.

Preprints (www.preprints.org) | NOT PEER-REVIEWED | Posted: 28 April 2021 doi:10.20944/preprints202104.0750.v1

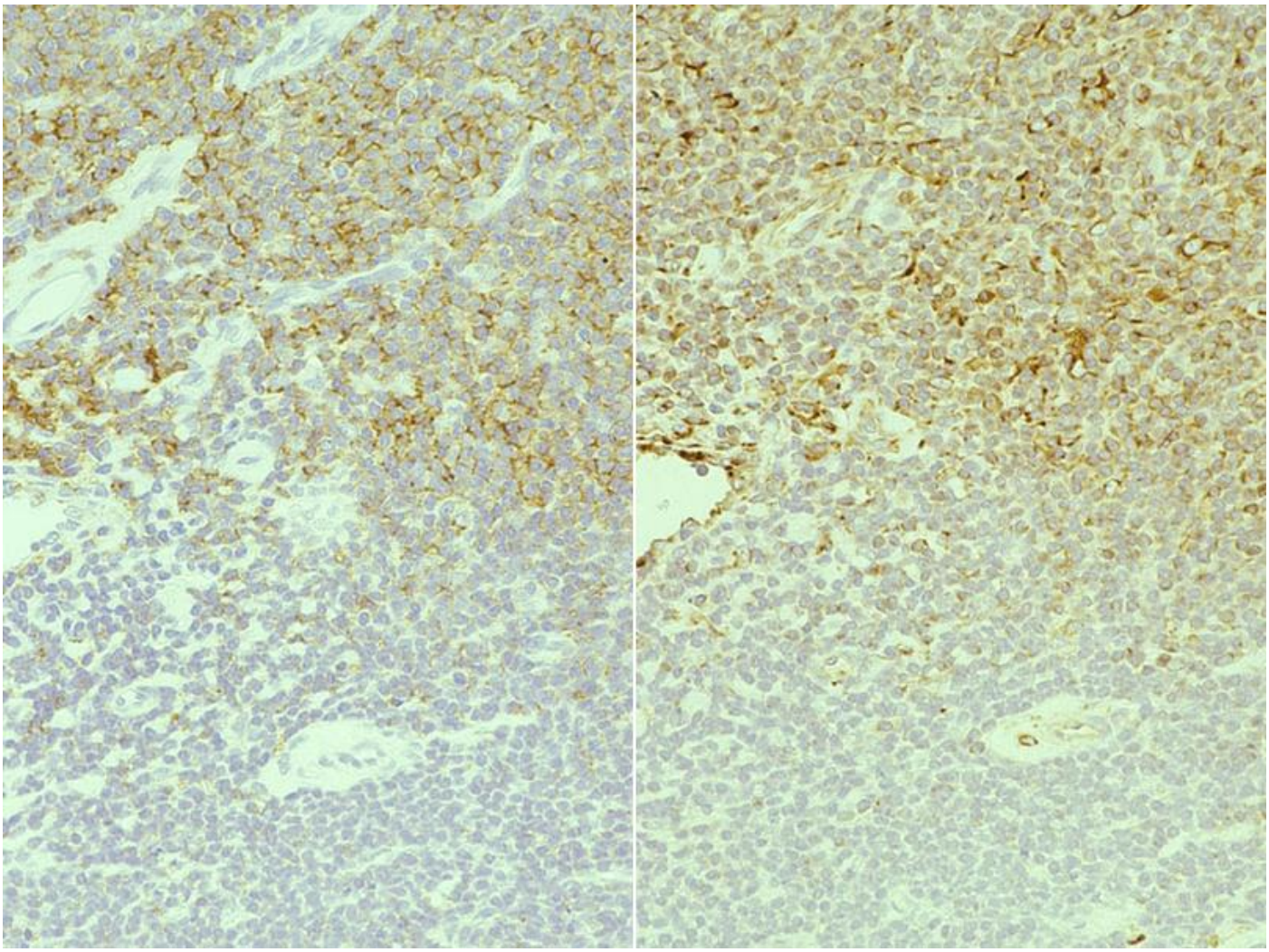

Figure 14. Vimentin internal control. Diffuse large B-cell lymphoma. **Left**: vimentin, **Right**: CD20. The poorly fixed central part is false-negative for both vimentin and CD20. The expression of lymphocyte surface markers should be judged, based on the positivity in appropriately fixed peripheral area.

Preprints (www.preprints.org) | NOT PEER-REVIEWED | Posted: 28 April 2021 doi:10.20944/preprints202104.0750.v1

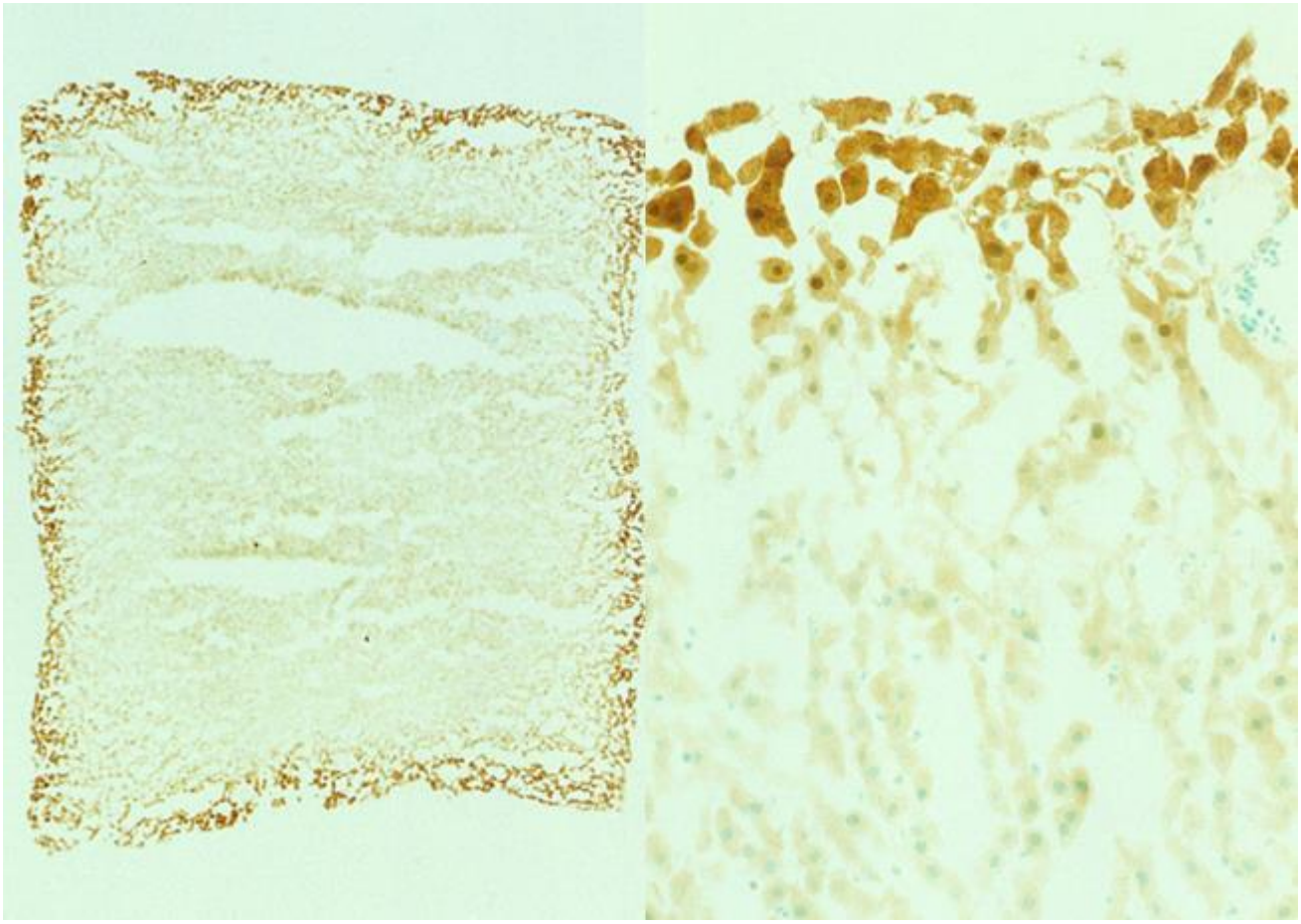

Figure 15. Glutathione peroxidase immunostaining using a frozen section prepared from 4% paraformaldehyde-fixed rat liver tissue (**left**: low power, **right**: high power). Positive immunoreactivity in the cytoplasm and nucleus of the hepatocyte is seen just at the outermost part of the section.

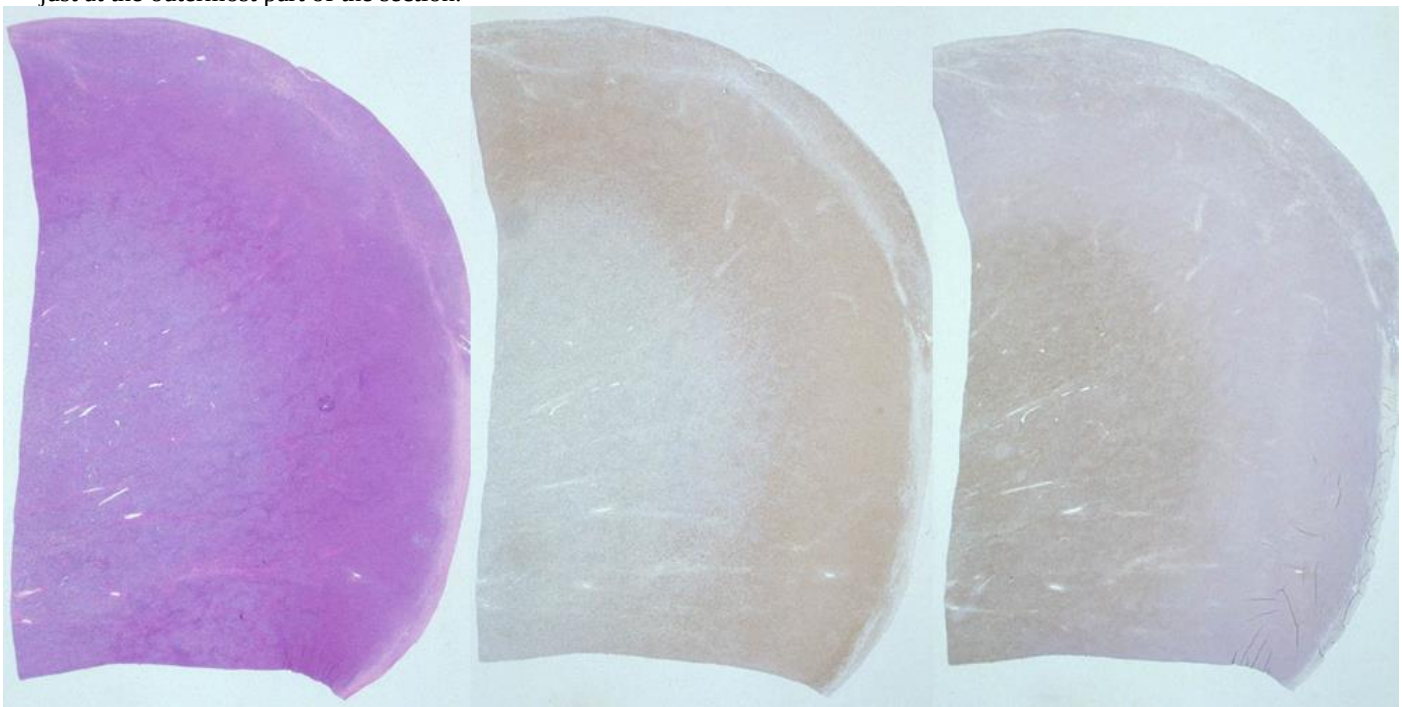

Figure 16. Paradoxical localization of CD45 and vimentin in FFPE malignant lymphoma tissue. **Left**: H&E, **Center**: vimentin, **Right**: CD45 (leukocyte common antigen: LCA). Vimentin is positive in the peripheral zone but negative in the poorly fixed central area. A reversed pattern is recognizable for CD45 localization.

Preprints (www.preprints.org) | NOT PEER-REVIEWED | Posted: 28 April 2021 doi:10.20944/preprints202104.0750.v1

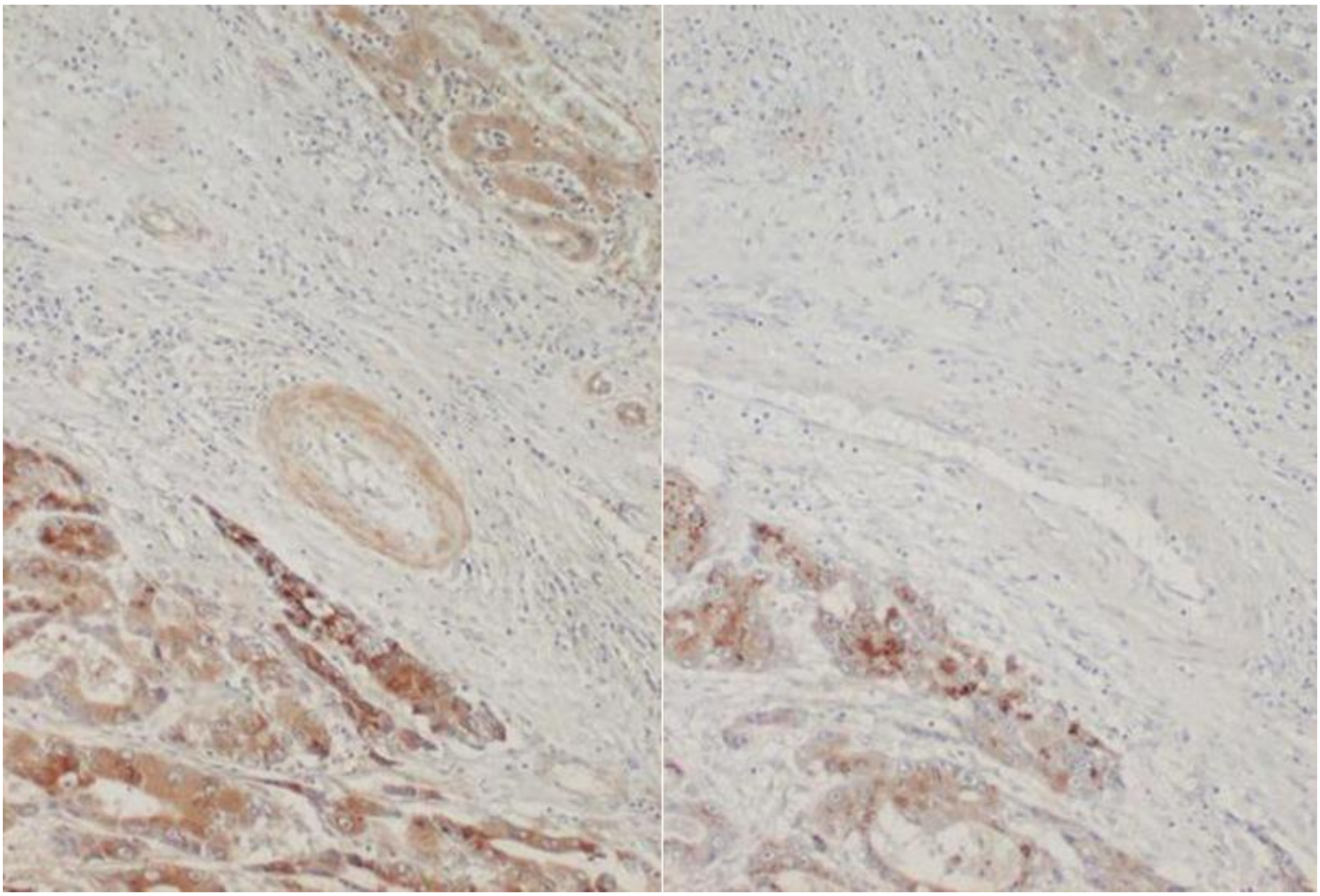

Figure 17. The need for appropriate dilution of the primary rabbit antiserum. Alpha-fetoprotein (AFP) immunostaining (using the polymer method) for hepatocellular carcinoma (**left**: 1:400 dilution, **right**: 1:3,200 dilution). With 1:400 diluted antiserum, non-neoplastic hepatocytes, bile ducts and arterial wall reveal nonspecific staining. At an appropriate dilution (1:3,200), positive signals of AFP are seen only in the hepatoma cells.

Preprints (www.preprints.org) | NOT PEER-REVIEWED | Posted: 28 April 2021 doi:10.20944/preprints202104.0750.v1

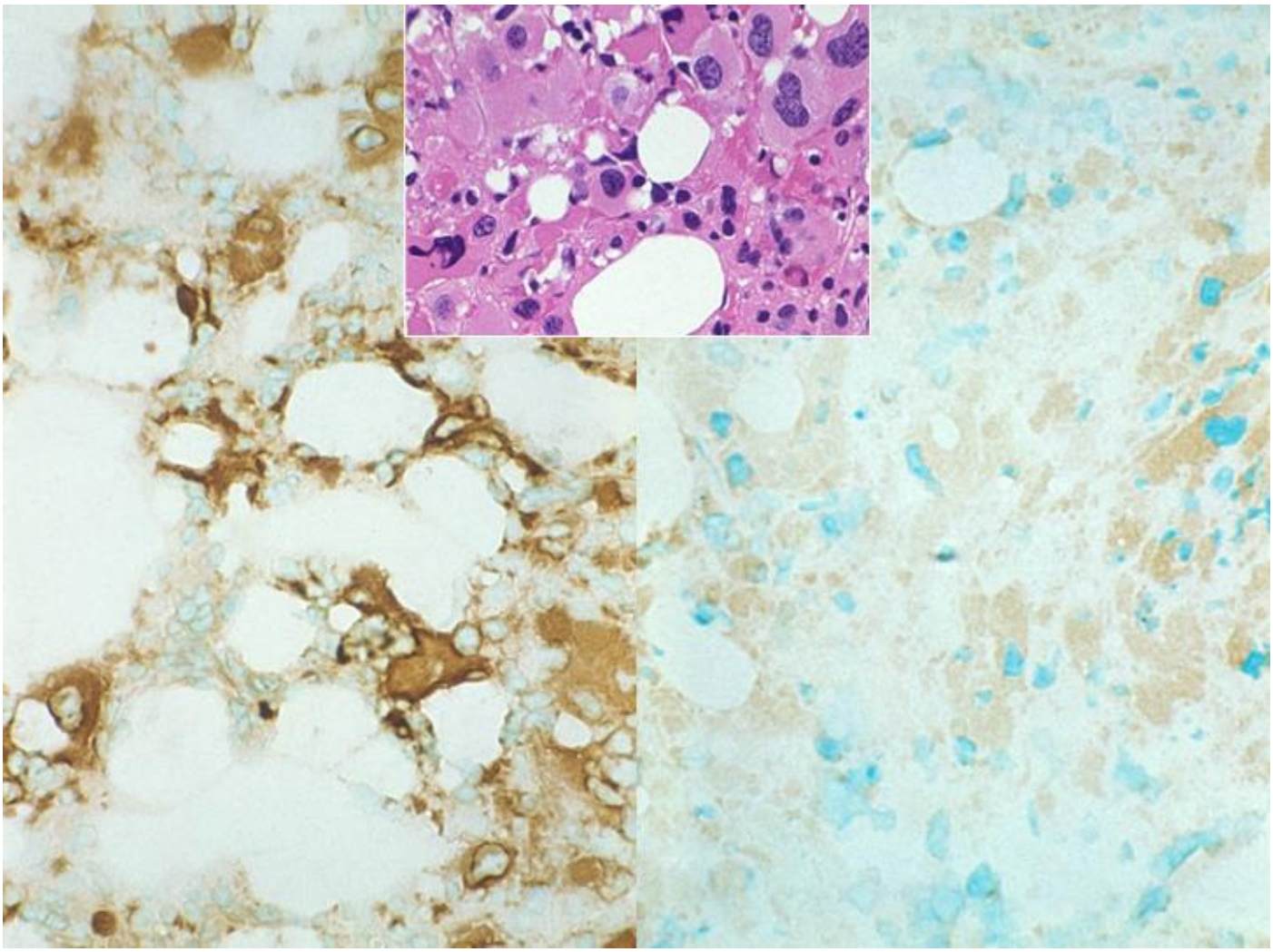

Figure 18. Antigenic loss of surface markers by the endogenous peroxidase blockage in fresh-frozen sections. Aspirated clot of essential thrombocythemia. Immunostaining for glycoprotein IIbIIIa, a megakaryocytic marker. **Left**: without endogenous peroxidase blockage, **Right**: with endogenous peroxidase blockage, **inset**: H&E. Endogenous peroxidase blockage in 0.3% hydrogen peroxide in methanol significantly hampers the immunoreactivity.

Preprints (www.preprints.org) | NOT PEER-REVIEWED | Posted: 28 April 2021 doi:10.20944/preprints202104.0750.v1

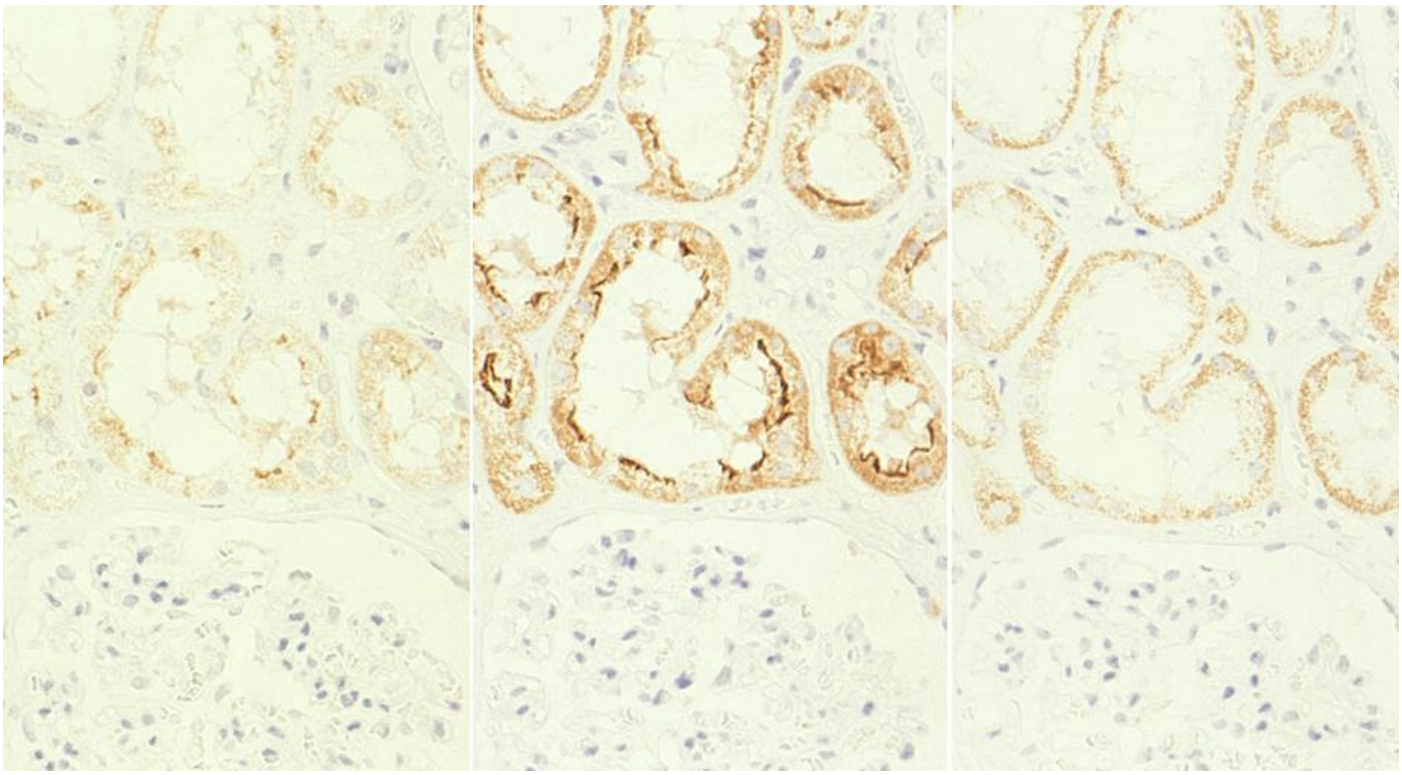

Figure 19. Retrieval of endogenous biotin activity by heating pretreatment (LSAB immunostaining for villin in the normal kidney with pressure pan heating in 10 mM citrate buffer, pH 6 (**left**), 10 mM citrate buffer, pH 7 (**center**), and 10mM citrate buffer, pH 7, without primary antibody (**right**). The brush border of proximal renal tubules is immunoreactive for villin. Hydrated heating in citrate buffer, pH 7, enhances retrieval of endogenous biotin activity, typically represented by the right panel. Coarse granular positivity is observed in the cytoplasm.

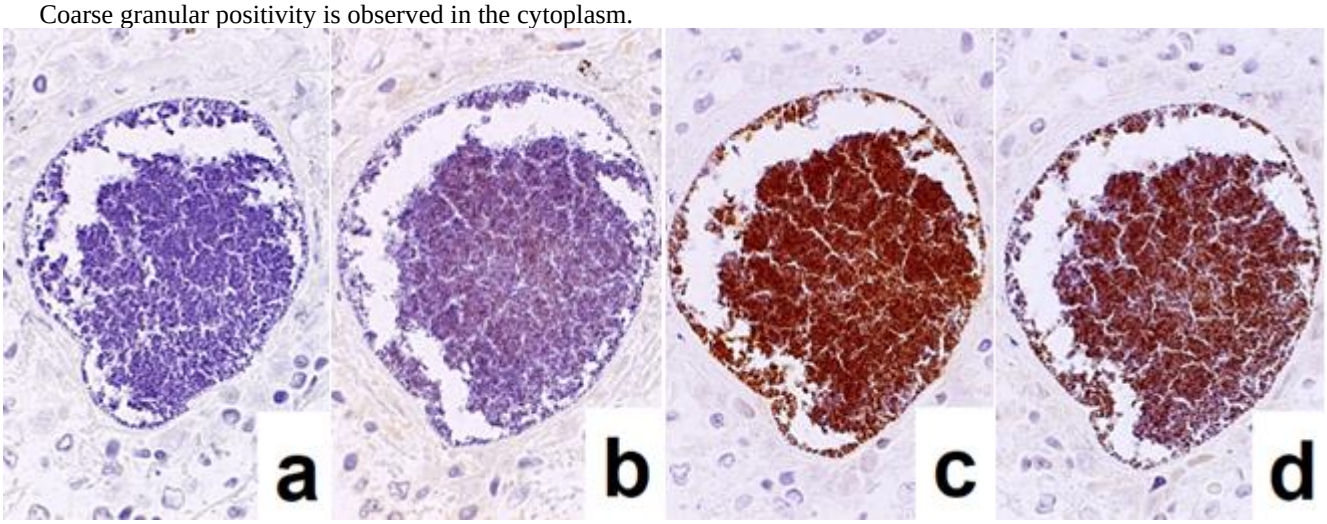

Figure 20. Retrieval of protein A activity by heating pretreatment in 1 mM EDTA, pH 8. Methicillin-resistant *Staphylococcus aureus* infection in the lung. a: without primary antibody (negative control), b: incubation with rabbit antibody, F(ab')2 fragments, against mouse immunoglobulins, c: incubation with rabbit antibody, whole IgG, against mouse immunoglobulins, d: incubation with mouse monoclonal antibody against *Pseudomonas aeruginosa* as an indifferent antibody. It is evident that the colony of *S. aureus* in the lung binds to rabbit and mouse IgG, as shown in c and d. The F(ab')2 fragments of IgG lack the binding (b), so that the nonspecific binding is caused through the Fc portion of IgG.

Preprints (www.preprints.org) | NOT PEER-REVIEWED | Posted: 28 April 2021 doi:10.20944/preprints202104.0750.v1

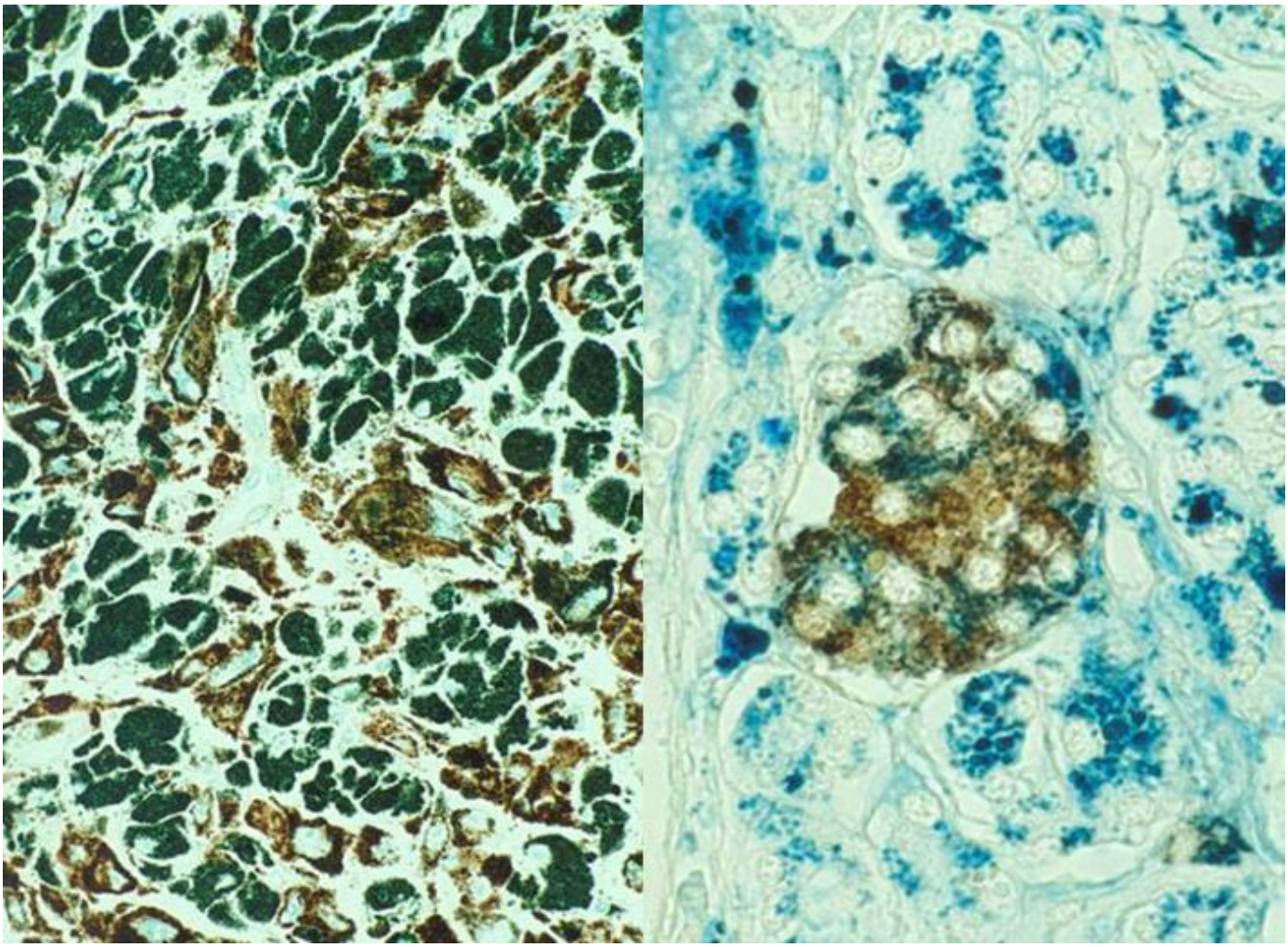

Figure 21. Metachromasia of melanin by methylgreen counterstaining in heavily pigmented nasal malignant melanoma (**left**: immunostaining for HMB45) and Berlin blue counterstaining for hemosiderin in pancreatic hemochromatosis (**right**: immunostaining for insulin). Brown-colored pigments such as melanin and hemosiderin hamper the judgment of DAB coloration. Counterstaining with methylgreen and Berlin blue is quite effective for distinguishing the DAB color from the endogenous pigments. The rich distribution of HMB45-negative melanophages is noted in the left panel. In the right panel, hemosiderin deposition is observed in insulin-positive β-cells of the pancreatic islet.

Preprints (www.preprints.org) | NOT PEER-REVIEWED | Posted: 28 April 2021 doi:10.20944/preprints202104.0750.v1

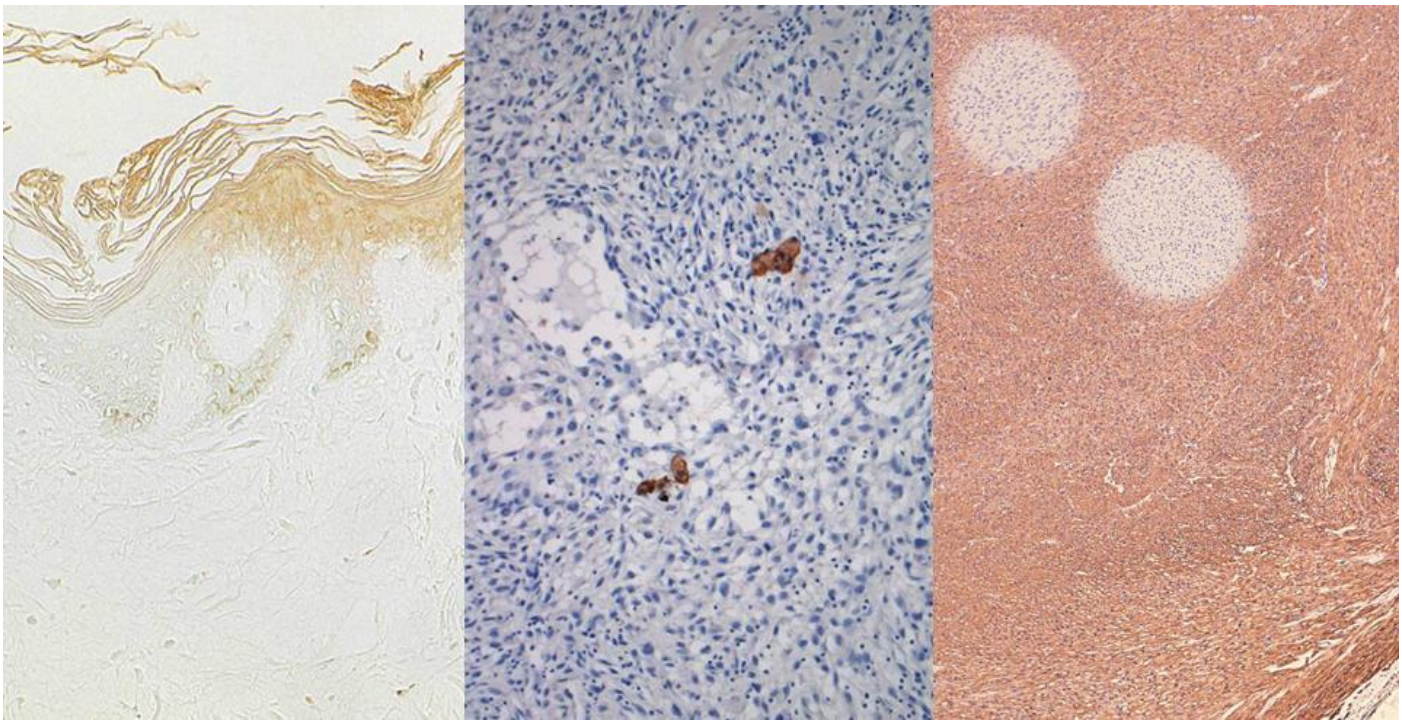

Figure 22. Technical artifacts. Effects of dewatering (**left**: surfactant apoprotein immunostaining for the skin), contamination of cytokeratin-positive squams (**center**: cytokeratin immunostaining for spindle cell sarcoma), and insufficient deparaffinization (**right**: smooth muscle actin immunostaining for leiomyosarcoma). Drying of sections during antibody incubation causes nonspecific binding in the dried area (left). Contaminated cytokeratin-positive squams on the section should be distinguished from true positivity (center). False-negative rounded areas result from insufficient deparaffinization (right).

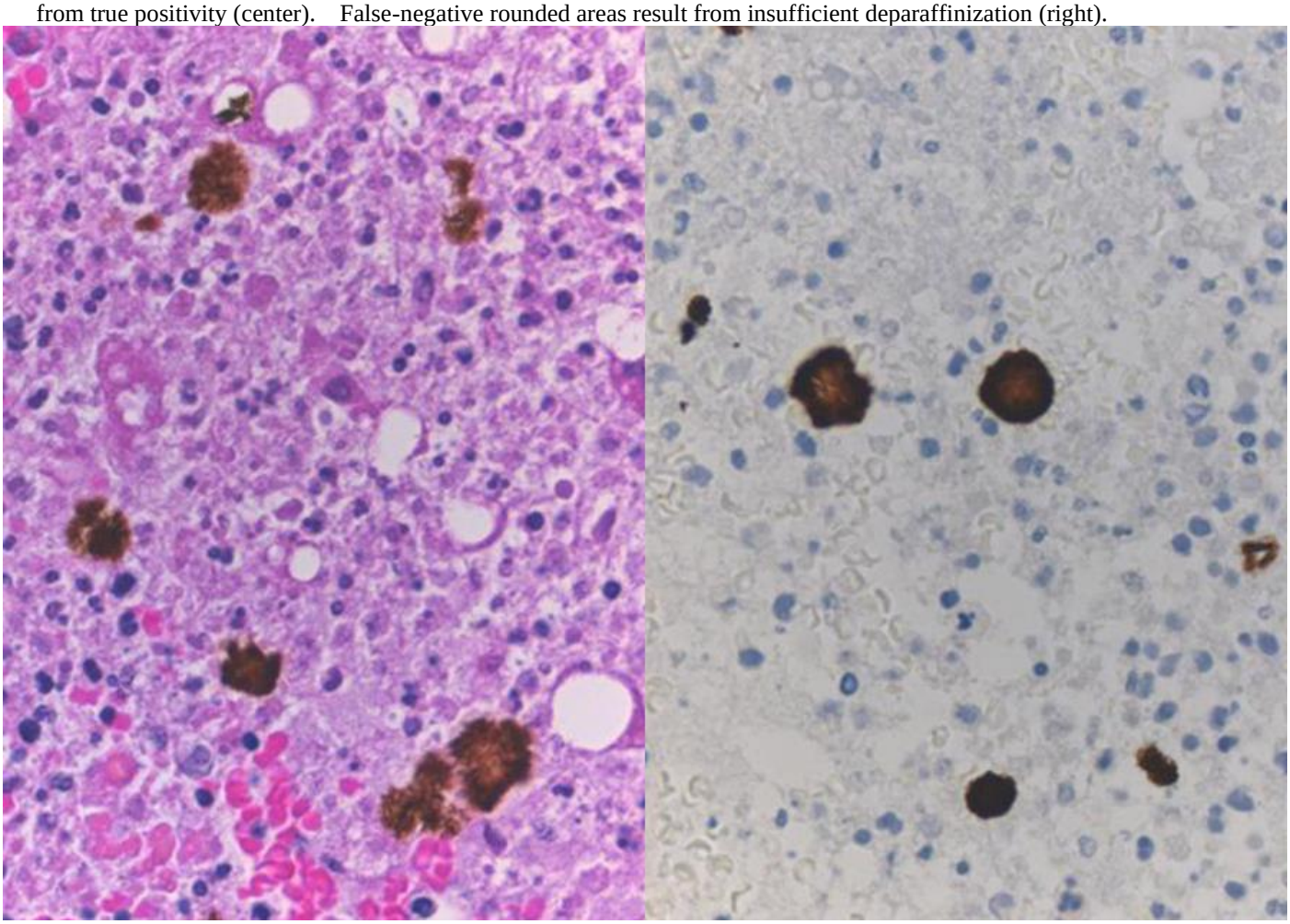

Preprints (www.preprints.org) | NOT PEER-REVIEWED | Posted: 28 April 2021 doi:10.20944/preprints202104.0750.v1

Figure 23. Concentrated bile pigments in a cell block preparation of liver abscess clinically suspected of amebic infection. **Left**: H&E, **Right**: Immunostaining using a monoclonal antibody against *Entamoeba histolytica*. Brown-colored structures of concentrated bile pigments somewhat resemble strongly immunoreactive amebic trophozoites. Careful comparison with H&E histology is needed in order to avoid to judge falsely as positive immunohistochemical signals.

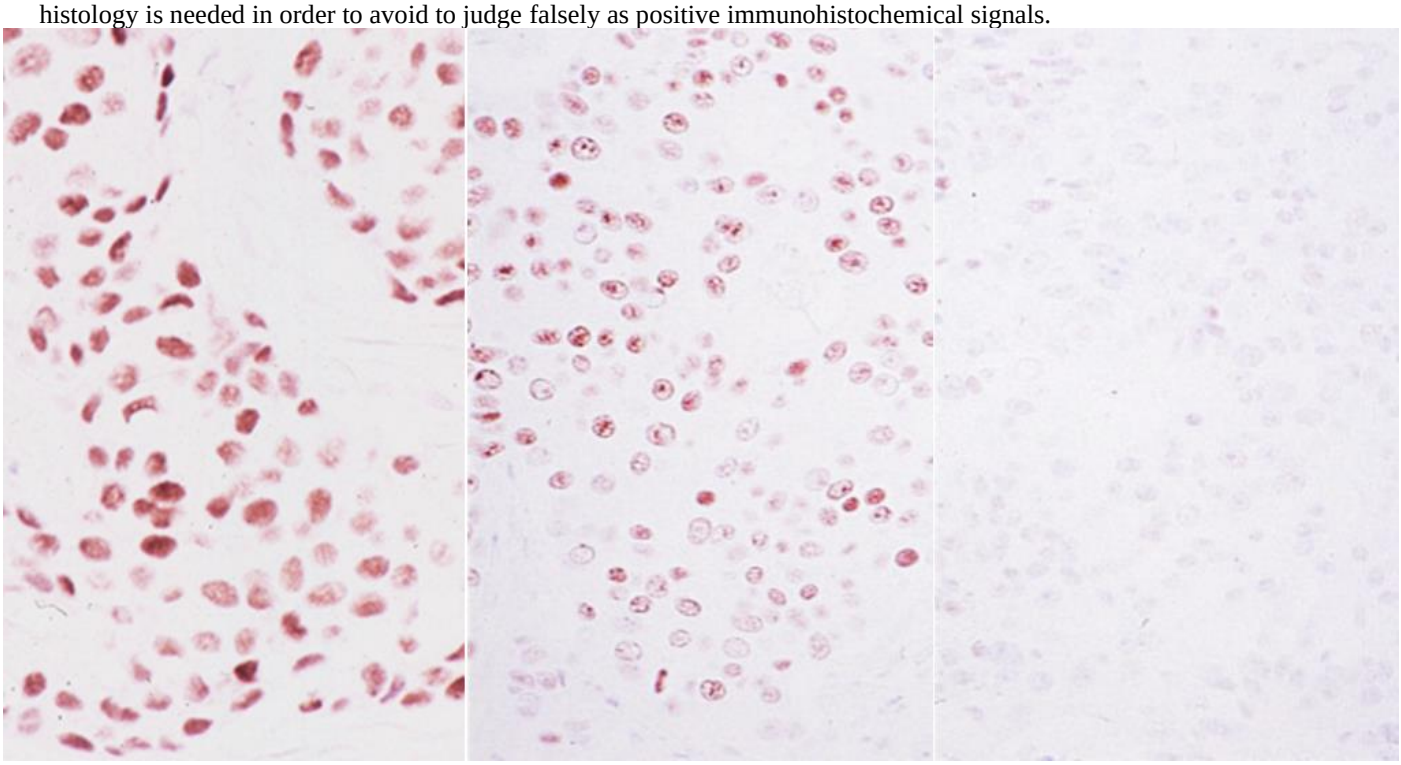

Figure 24. Effect of prolonged storage of unstained sections (ER immunostaining for breast cancer). Immunostaining just after cutting (**left**) and immunostaining after prolonged storage for 6 months in a -20C freezer (**center**) or at room temperature (**right**). The prolonged storage at room temperature severely deteriorates the immunoreactivity of nuclear antigens such as ER. The storage in the freezer is effective for avoiding such false negativity.

Preprints (www.preprints.org) | NOT PEER-REVIEWED | Posted: 28 April 2021 doi:10.20944/preprints202104.0750.v1

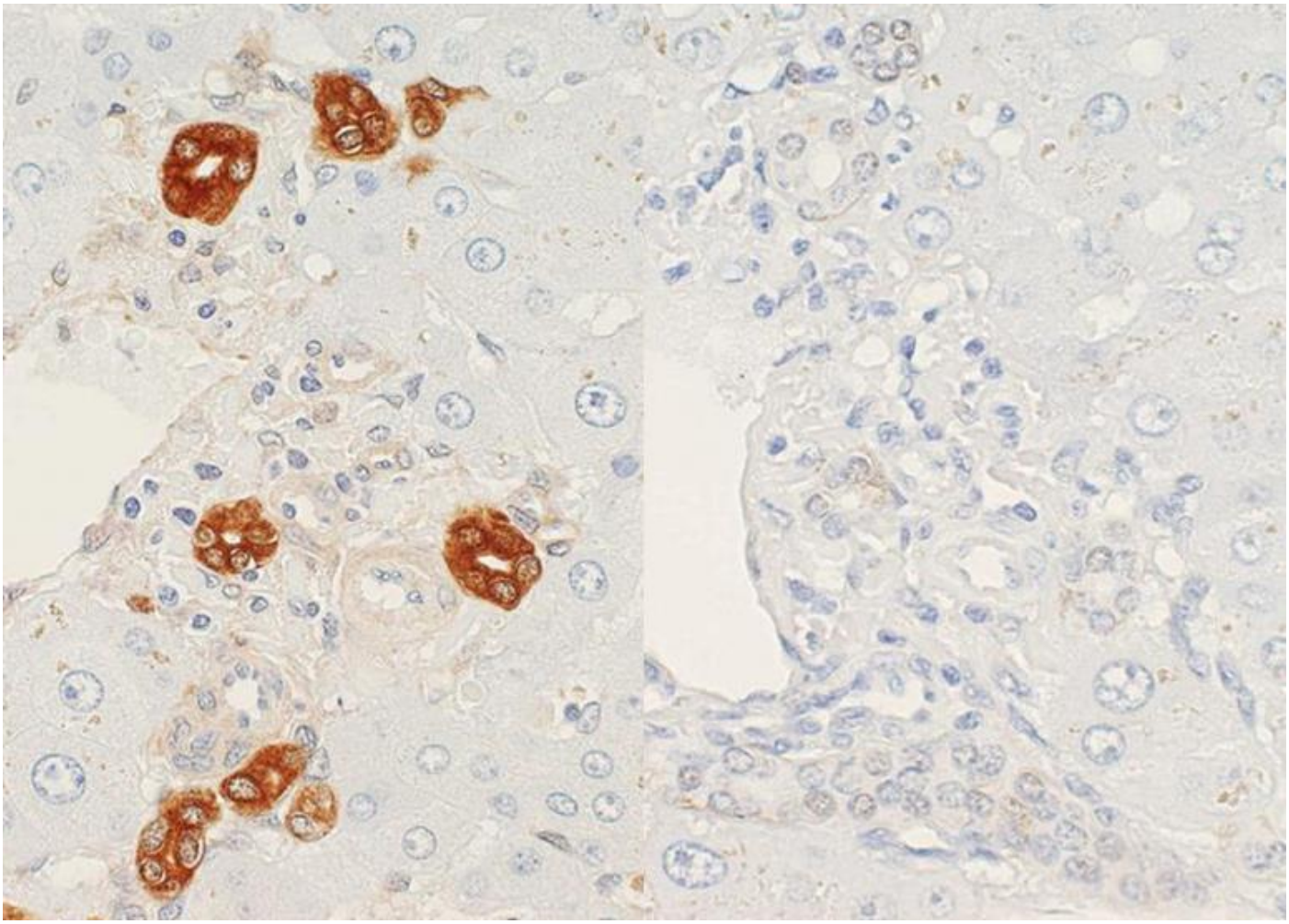

Figure 25. Antigenic loss by stretching sections on a hot plate. Immunostaining for glutathione-S-transferase (GST)-π in the normal liver after stretching on a hot plate at 50C for 10 seconds (**left**) and at 70C for 3 seconds (**right**). The cytoplasmic immunoreactivity of GST-π in the bile duct cells is completely lost by high temperature stretching at 70C for a very short period.

Preprints (www.preprints.org) | NOT PEER-REVIEWED | Posted: 28 April 2021 doi:10.20944/preprints202104.0750.v1

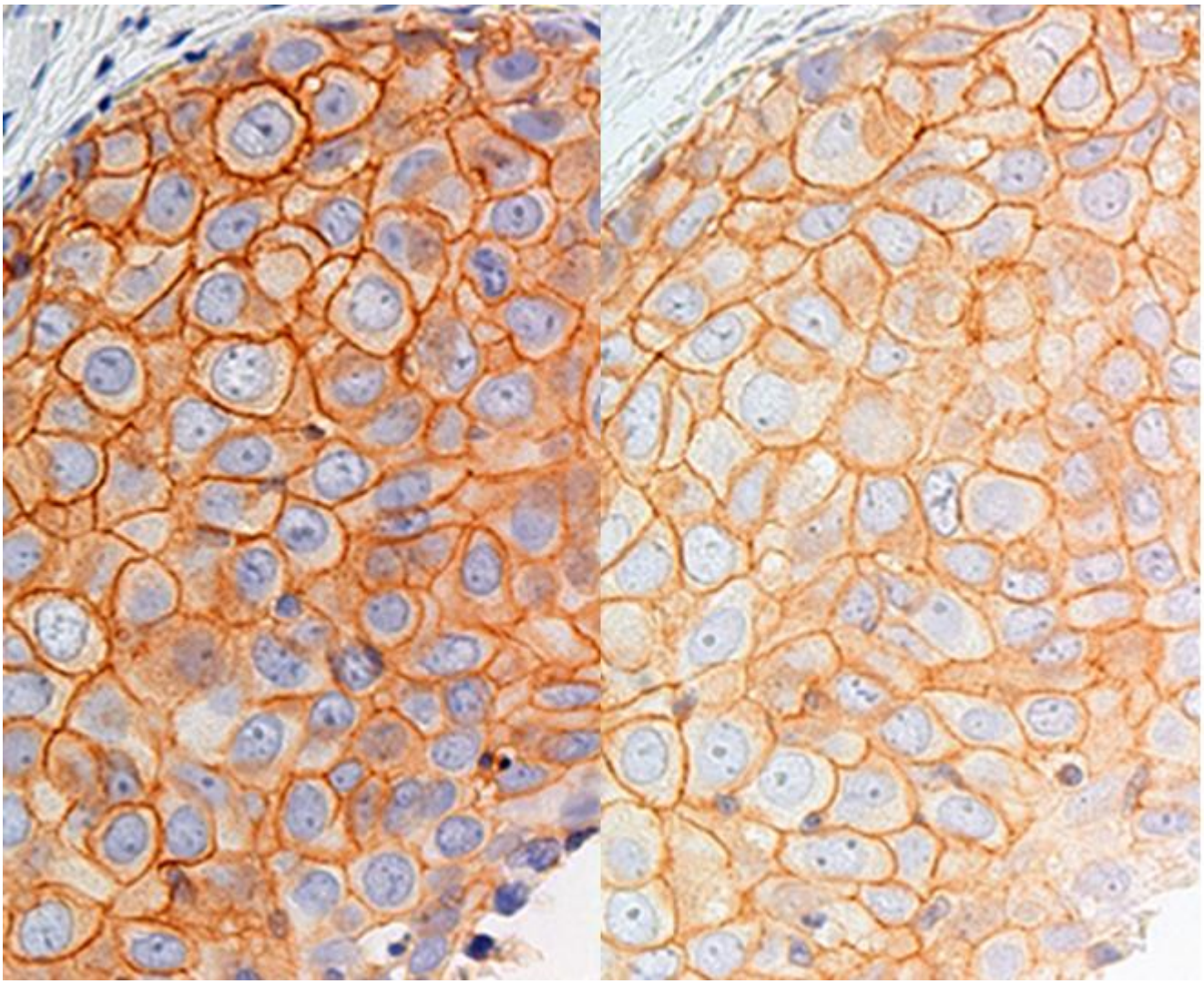

Figure 26. Weakened HER2 immunoreactivity on breast cancer cells by prolonged drying of unstained sections. Drying in an incubator at 40C for 1 hour (**left**) and for 3 days (**right**). The intensity of HER2 immunostaining is considerably weakened after prolonged drying in the incubator during the weekend.

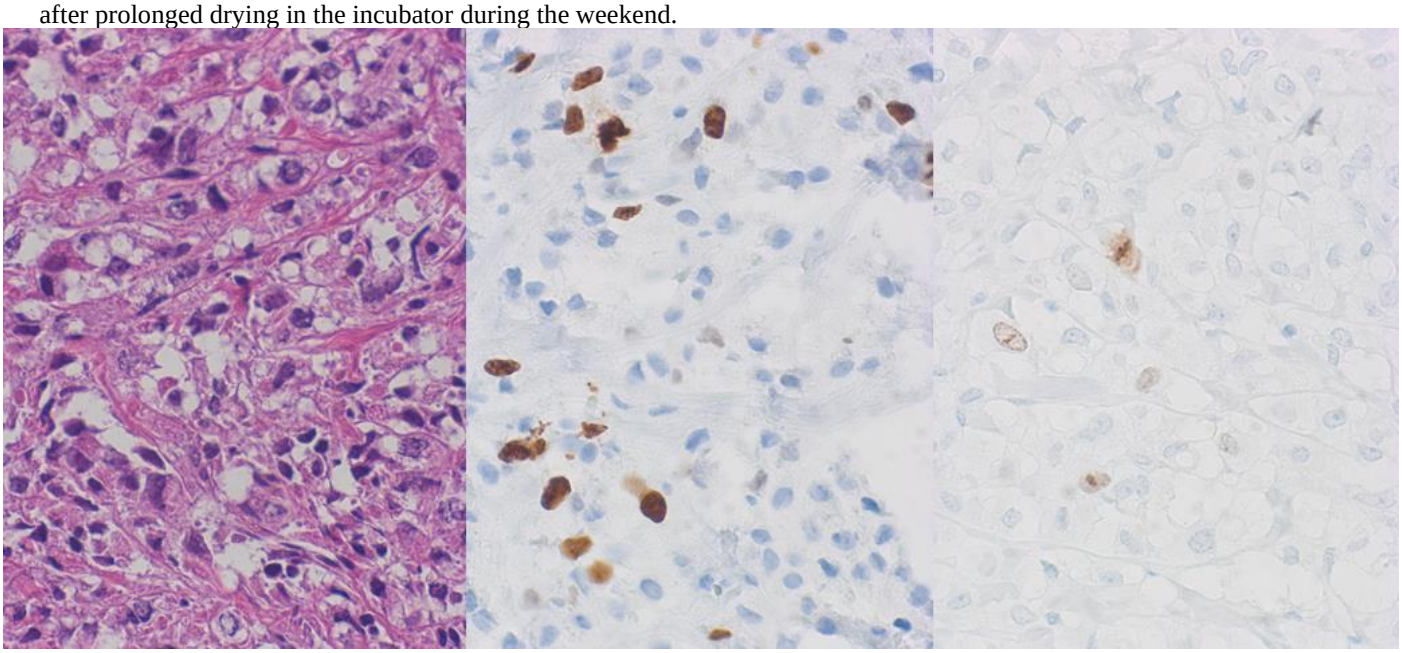

Preprints (www.preprints.org) | NOT PEER-REVIEWED | Posted: 28 April 2021 doi:10.20944/preprints202104.0750.v1

Figure 27. Loss of Ki-67 immunoreactivity in breast cancer (with foci of dystrophic calcification) by surface decalcification with 5% trichloroacetic acid for 1 hour. **Left**: H&E, **Center**: Immunostaining without surface decalcification, **Right**: Immunostaining after surface decalcification with trichloroacetic acid. Surface decalcification significantly deteriorates Ki-67 immunoreactivity.

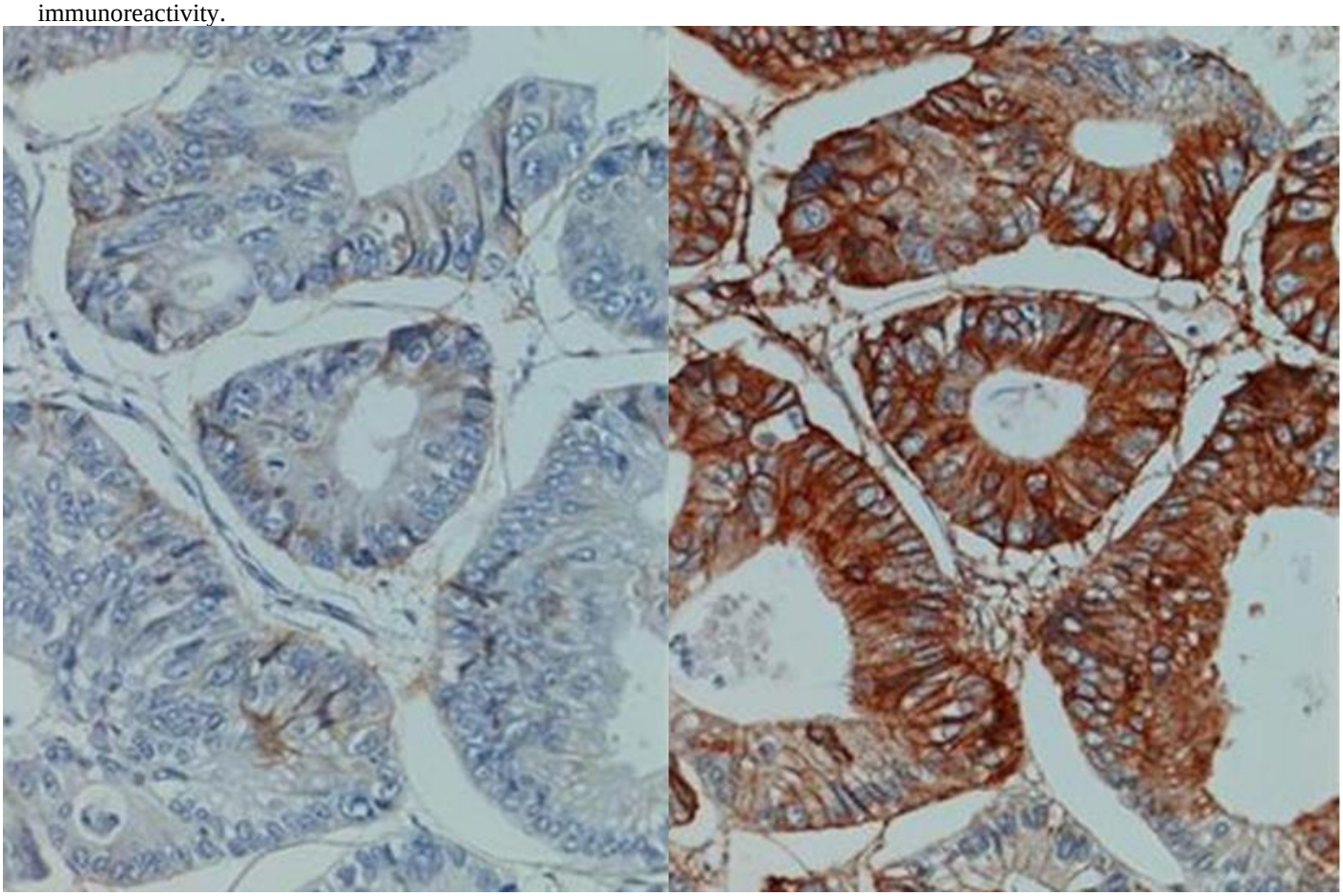

Figure 28. PharmDx™ for EGFR immunostaining in colonic adenocarcinoma. The kit supplied from Agilent/Dako gives a faint immunoreactivity (**left**), which may affect the appropriate judgment. When the secondary reagent is replaced from the EnVision to the CSA-II (available from the same company), very strong EGFR immunoreactivity can be observed (**right**).

Preprints (www.preprints.org) | NOT PEER-REVIEWED | Posted: 28 April 2021 doi:10.20944/preprints202104.0750.v1

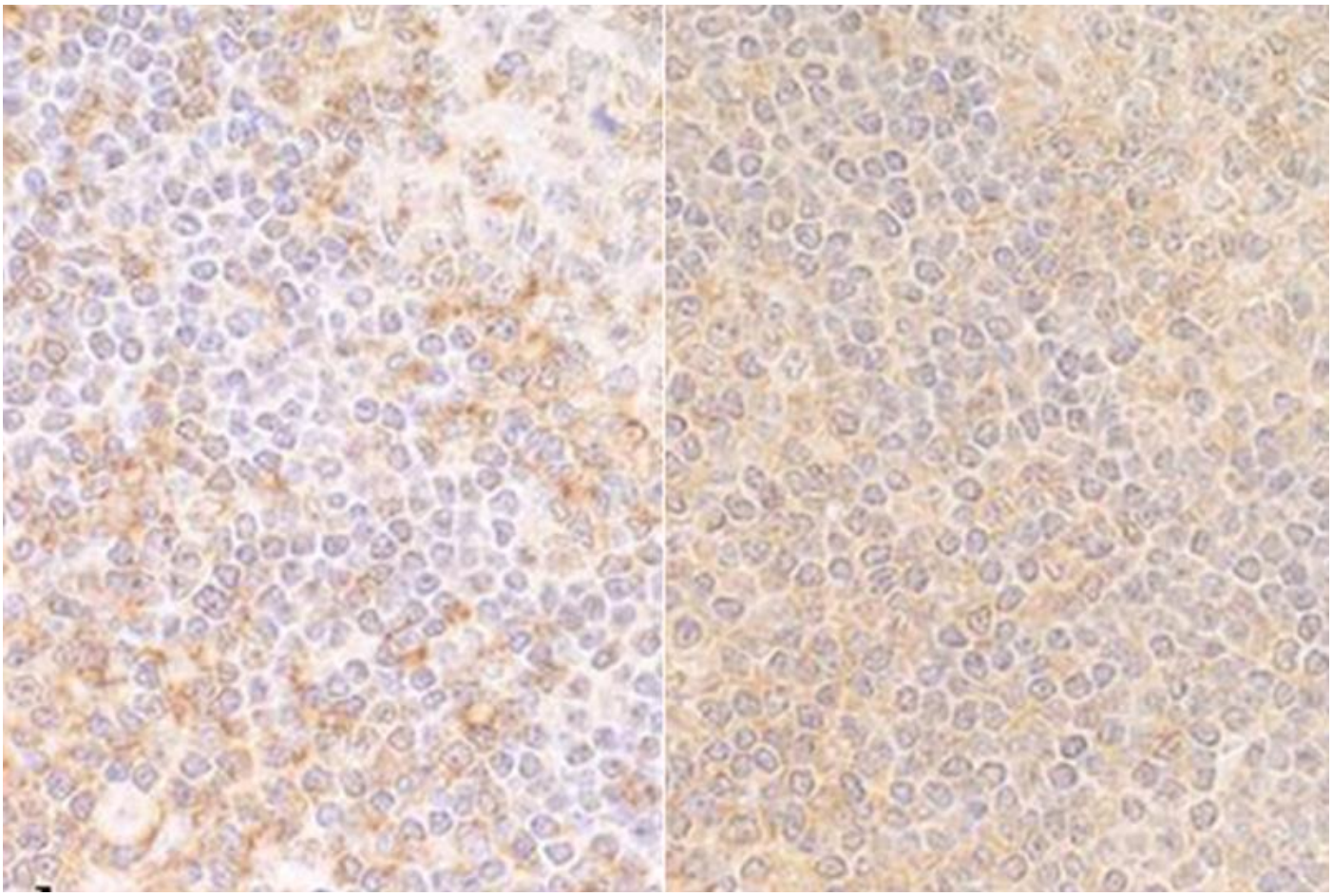

Figure 29. Paradoxical weakening of the antigenicity in CSA-II-mediated immunostaining when the primary antibody concentration is high. CD4 immunostaining of the pharyngeal tonsil after HIER using CD4 monoclonal antibody diluted at 1:500 (**left**) and 1:50 (**right**). Equivocal CD4 immunostaining with high background happens when the primary antibody concentration is 10 times-high.

Preprints (www.preprints.org) | NOT PEER-REVIEWED | Posted: 28 April 2021 doi:10.20944/preprints202104.0750.v1

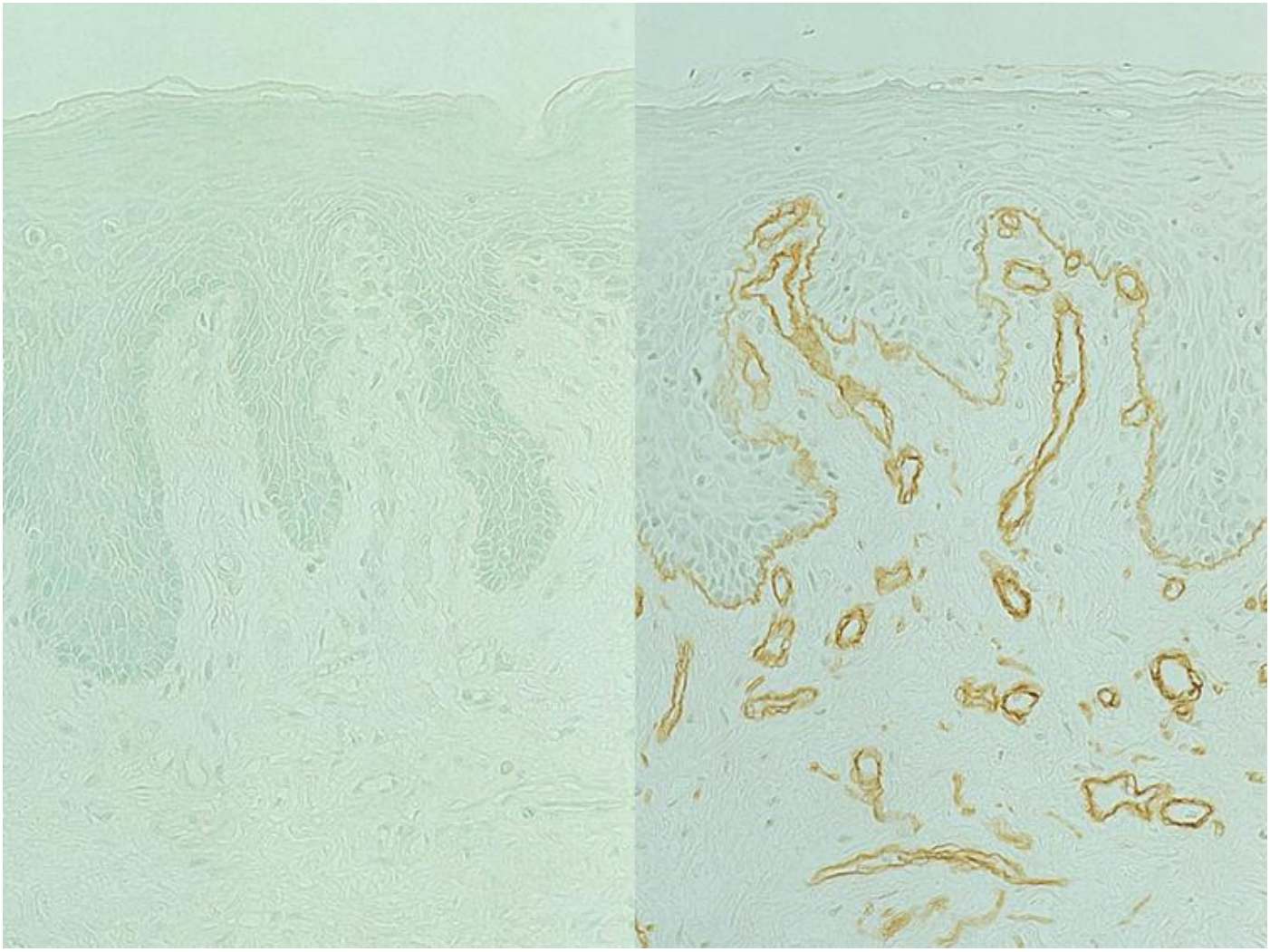

Figure 30. Effect of trypsin digestion in immunostaining for type 4 collagen in the normal skin. **Left**: immunostaining without treatment, **Right**: after 0.1% trypsin digestion at 37C for 30 minutes. Type 4 collagen immunoreactivity in the basement membrane is clearly visualized after trypsin digestion.

Preprints (www.preprints.org) | NOT PEER-REVIEWED | Posted: 28 April 2021 doi:10.20944/preprints202104.0750.v1

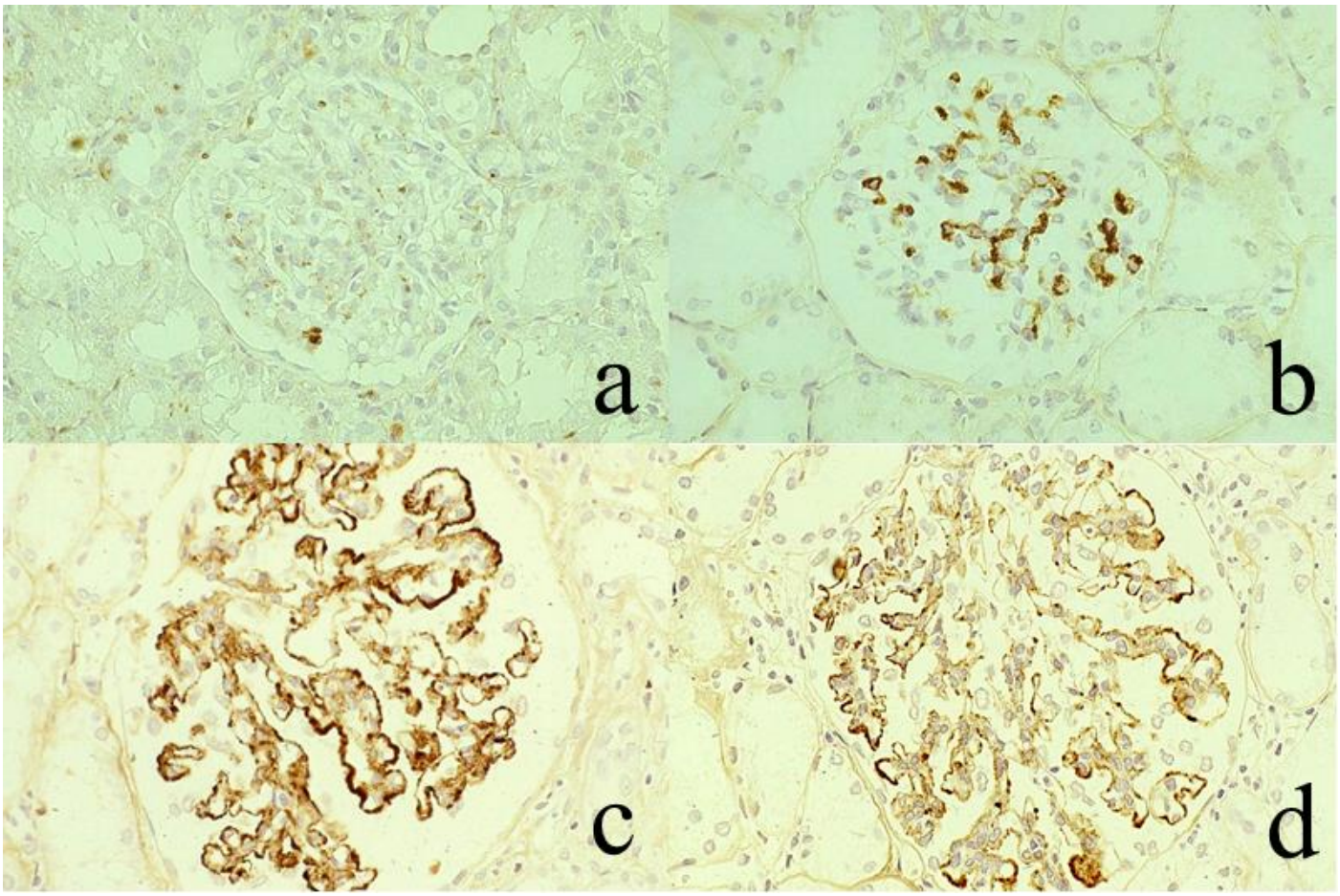

Figure 31. Detection of glomerular deposits of immunoglobulins and complement in FFPE renal biopsy sections with the aid of prolonged 0.1% trypsin digestion for 120 minutes. a&b: IgA nephropathy (IgA staining, a: without digestion, b: after digestion). Mesangial deposition of IgA is evident in b. c&d: Membranous nephropathy after 0.1% trypsin digestion for 120 minutes (c: IgG, d: C3). Granular deposition of IgG and C3 is observed along the capillary loop, diagnostic features of membranous nephropathy.

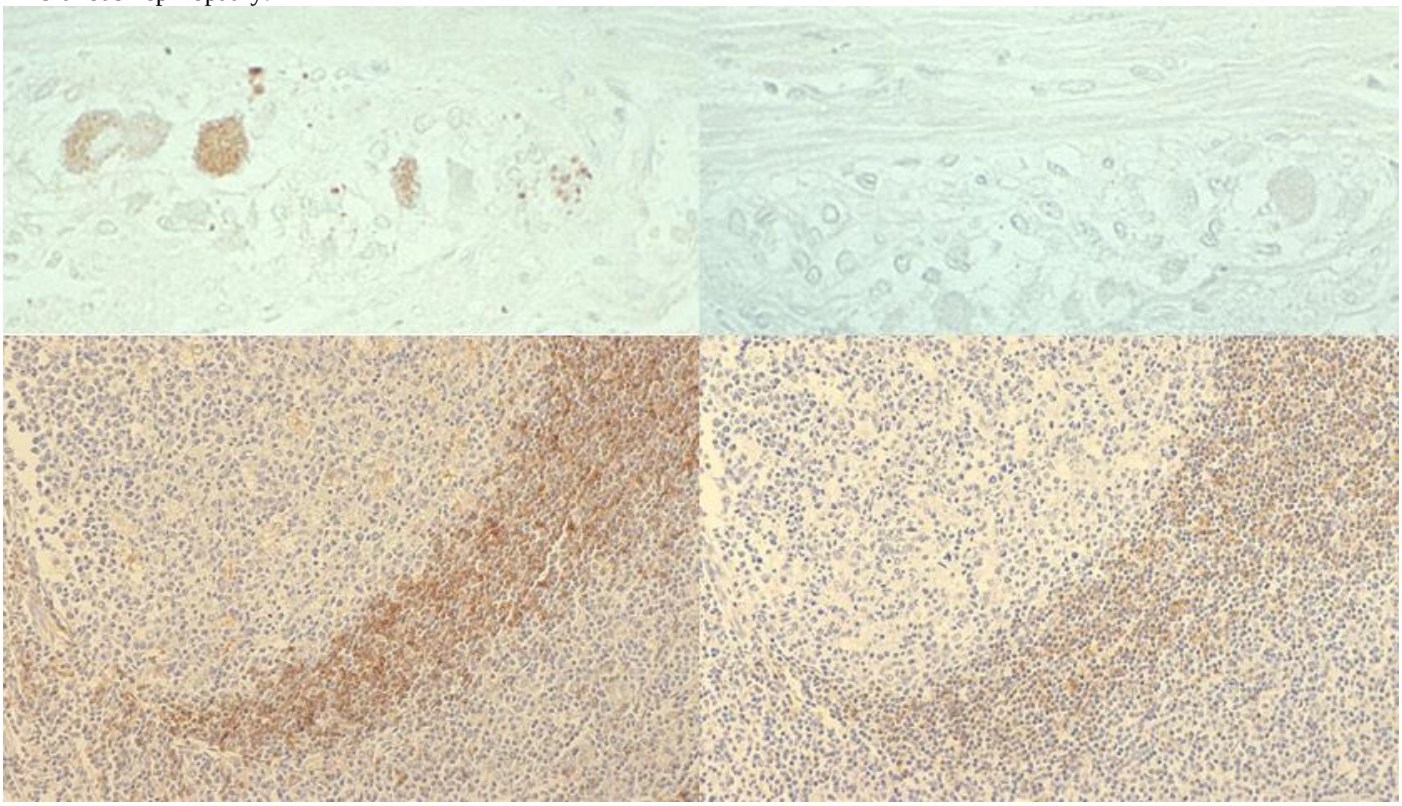

Preprints (www.preprints.org) | NOT PEER-REVIEWED | Posted: 28 April 2021 doi:10.20944/preprints202104.0750.v1

Figure 32. Deterioration of the antigenicity by protease pretreatment. **Left**: without treatment, **Right**: after trypsin digestion for 15 minutes. **Top panels**: substance P in the myenteric plexus of the small bowel, **Bottom panels**: IgD in the mantle zone of the pharyngeal tonsil. Immunoreactivity of substance P and IgD is lost or markedly decreased by the enzymatic pretreatment.

Figure 33. Recommendation of French cuisine with a pressure pan available from T-FAL Co. The pressure pan made by T-FAL (Rumilly, Haute-Savoie, France) is easy to handle and cook for HIER in a diagnostic pathology laboratory.

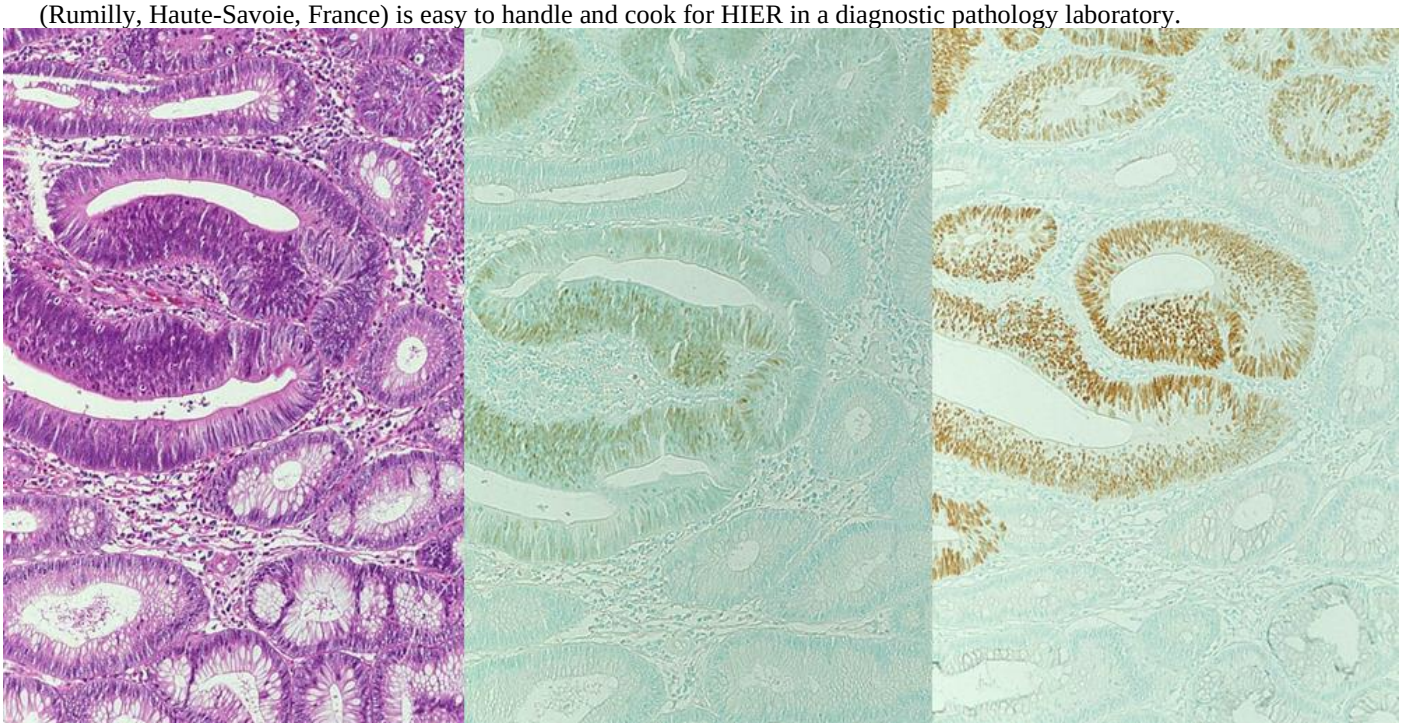

Figure 34. Application of HIER (I). p53 expression in cancer in adenoma of the colon. **Left**: H&E, **Center**: immunostaining without HIER, **Right**: immunostaining after HIER with autoclaving in 10 mM citrate buffer, pH 6.0 for 10 minutes. The nuclei of adenocarcinoma cells express p53, while the surrounding adenoma cells remain negative.

Preprints (www.preprints.org) | NOT PEER-REVIEWED | Posted: 28 April 2021 doi:10.20944/preprints202104.0750.v1

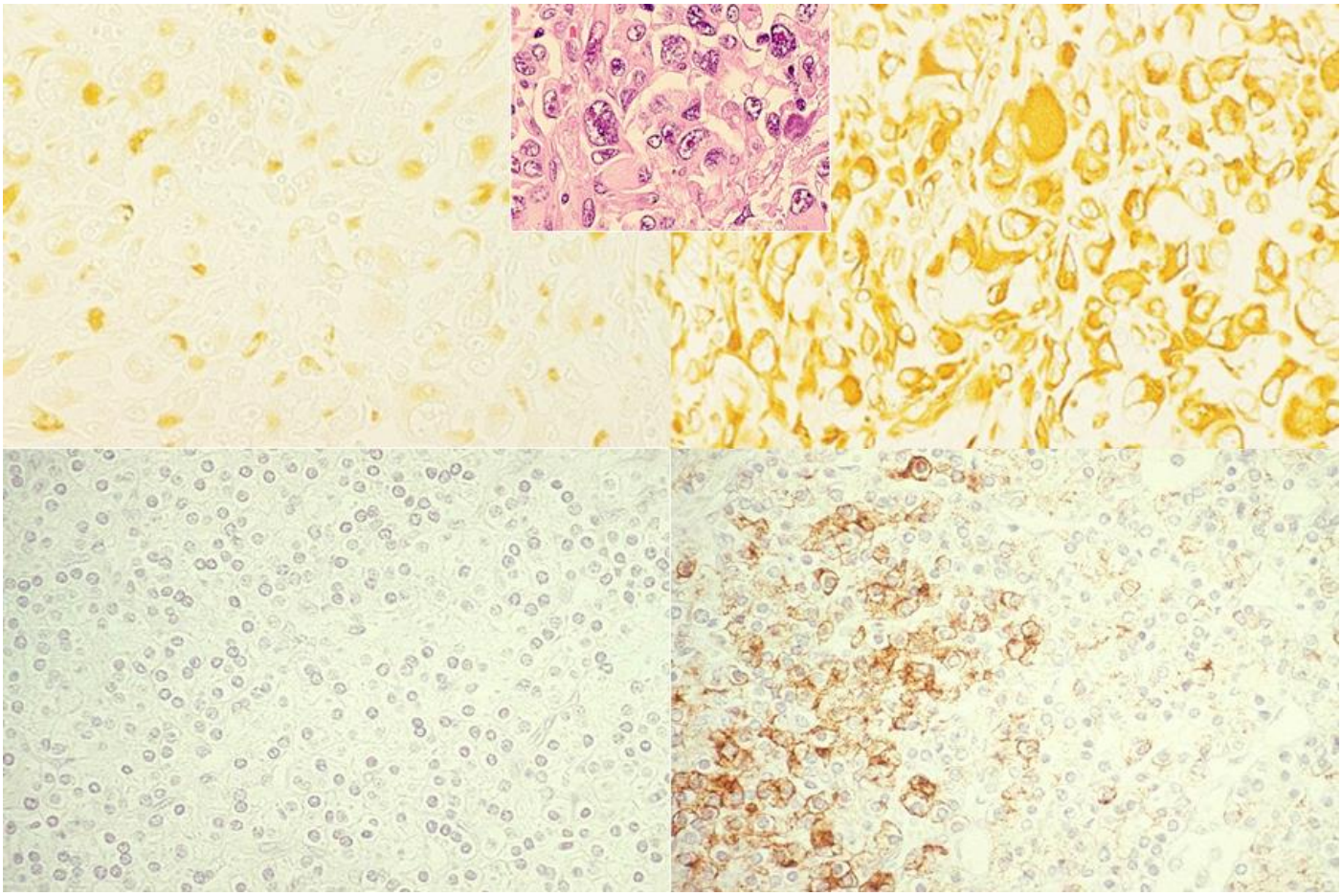

Figure 35. Application of HIER (II). **Left**: without HIER treatment, **Right**: after HIER with autoclaving in 10 mM citrate buffer, pH 6. **Top panels**: vimentin in lung metastasis of anaplastic thyroid carcinoma (**inset**: H&E). **Bottom panels**: parathyroid hormone in normal parathyroid gland. Immunoreactivities of vimentin and parathyroid hormone are significantly retrieved by the hydrated heating pretreatment.

Preprints (www.preprints.org) | NOT PEER-REVIEWED | Posted: 28 April 2021 doi:10.20944/preprints202104.0750.v1

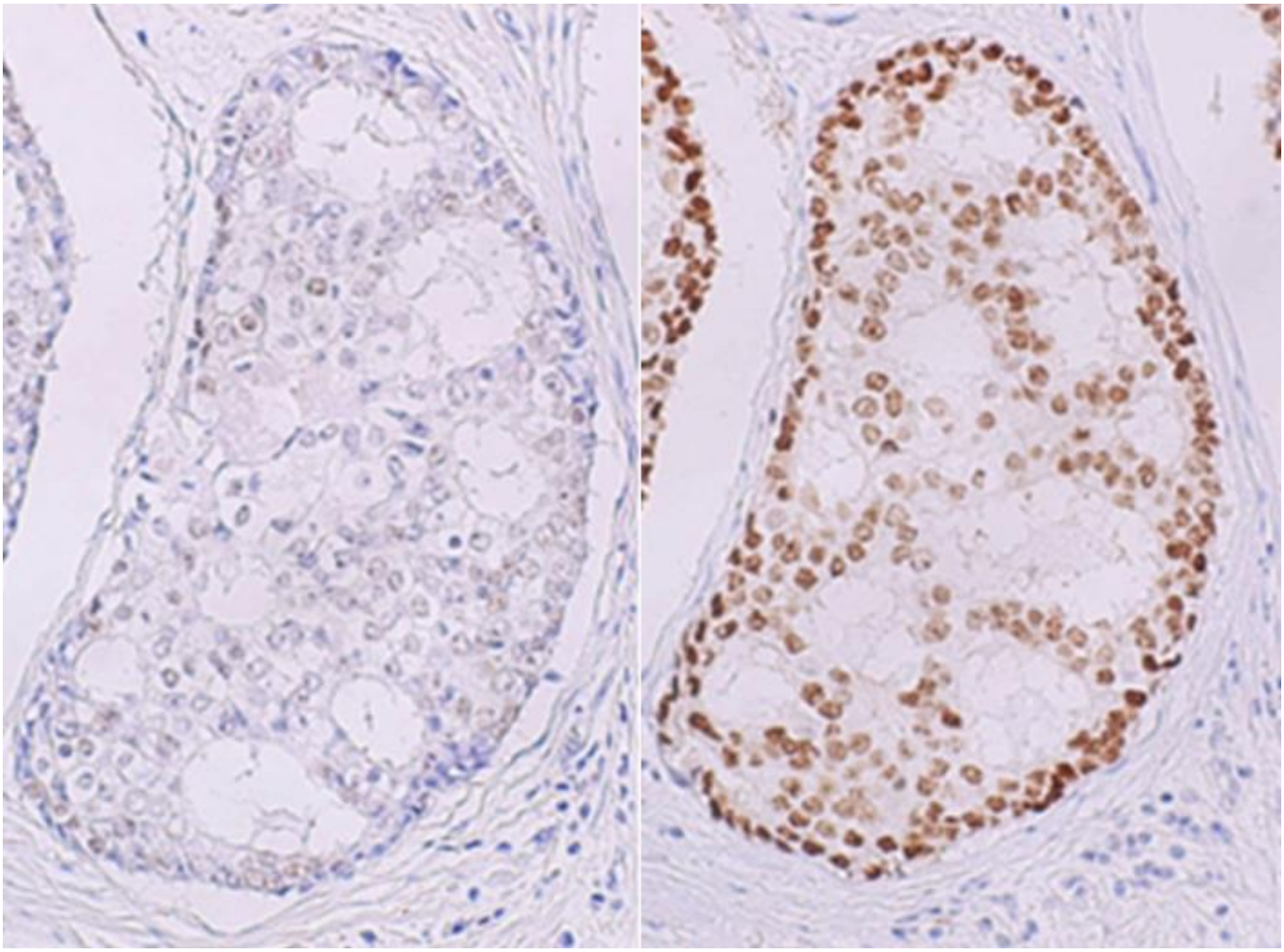

Figure 36. Choice of the aqueous solution for appropriate HIER. ER immunostaining for breast cancer. **Left**: 10 mM citrate buffer, pH 6.0, **Right**: 1 mM EDTA, pH 8.0. ER in cribriforming ductal carcinoma *in situ* is effectively retrieved by HIER in 1 mM EDTA solution, pH 8.0.

Preprints (www.preprints.org) | NOT PEER-REVIEWED | Posted: 28 April 2021 doi:10.20944/preprints202104.0750.v1

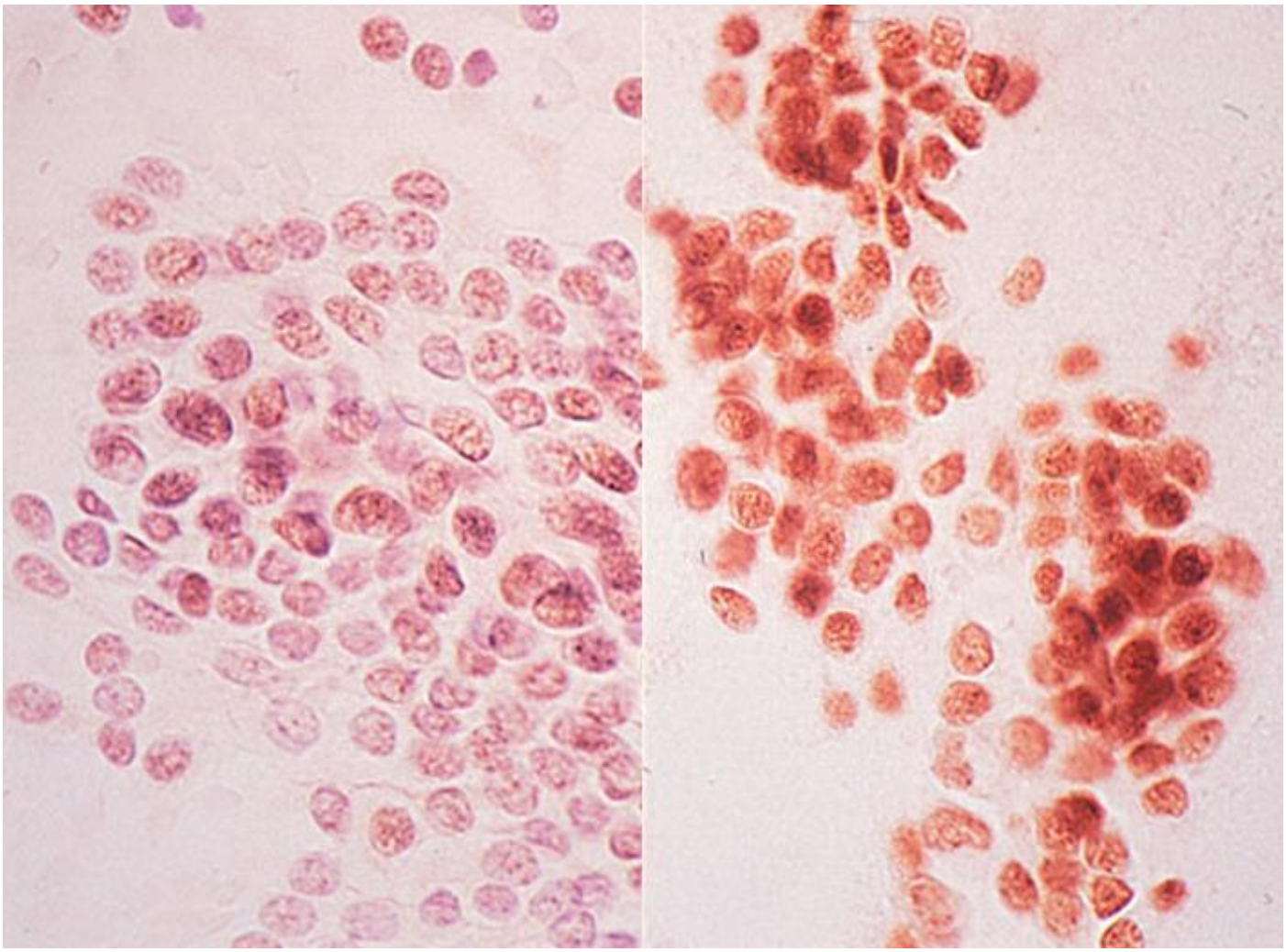

Figure 37. ER immunostaining for an aspiration cytology preparation with ethanol fixation. **Left**: without pretreatment, **Right**: HIER in 10 mM citrate buffer, pH 7.0. HIER is effective for ER immunolocalization even in the cytology specimen.

Preprints (www.preprints.org) | NOT PEER-REVIEWED | Posted: 28 April 2021 doi:10.20944/preprints202104.0750.v1

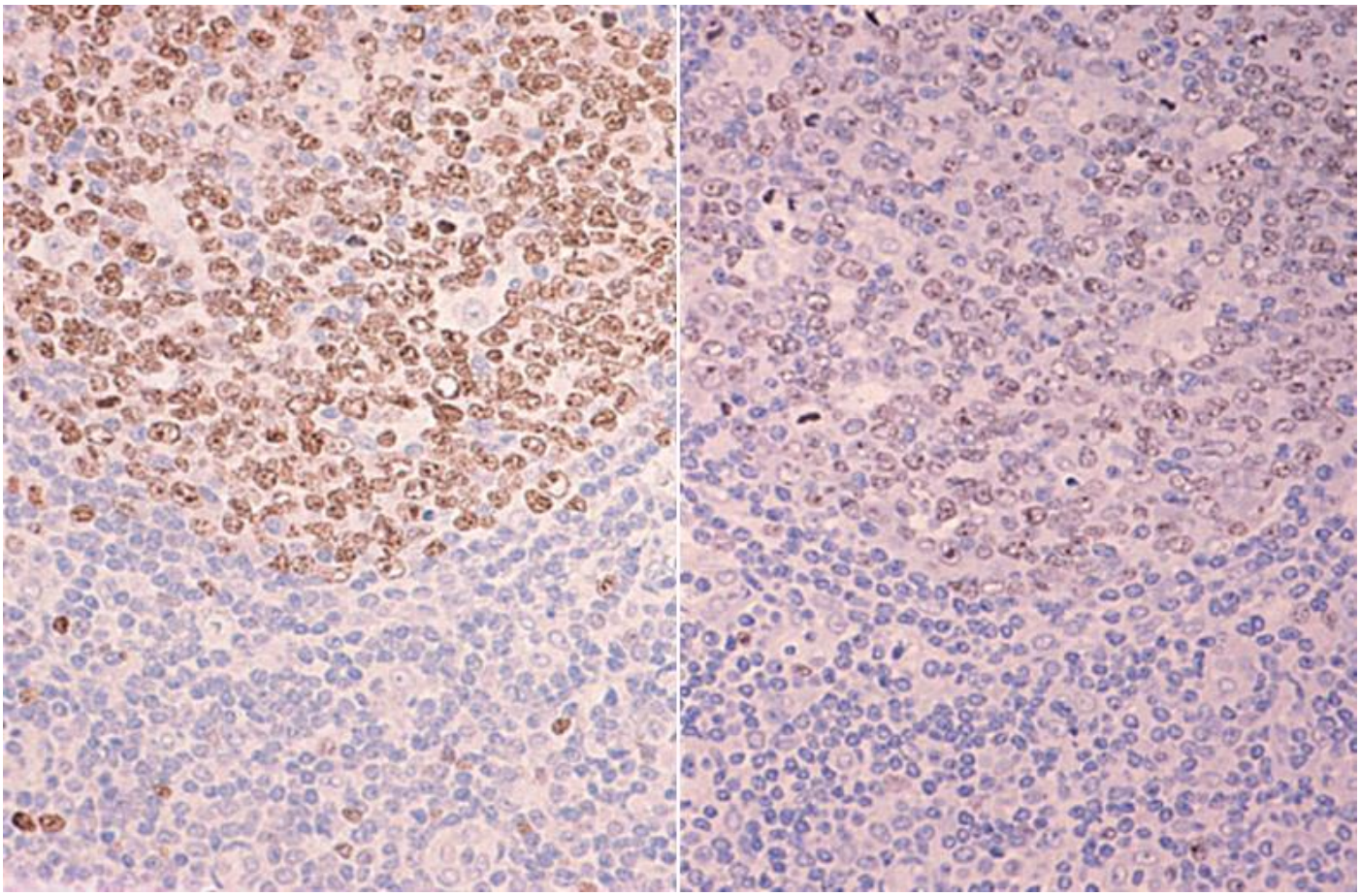

Figure 38. Weakening of Ki-67 immunoreactivity by overnight antibody incubation after HIER in 10 mM citrate buffer, pH 6.0. **Left**: 1 hour antibody incubation, **Right**: overnight incubation. Ki-67 labeling in the germinal center lymphocytes of the pharyngeal tonsil, clearly seen in 1 hour antibody incubation, is significantly weakened after overnight incubation.

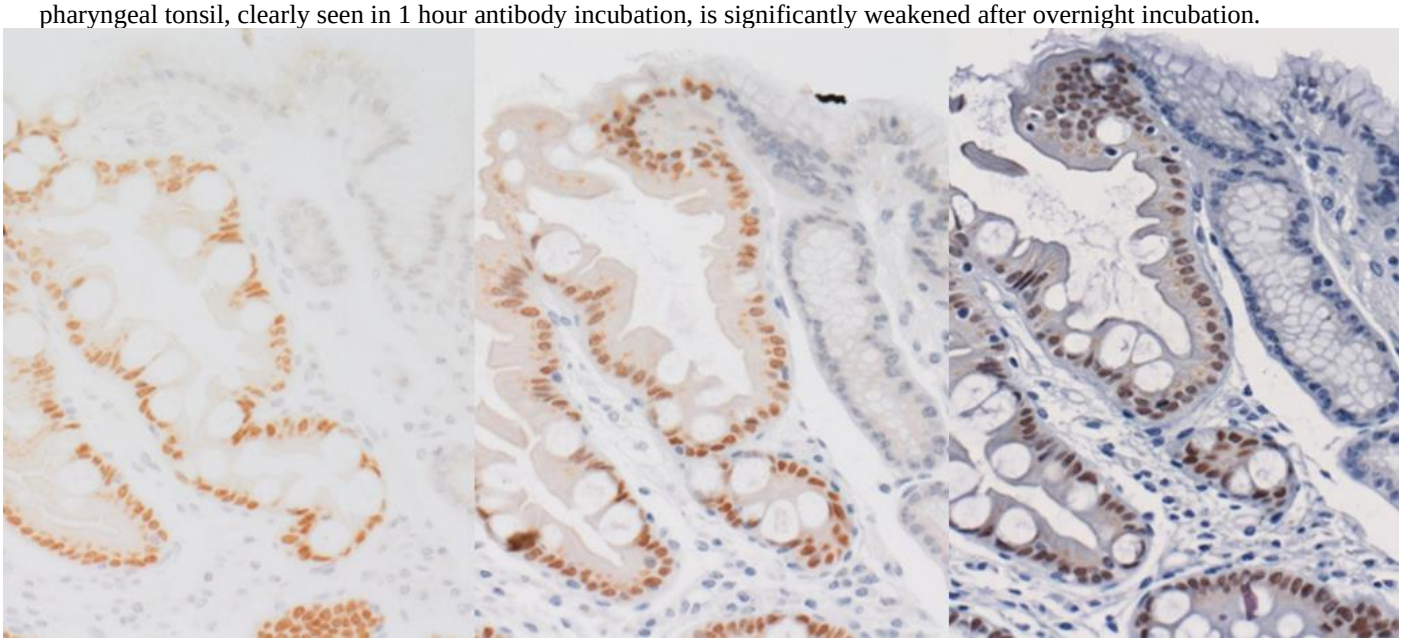

Figure 39. Poor nuclear stainability by hematoxylin after EDTA-mediated HIER. CDX2 (caudal-type homeobox-2) immunoreactivity in intestinal metaplasia of the stomach. Mayer's hematoxylin staining for 10 seconds (**left**), 1 minute (**center**) and 3 minutes (**right**). Prolonged nuclear staining is needed after HIER in 1 mM EDTA solution, pH 8.0.

Preprints (www.preprints.org) | NOT PEER-REVIEWED | Posted: 28 April 2021 doi:10.20944/preprints202104.0750.v1

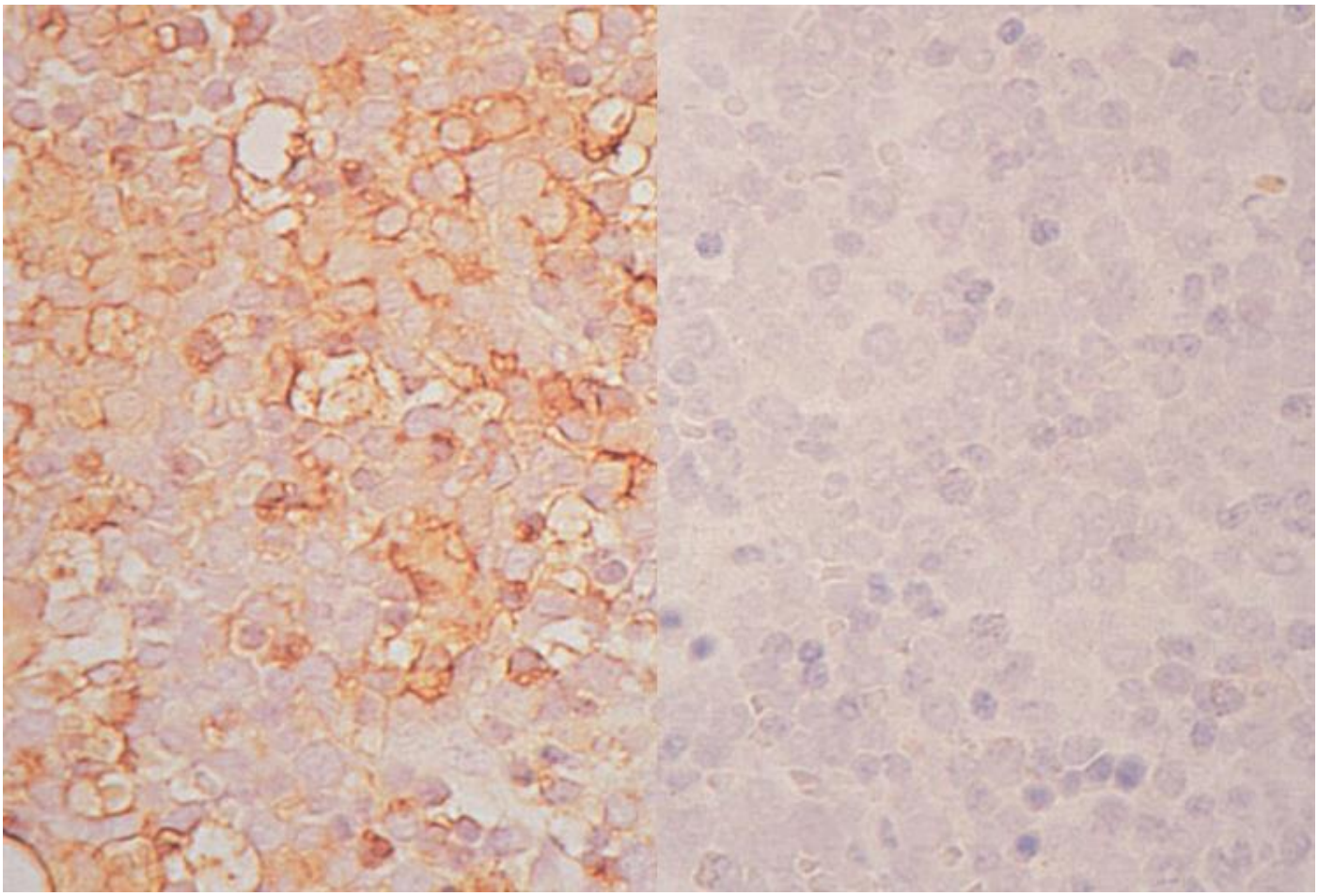

Figure 40. Antigenic loss by HIER in 10 mM citrate buffer, pH 6.0. BM-1 (a myeloid marker) in FFPE bone marrow aspiration. **Left**: without HIER, **Right**: after HIER. BM-1 immunoreactivity is quite susceptible to heating.

Preprints (www.preprints.org) | NOT PEER-REVIEWED | Posted: 28 April 2021 doi:10.20944/preprints202104.0750.v1

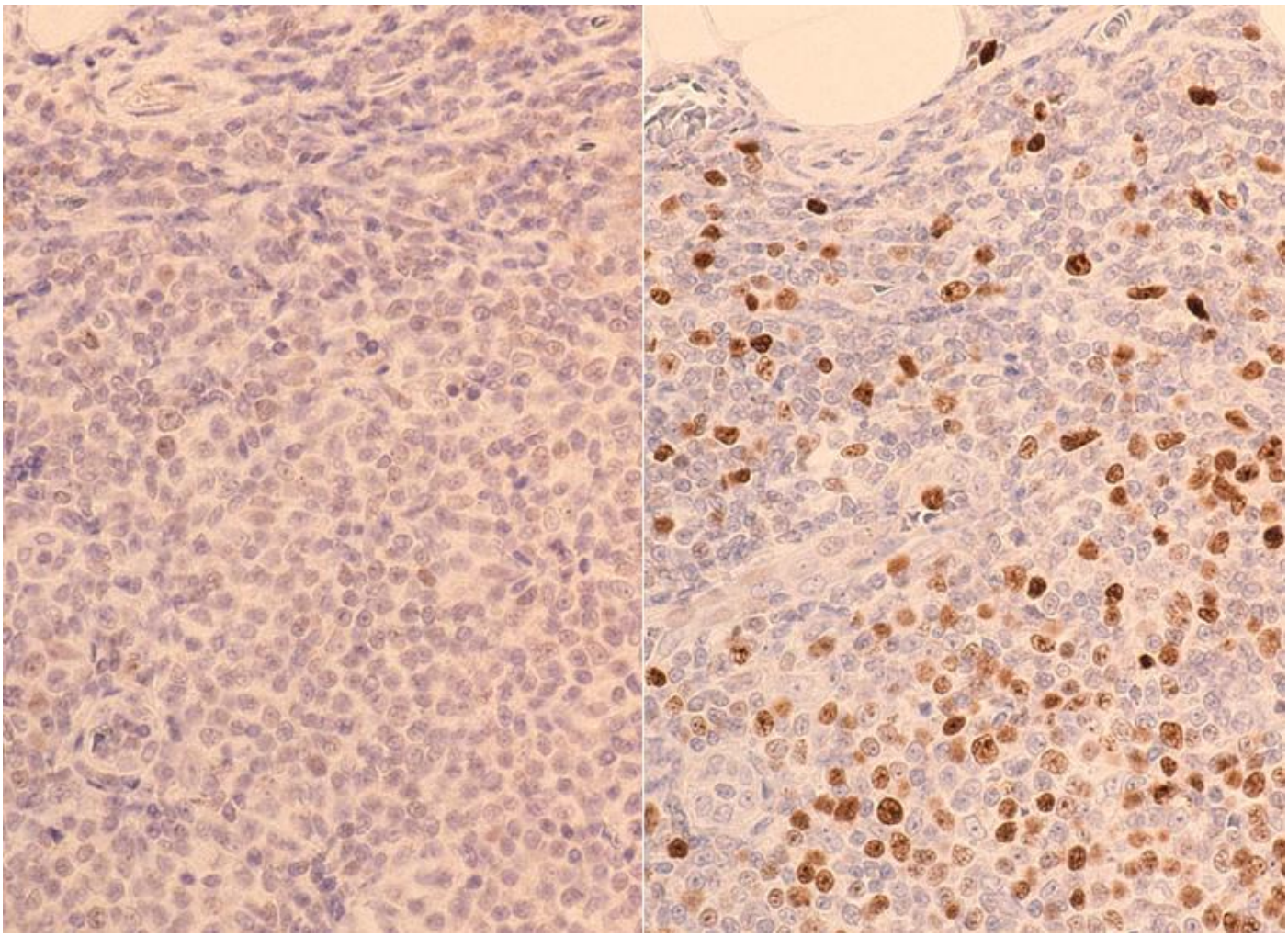

Figure 41. How to cool down after HIER. **Left**: rapid cooling by soaking in tap water, **Right**: gradual cooling by leaving the slide container at room temperature. Ki-67 antigenicity in reactive lymphadenopathy becomes undetectable after rapid cooling. Sections after gradual cooling reveal distinct nuclear labeling.

Preprints (www.preprints.org) | NOT PEER-REVIEWED | Posted: 28 April 2021 doi:10.20944/preprints202104.0750.v1

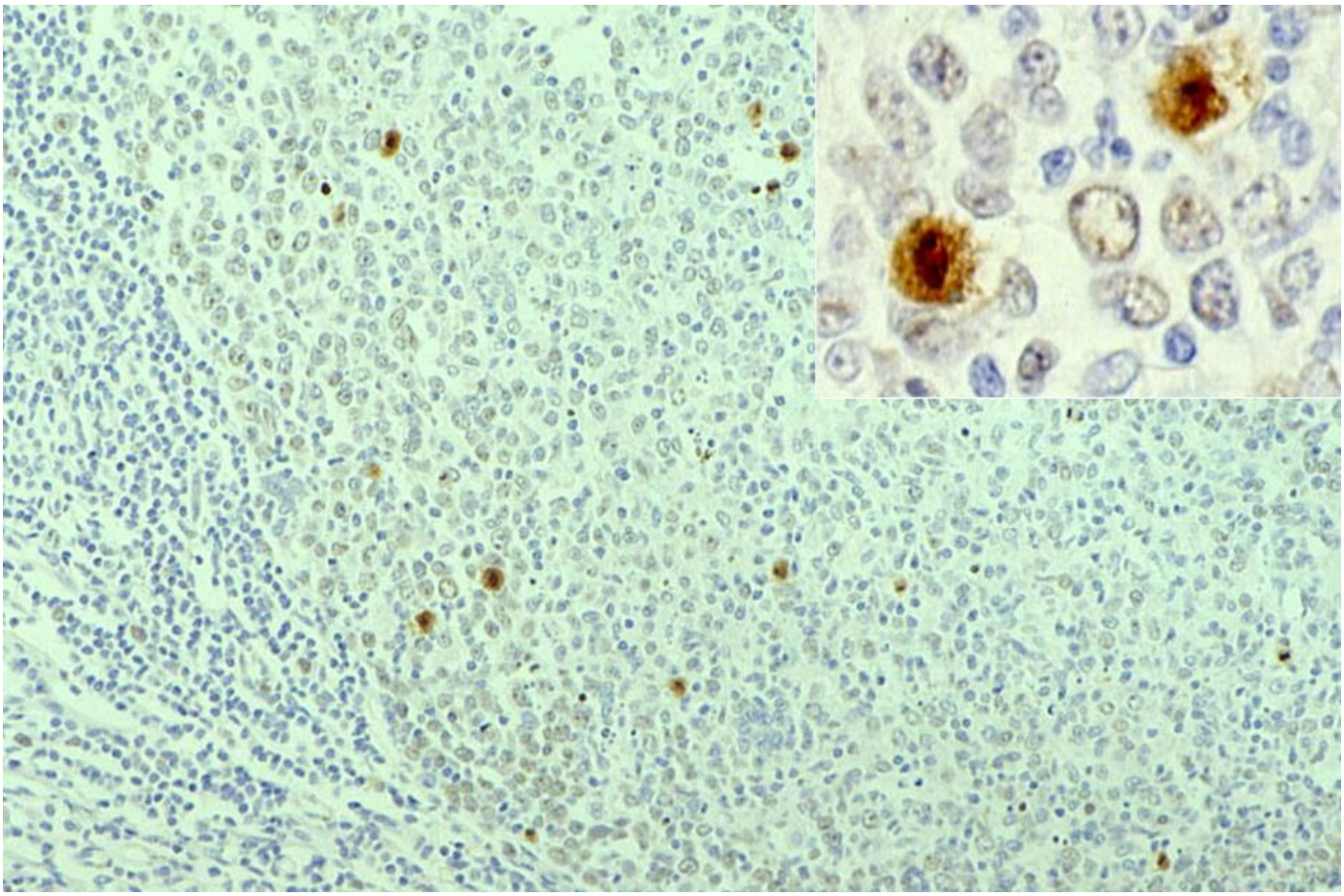

Figure 42. Labeling of mitotic cells by Ki-67 immunostaining in the pharyngeal tonsil (**inset**: high-powered view). A high molecular weight polymer reagent in the EnVision provokes a false negative result for Ki-67 nuclear labeling of proliferative cells. Only mitotic cells are labeled. The reason seems that the huge molecules of the secondary reagent do not penetrate the nuclear membrane.

Preprints (www.preprints.org) | NOT PEER-REVIEWED | Posted: 28 April 2021 doi:10.20944/preprints202104.0750.v1

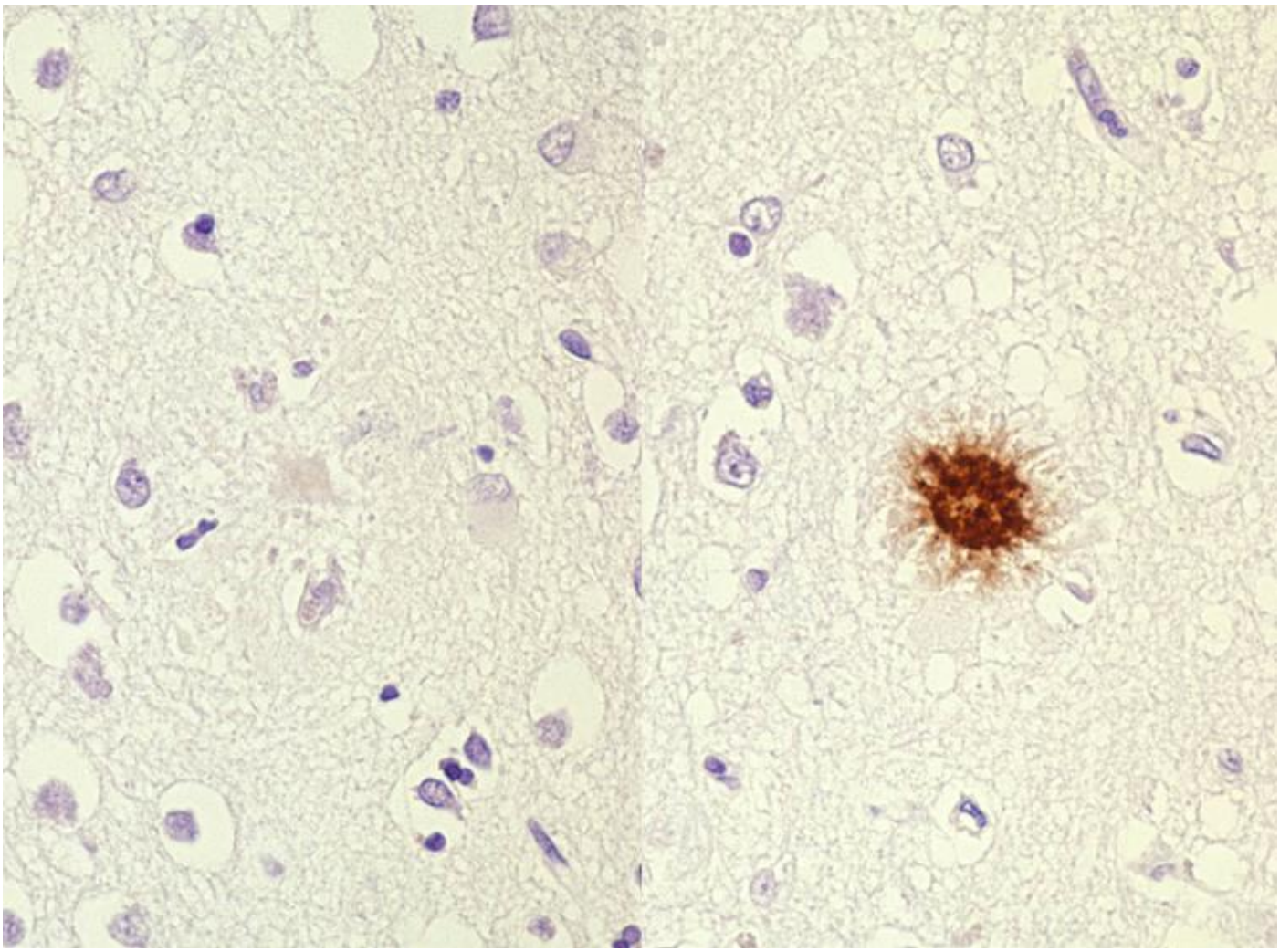

Figure 43. Retrieval of β-amyloid immunoreactivity in the brain by formic acid pretreatment. **Left**: without treatment, **Right**: 100% formic acid treatment for 5 minutes. Brief soaking in formic acid retrieves β-amyloid immunoreactivity of senile plaques in Alzheimer's disease.

Preprints (www.preprints.org) | NOT PEER-REVIEWED | Posted: 28 April 2021 doi:10.20944/preprints202104.0750.v1

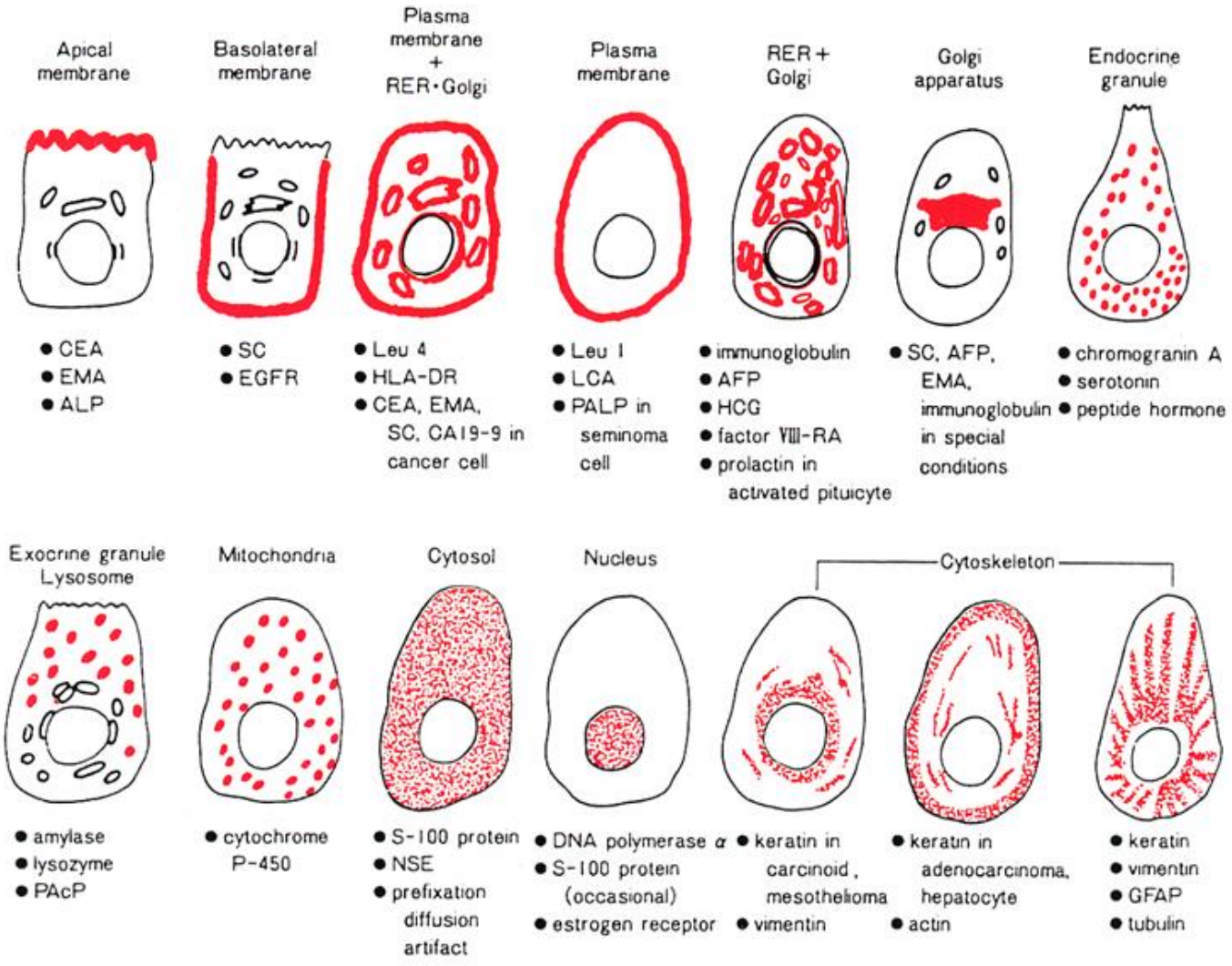

Figure 44. Schematic illustration of intracellular localization of antigens. The specificity of immunostaining can be judged by the intracellular localization pattern of the antigenic substances: either membranous, diffuse cytoplasmic, granular/vesicular cytoplasmic or nuclear in microscopic localization.

Preprints (www.preprints.org) | NOT PEER-REVIEWED | Posted: 28 April 2021 doi:10.20944/preprints202104.0750.v1

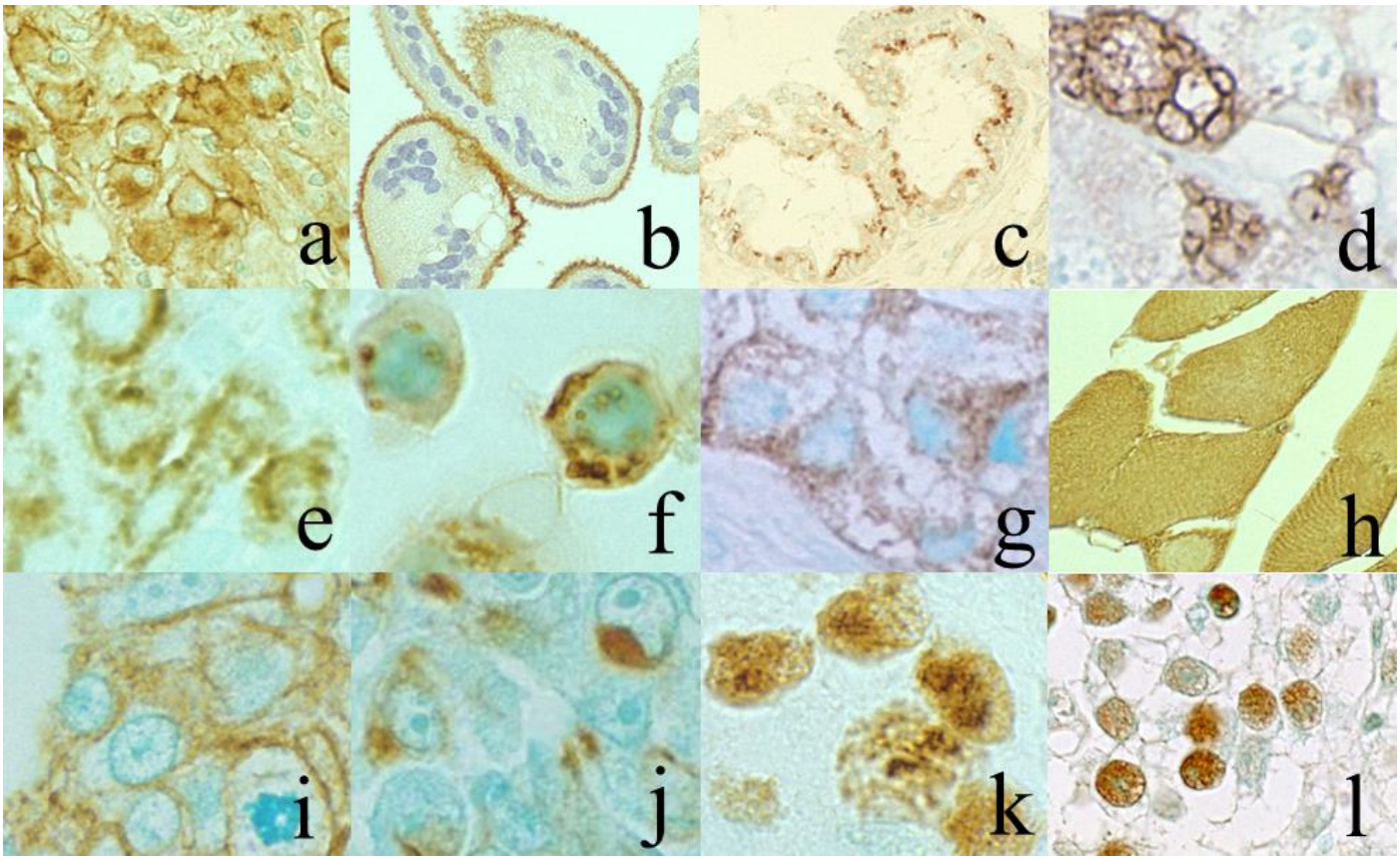

Figure 45. Representative immunohistochemical markers showing various intracellular localization patterns. a: CD30 in anaplastic large cell (Ki-1) lymphoma, b: placental ALP on the villi of the normal placenta, c: CA125 in ovarian serous adenocarcinoma, d: IgG in plasmacytoma, e: intrinsic factor in parietal cells in the oxyntic gastric mucosa, f: nonspecific cross-reacting antigen in lysosomes of lung adenocarcinoma cells (cell line PC-9), g: insulin in pancreatic insulinoma, h: creatine kinase, mm isotype in normal striated muscle, i: cytokeratin in well-differentiated gastric adenocarcinoma, j: cytokeratin in poorly differentiated gastric adenocarcinoma, k: Ki-67 in breast cancer, l: proliferating cell nuclear antigen (PCNA) in testicular seminoma.

Preprints (www.preprints.org) | NOT PEER-REVIEWED | Posted: 28 April 2021 doi:10.20944/preprints202104.0750.v1

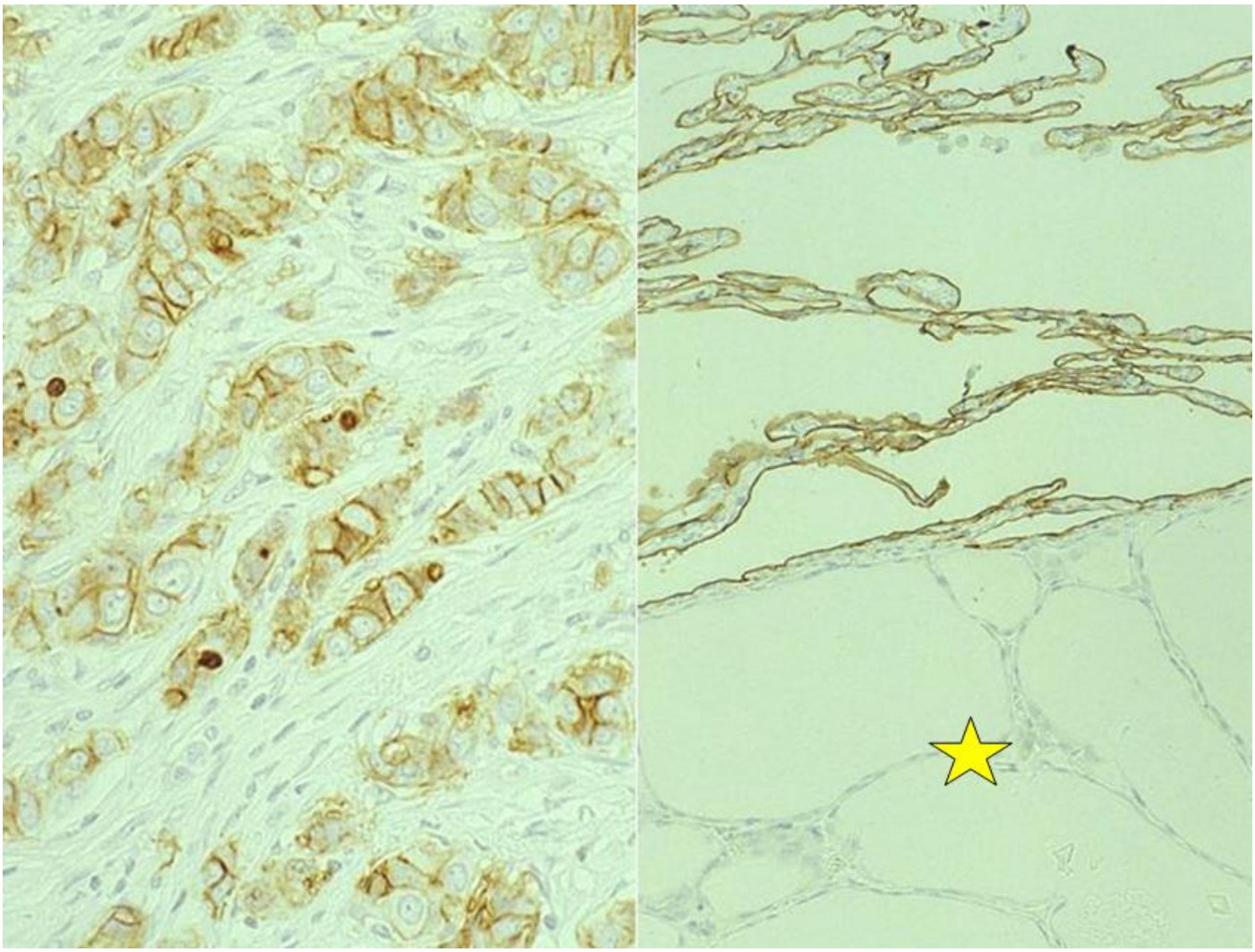

Figure 46. Plasma membrane localization of Ki-67. **Left**: breast cancer, **Right**: Lung with ectopic thyroid tissue. Ki-67 may show strange, cross-reactive localization on the plasma membrane. Membranous positivity in invasive ductal carcinoma cells and alveolar type I pneumocytes is unique but nonspecific. Asterisk indicates ectopic thyroid tissue.

Preprints (www.preprints.org) | NOT PEER-REVIEWED | Posted: 28 April 2021 doi:10.20944/preprints202104.0750.v1

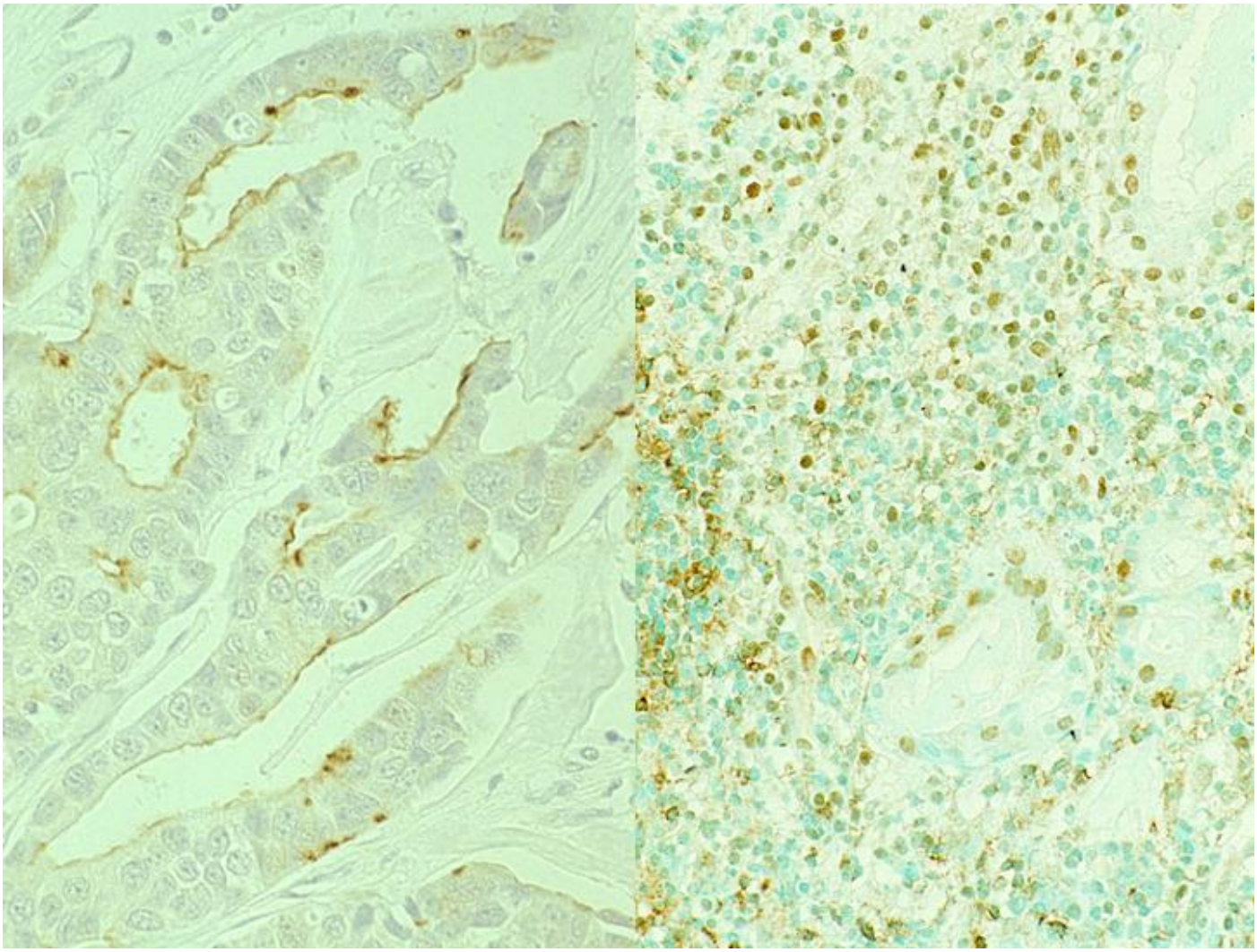

Figure 47. Examples of nonspecific immunostaining. **Left**: membranous positivity of PgR in breast cancer, **Right**; nuclear positivity of CD45RO (UCHL1) in nasal NK-cell lymphoma. The intracellular localization pattern is unusual, so that the results must be regarded as nonspecific.

Preprints (www.preprints.org) | NOT PEER-REVIEWED | Posted: 28 April 2021 doi:10.20944/preprints202104.0750.v1

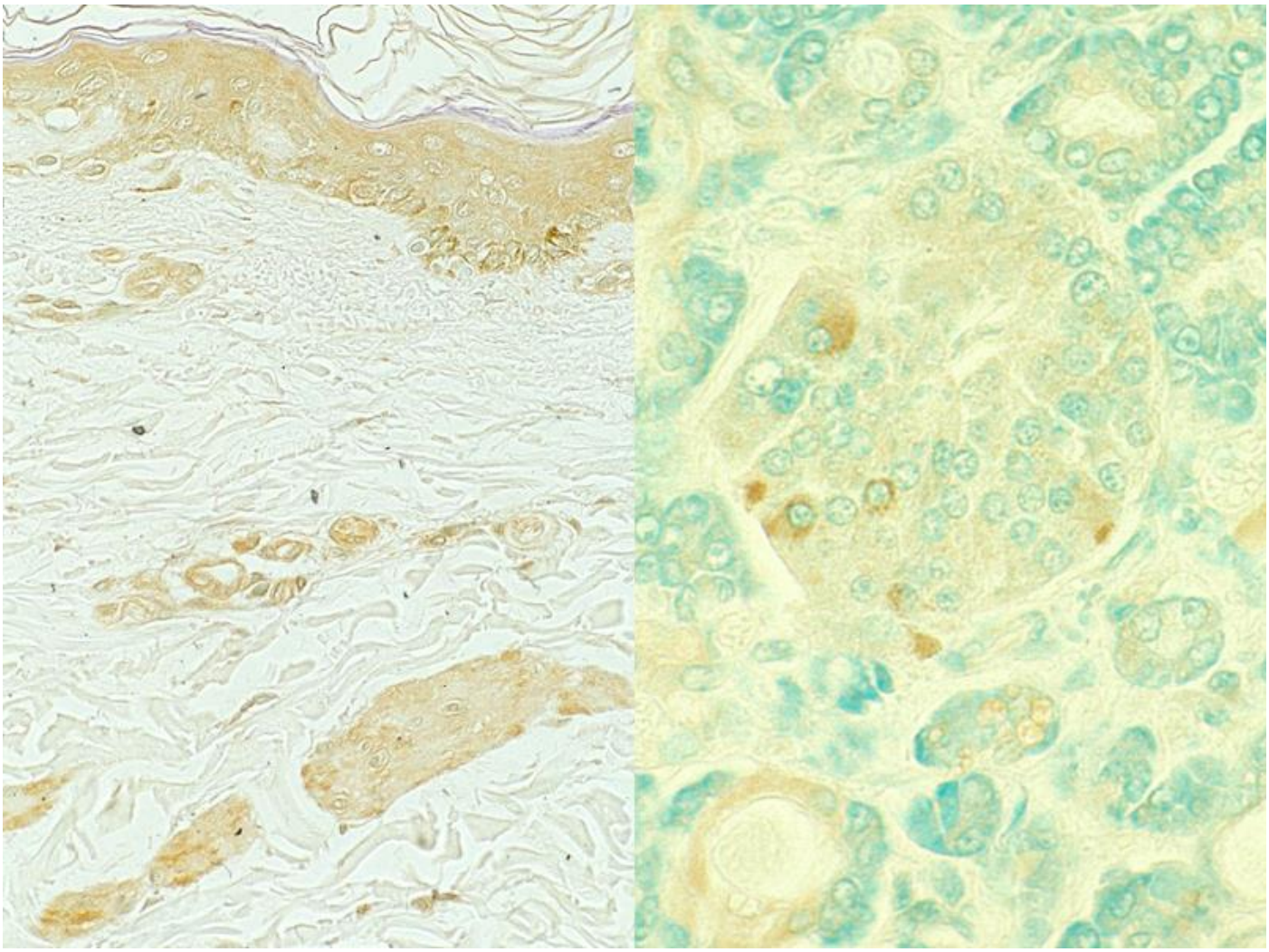

Figure 48. Myoglobin immunostaining in the skin (**left**) and pancreas (**right**) using a commercial rabbit antiserum. Rabbit antiserum may contain natural antibodies against intermediate filament proteins. In the skin, epidermal keratinocytes, vascular endothelial cells and smooth muscle cells of erector pili are weakly stained. In the pancreas, some islet cells are faintly immunostained by the incidentally contaminated antibodies.

Preprints (www.preprints.org) | NOT PEER-REVIEWED | Posted: 28 April 2021 doi:10.20944/preprints202104.0750.v1

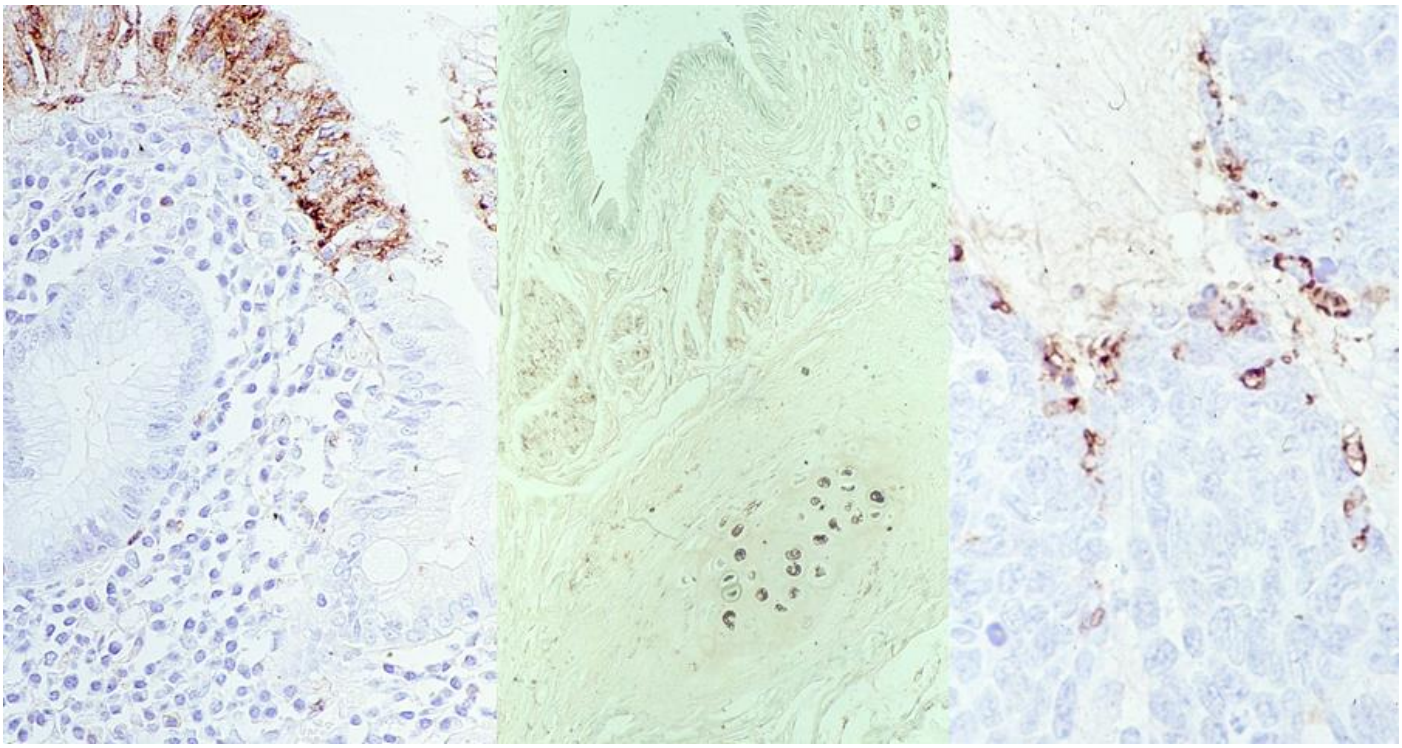

Figure 49. Cross-reactive antibodies against the carrier protein. Cholecystokinin (CCK) is a polypeptide with 33 amino acid residues. The CCK antiserum was raised in a rabbit by using the *Ascaris* extract as carrier proteins. *Ascaris* protein-like (cross-reactive) immunoreactivities are observed in the gastric foveolar cells (**left**), smooth muscle cells and cartilage in the bronchial wall (**center**), and small cell lung carcinoma cells (**right**).

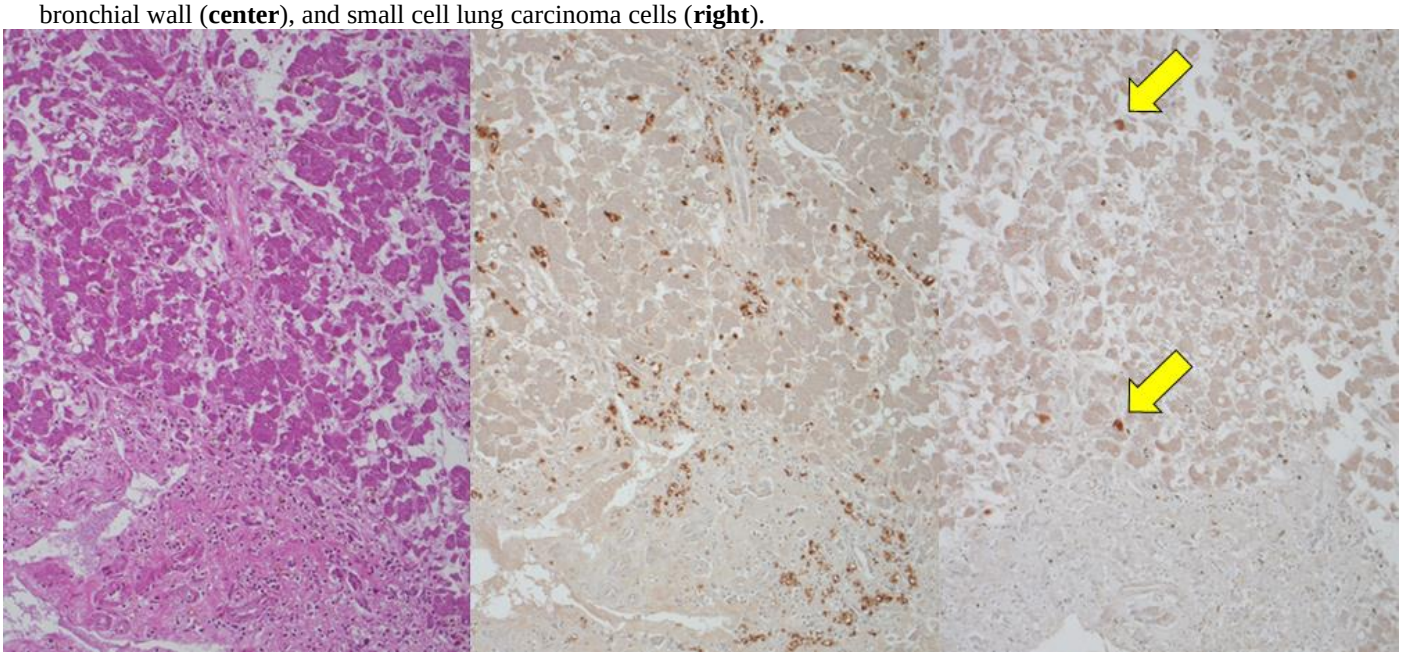

Figure 50. Cross-reactive immunostaining of *Mycobacterium leprae* in the liver by a rabbit anti-HBs antiserum, immunized with complete adjuvant containing the extract of *Mycobacterium tuberculosis*. **Left**: H&E, **Center**: anti-HBs rabbit antiserum, **Right**: anti-HBs monoclonal antibody. Leproma is seen mainly in the portal area. The antiserum visualizes *M. leprae* richly distributed both in the portal triad and in the sinusoidal Kupffer cells. The monoclonal antibody detects HBs antigen-positive hepatocytes (arrows) without background cross-reactivity.

Preprints (www.preprints.org) | NOT PEER-REVIEWED | Posted: 28 April 2021 doi:10.20944/preprints202104.0750.v1

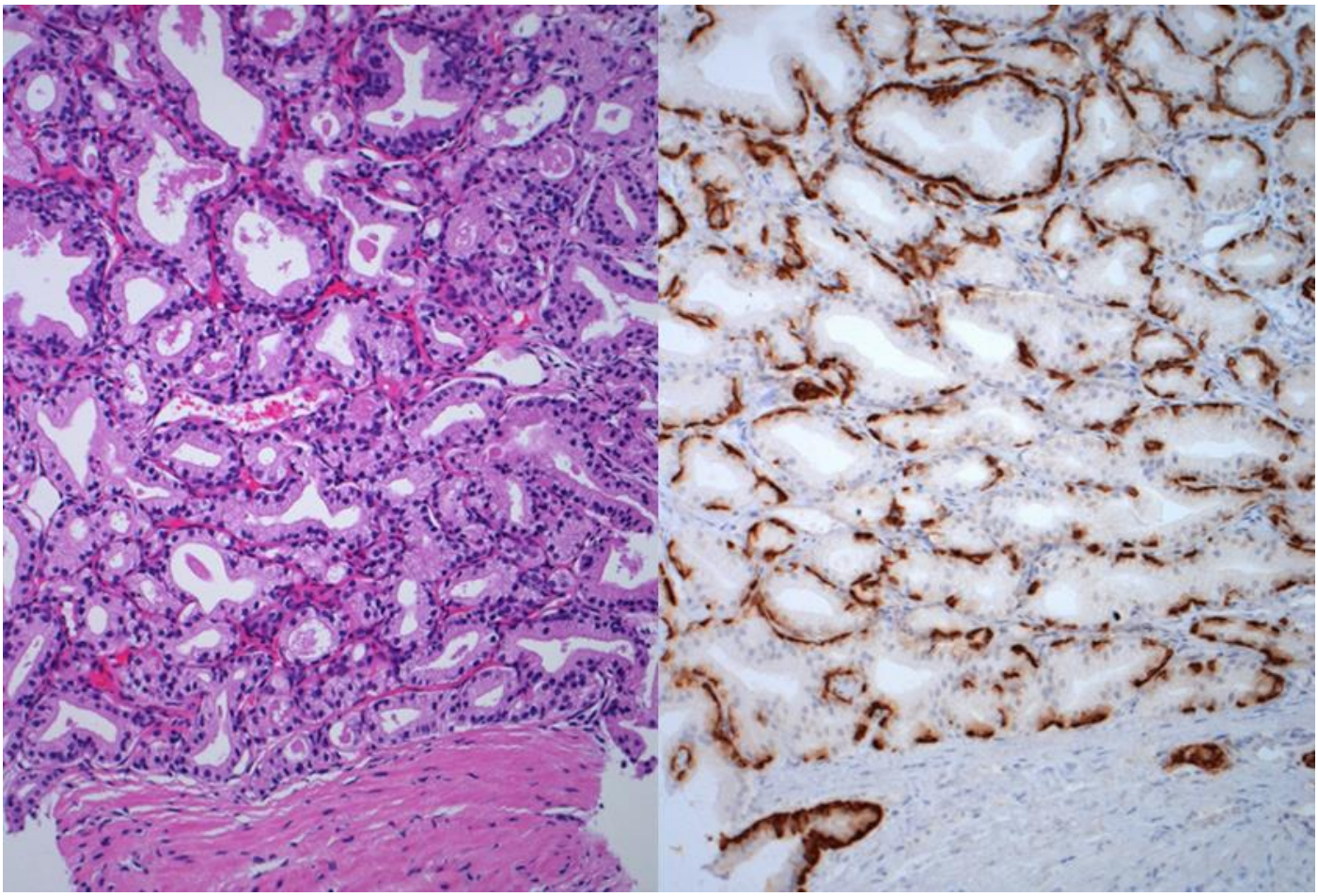

Figure 51. Postatrophic hyperplasia of the prostate. **Left**: H&E, **Right**: immunostaining for cytokeratin 5/6. H&E histology resembles well-differentiated prostatic adenocarcinoma. Immunostaining for cytokeratin 5/6, a basal cell marker, clearly demonstrates the consistent association of basal cells around the acini, definitely indicating a benign lesion.

Preprints (www.preprints.org) | NOT PEER-REVIEWED | Posted: 28 April 2021 doi:10.20944/preprints202104.0750.v1

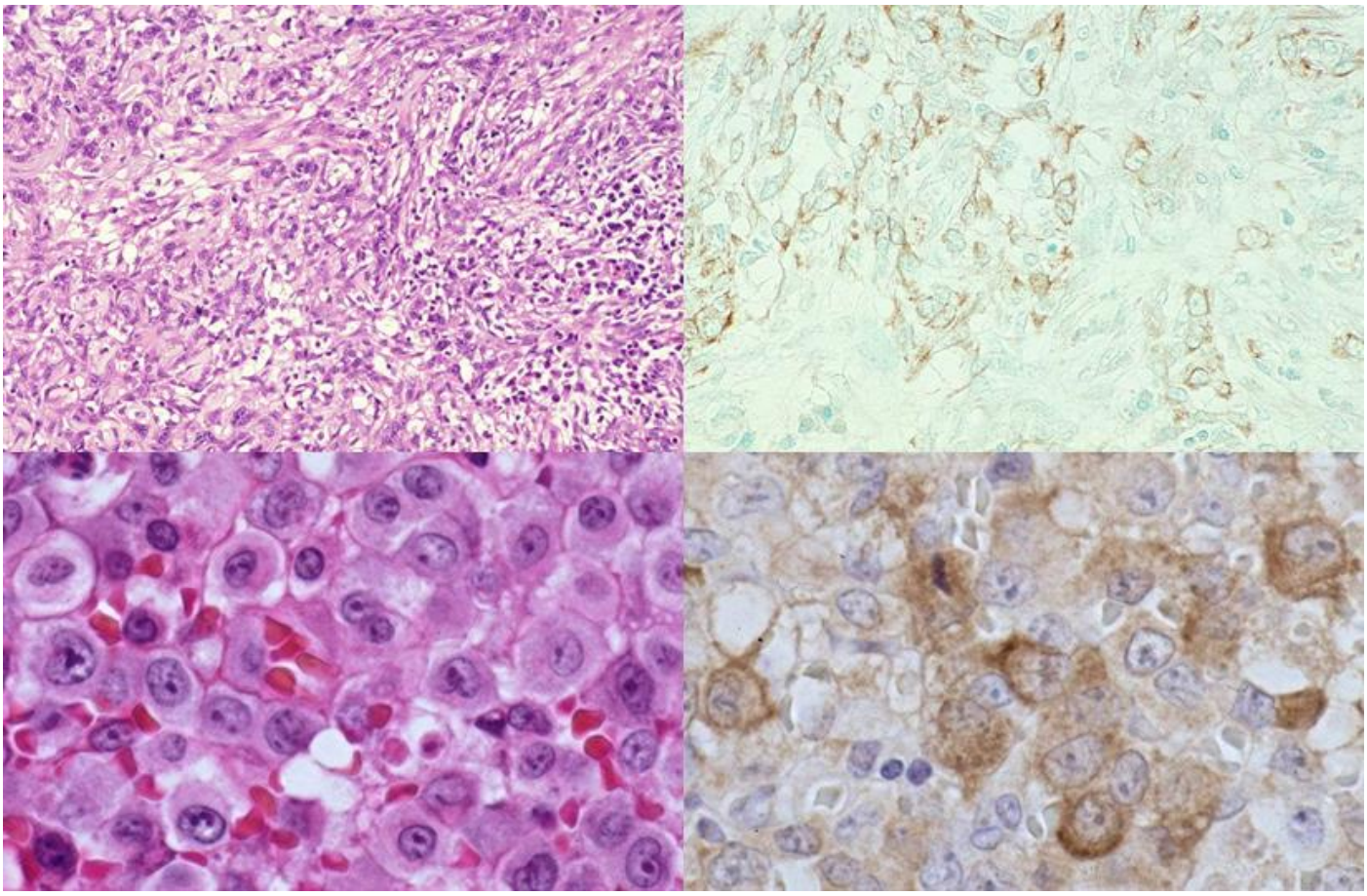

Figure 52. Diagnostic utility of cytokeratin immunostaining. **Left**: H&E, **Right**: immunostaining with wide-spectrum anti-cytokeratin antiserum. **Top panels**: spindle cell carcinoma of the skin, **Bottom panels**: Anaplastic large cell (Ki-1) lymphoma. Cytokeratin expression confirms the epithelial nature of the spindle cells in the skin. Because of epithelioid morphology and cytokeratin expression in Ki-1 lymphoma, the diagnostic confusion with metastatic undifferentiated carcinoma may happen.

Preprints (www.preprints.org) | NOT PEER-REVIEWED | Posted: 28 April 2021 doi:10.20944/preprints202104.0750.v1

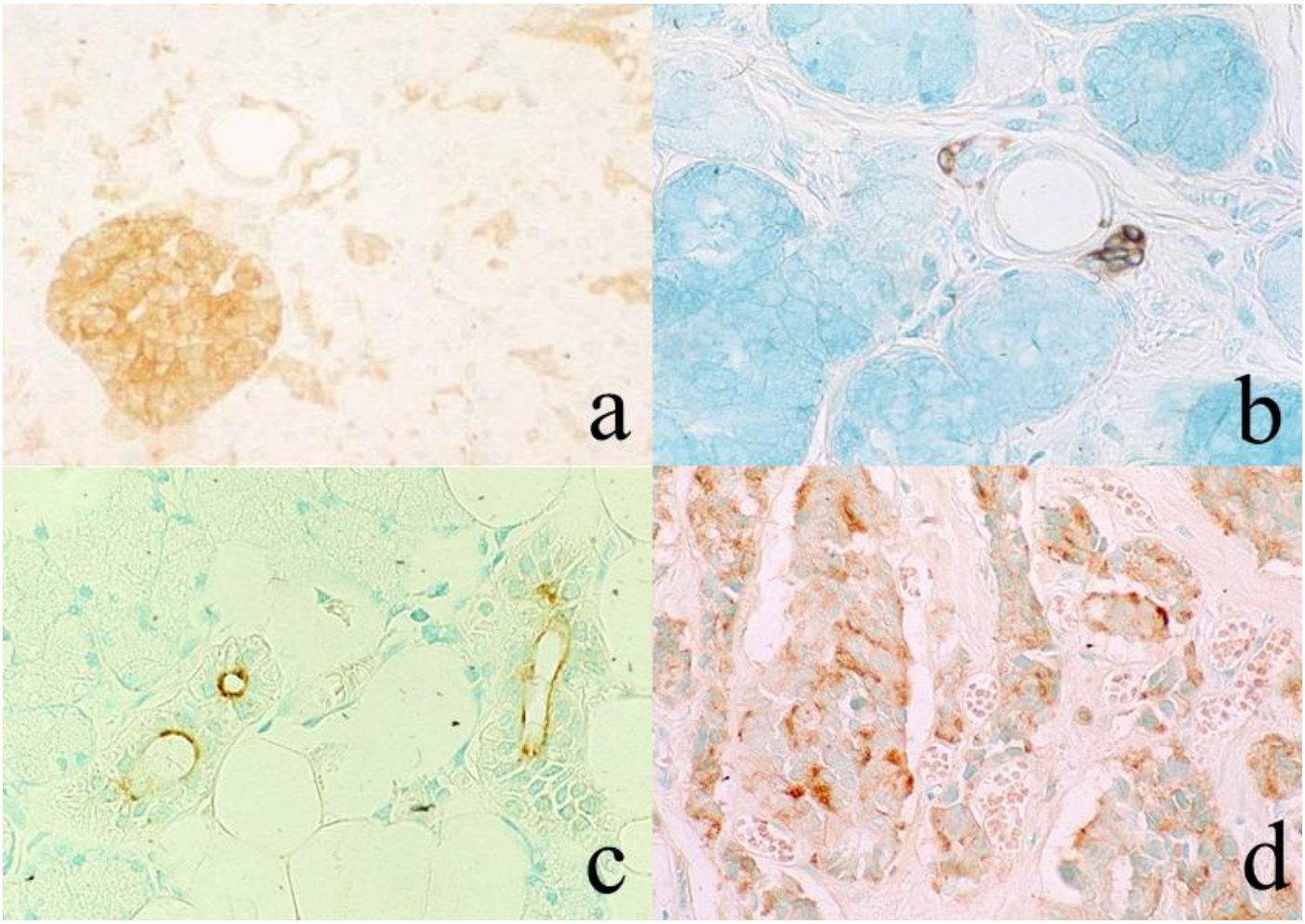

Figure 53. Expression of specific markers in indifferent cells. a: Neuron-specific enolase (NSE) in the normal pancreas, b: glial fibrillary acidic protein (GFAP) in the normal salivary gland, c: prostate-specific antigen (PSA) in the normal salivary gland, d: prostatic acid phosphatase (PAcP) in rectal carcinoid tumor. NSE is expressed not only in islets but also pancreatic ductal cells (a). In the salivary gland, GFAP immunostains part of myoepithelial cells (b), and PSA antiserum decorates the apical cytoplasm of the ductal cells (c). Rectal carcinoid tumor cells are frequently immunoreactive for PAcP (d).

Preprints (www.preprints.org) | NOT PEER-REVIEWED | Posted: 28 April 2021 doi:10.20944/preprints202104.0750.v1

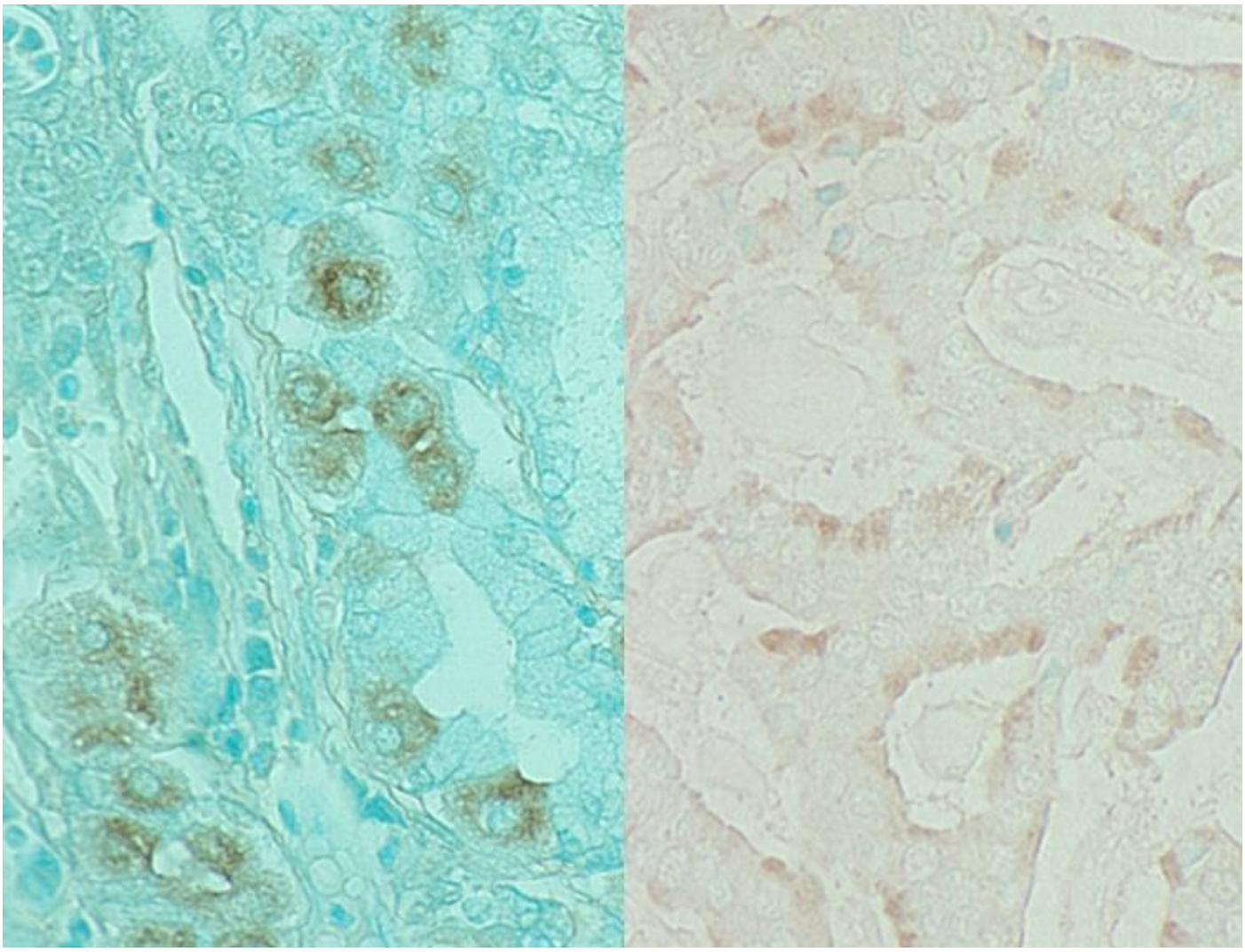

Figure 54. Nonspecific binding of IgG in certain cells in FFPE sections. **Left**: Glicentin (enteroglucagon) immunoreactivity in gastric parietal cells, **Right**: Motilin immunoreactivity in rectal carcinoid tumor. Certain cells may adsorb the antibody molecules nonspecifically, causing false positive immunostaining.

Preprints (www.preprints.org) | NOT PEER-REVIEWED | Posted: 28 April 2021 doi:10.20944/preprints202104.0750.v1

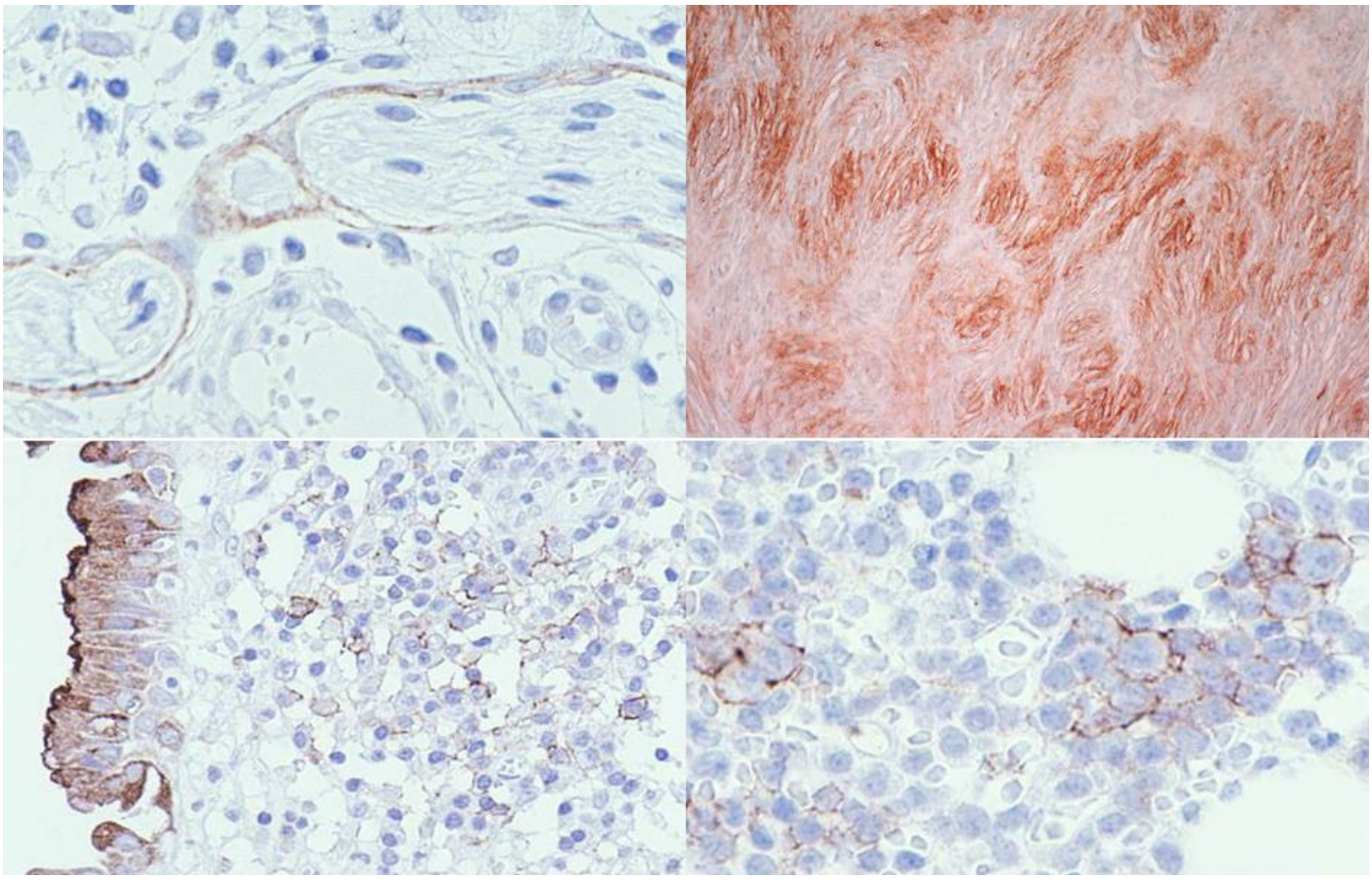

Figure 55. Epithelial membrane antigen (EMA) expression in normal (**left**) and neoplastic (**right**) perineurial cells (**top panels**) and plasma cells (**bottom panels**). It should be noted that EMA is positive in certain non-epithelial cells and their tumors (perineurioma and multiple myeloma). Perineurial cells surrounding the peripheral nerve sheath represent peripheral meningothelial cells. Chronic cervicitis containing numerous plasma cells is covered with EMA-positive columnar epithelial cells.

Preprints (www.preprints.org) | NOT PEER-REVIEWED | Posted: 28 April 2021 doi:10.20944/preprints202104.0750.v1

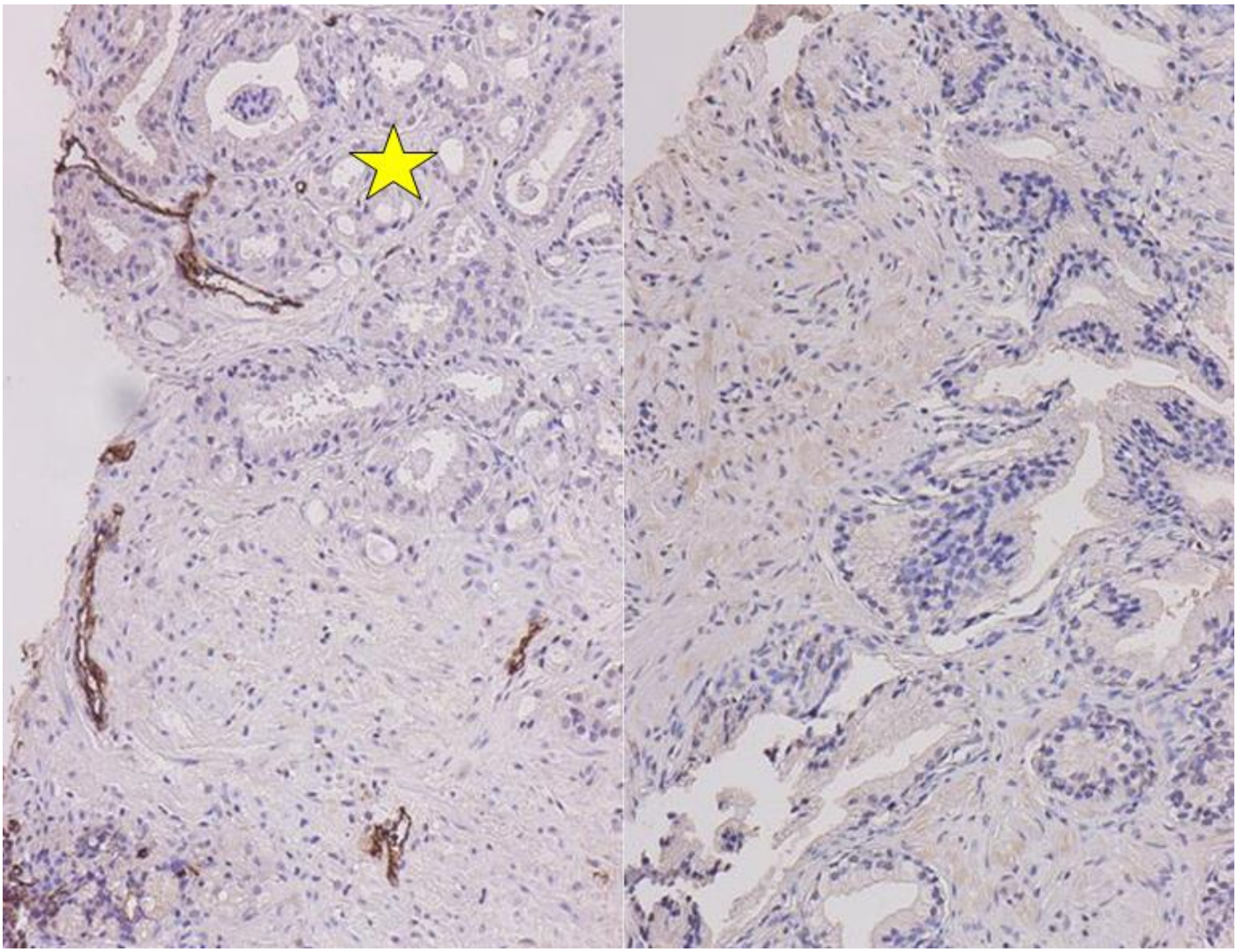

Figure 56. Immunohistochemical blood typing in needle biopsy specimens of the prostate. Specimens from two patients were mixed up in one tissue container. The blood group was type A in one patient, and type O in another. Immunostaining for type A substance is positive in endothelial cells in the **left** panel, but negative in the **right** panel. It is evident that the patient with type A blood group contains prostatic adenocarcinoma (asterisk).

Preprints (www.preprints.org) | NOT PEER-REVIEWED | Posted: 28 April 2021 doi:10.20944/preprints202104.0750.v1

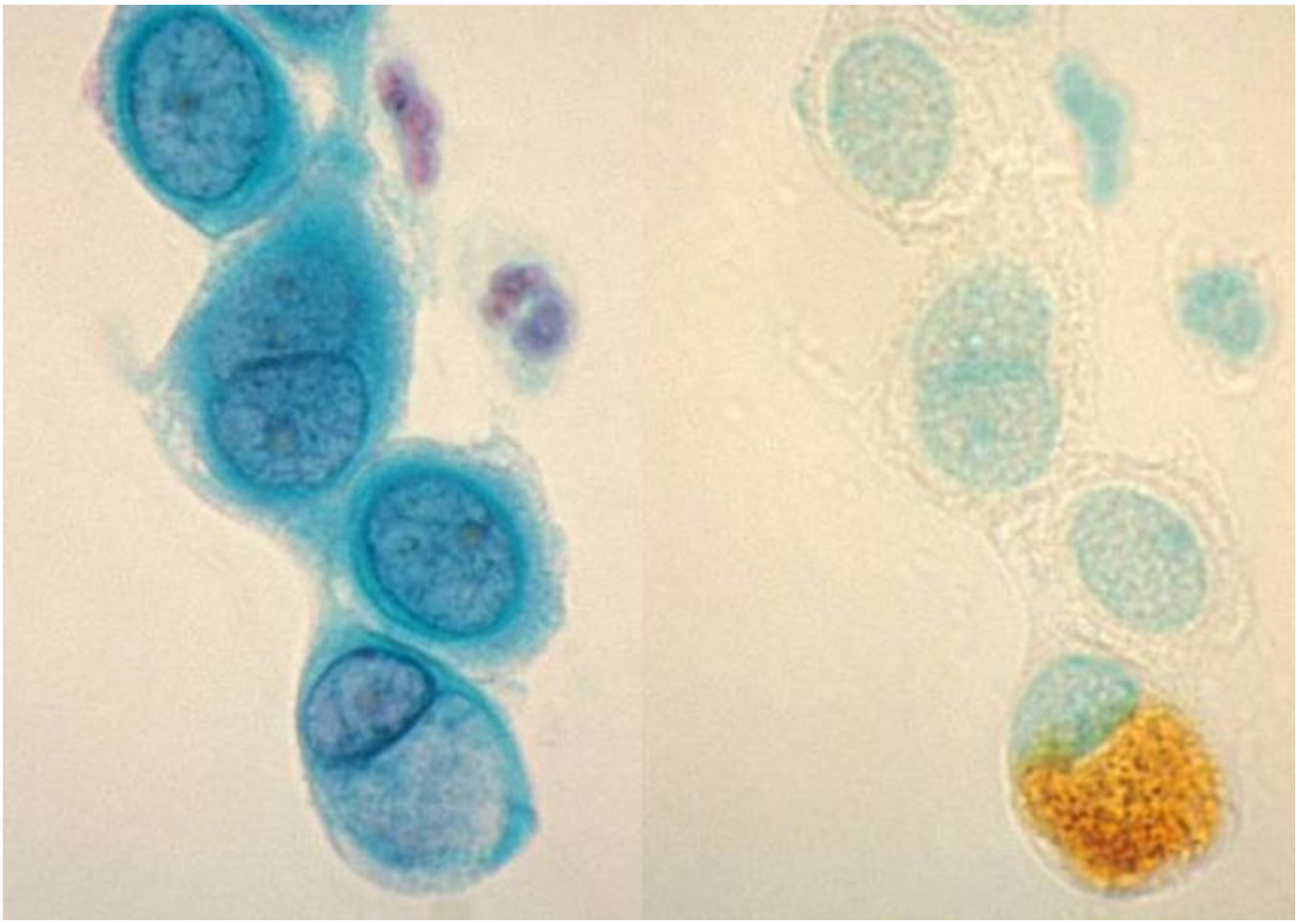

Figure 57. Re-staining for the cytology specimen with *Chlamydia trachomatis* infection. **Left**: Papanicolaou, **Right**: immunostaining with a mouse monoclonal antibody after removal of the cover glass and decoloration. A cytoplasmic "nevular" inclusion body in a cervical columnar cell is clearly immunoreactive for the *C. trachomatis* antigen, confirming the cytodiagnosis of chlamydiasis.

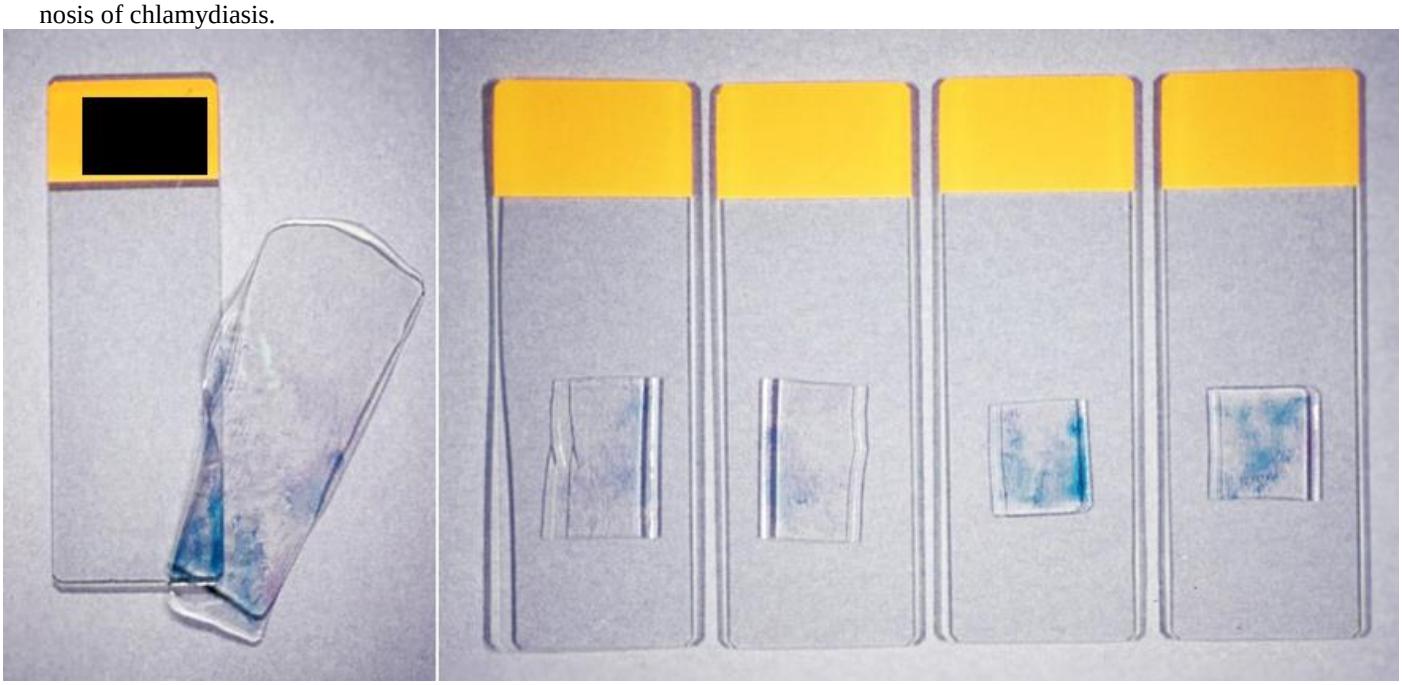

Figure 58. The cell transfer technique. After removal of the cover glass, the cell preparation is covered with mounting resin solution to be solidified as a thick membrane sheet. Cells are transferred to the solidified resin (**left**). After cutting into several pieces, the resin membrane is placed onto silane-coated glass slides, which should be fully dried in the incubator (**right**).

Preprints (www.preprints.org) | NOT PEER-REVIEWED | Posted: 28 April 2021 doi:10.20944/preprints202104.0750.v1

The resin component can easily be removed by dipping the specimens in xylene. Now, the specimens are ready for immunostaining using HIER.

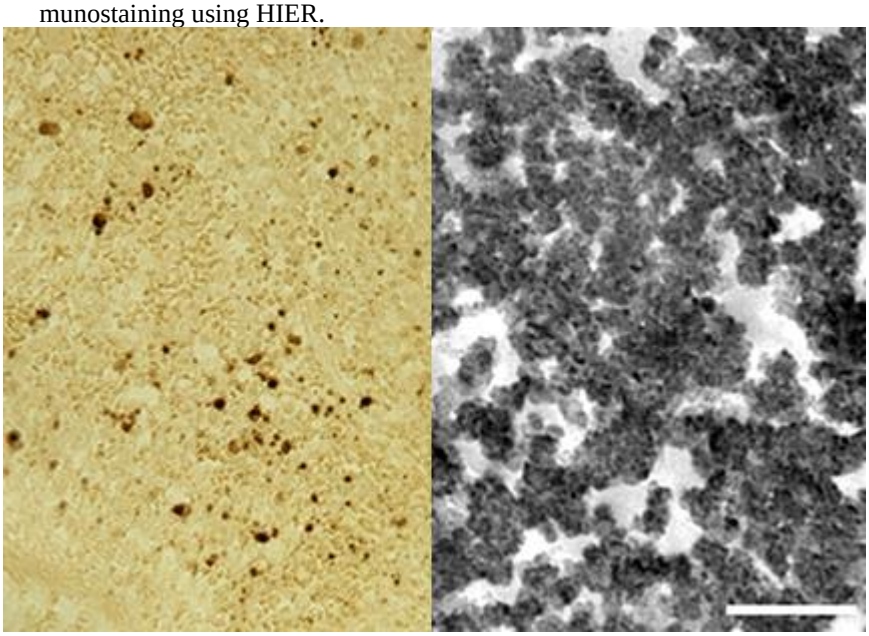

Figure 59. Pre-embedding immunoelectron microscopy for SFTS virus using a TACAS glass slide. **Left**: light microscopic immunostaining, **Right**: immunoreactive round-shaped viral particles, around 100 nm in size, at the ultrastructural level. The FFPE splenic red pulp from an autopsy case was immunostained with a monoclonal antibody to SFTS virus after HIER. For pre-embedding immunoelectron microscopy, the immunostained section was peeled off to transfer to an Epon-embedded block by the inverted beam capsule method. The miraculous TACAS glass slide prevents detaching off sections during immunostaining and allows the cell transfer after immunostaining. Bar indicates 500 nm.

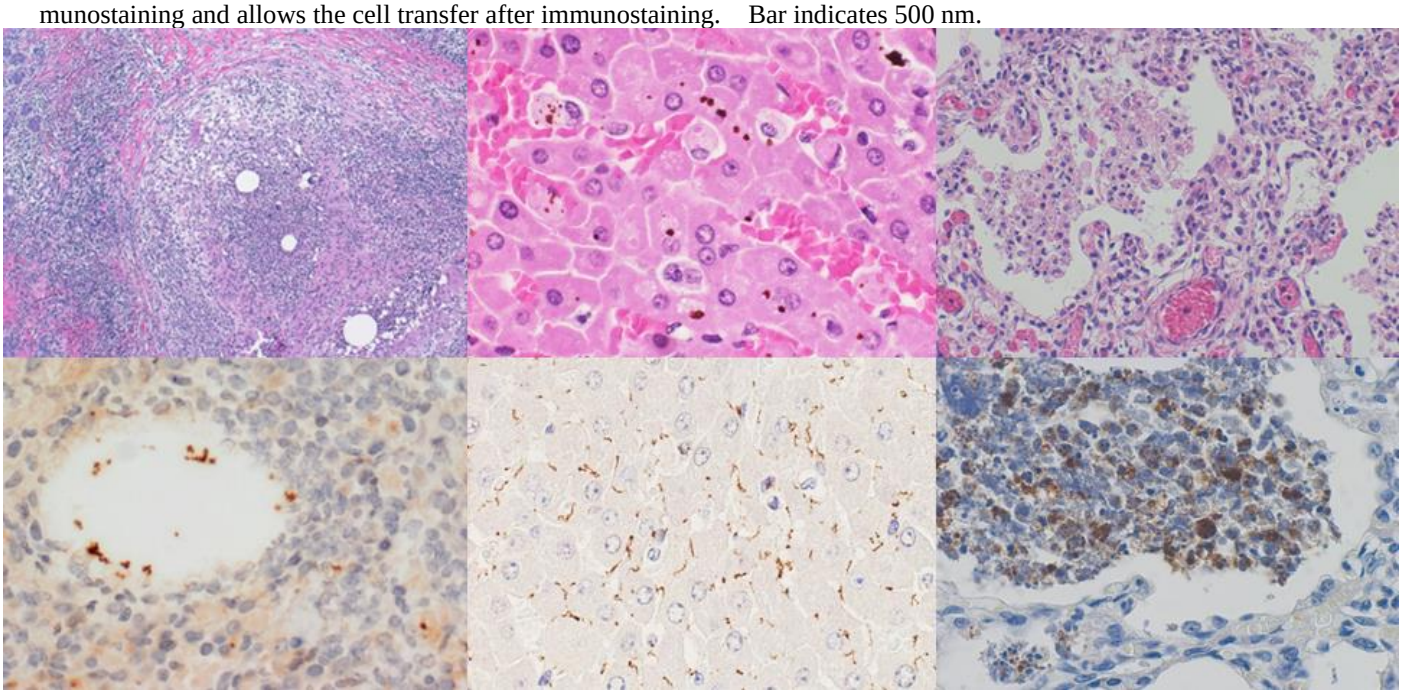

Figure 60. Visualization of bacteria in infectious lesions using cross-reactive antisera. **Top**: H&E, **Bottom**: immunostaining using commercially available antiserum against *Treponema pallidum* (left), *Escherichia coli* (center), and *Bacillus cereus* (right). **Left panels**: *Corynebacterium kroppenstedtii*-induced granulomatous mastitis, **Central panels**: leptospirosis (*Leptospira interrogans* infection or Weil's disease) in the liver, **Right panels**: *Haemophilus pertussis*-induced pneumonia. The causative bacteria are visible through the cross-reactivity of the antisera. Bacteria are not recognizable in H&E preparations.

Preprints (www.preprints.org) | NOT PEER-REVIEWED | Posted: 28 April 2021 doi:10.20944/preprints202104.0750.v1

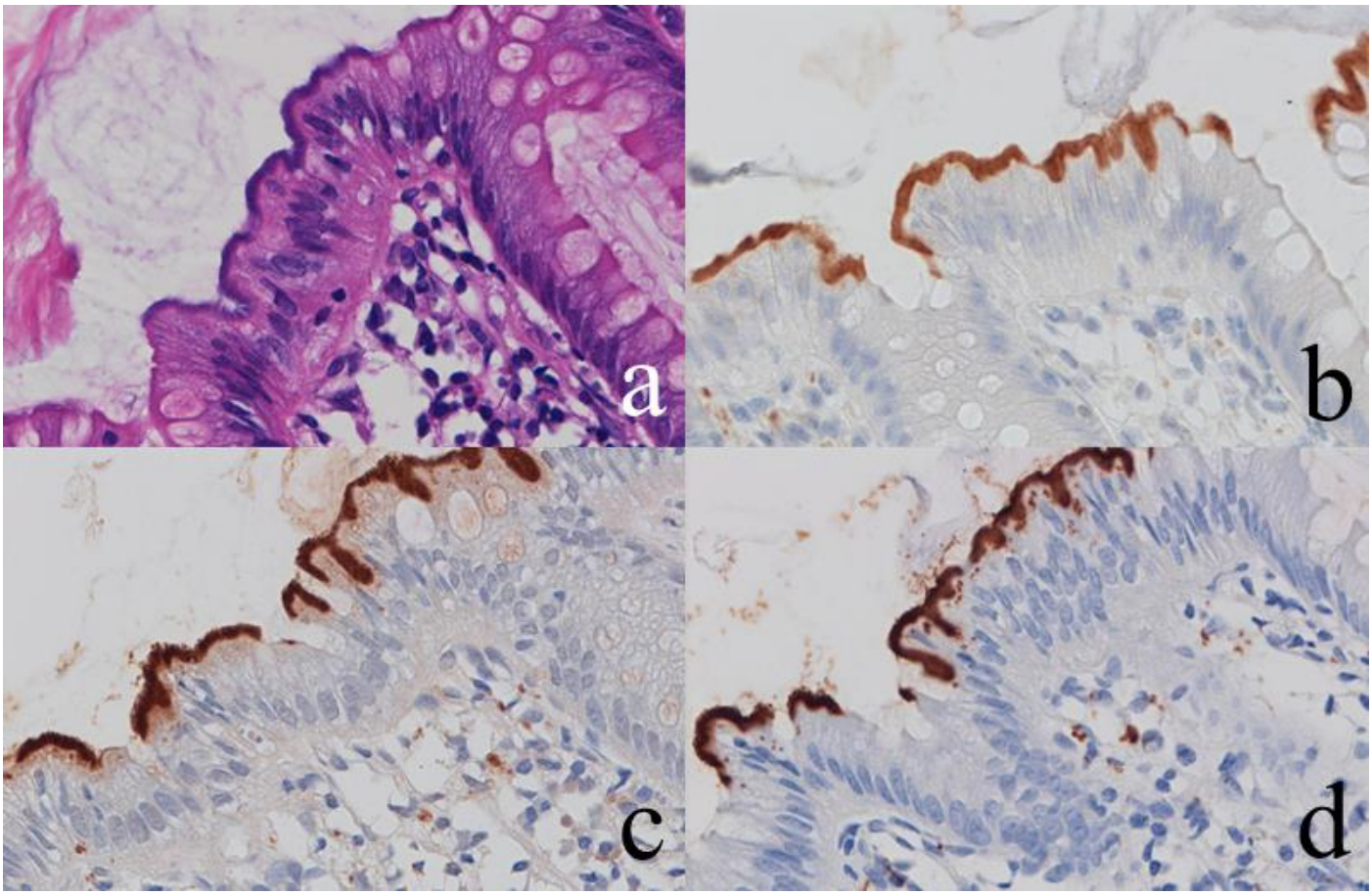

Figure 61. Intestinal spirochetosis caused by colonization of *Brachyspira aalborgi*. a: H&E, b-d: immunostaining using *Treponema pallidum* antiserum (b), BCG antiserum (c), and *E. coli* antiserum (d). Long and basophilic spiral bacteria closely attach onto the apical surface of the colonic columnar cells (a). They are clearly immunostained with plural antisera to *T. pallidum*, BCG and *E. coli*.

Preprints (www.preprints.org) | NOT PEER-REVIEWED | Posted: 28 April 2021 doi:10.20944/preprints202104.0750.v1

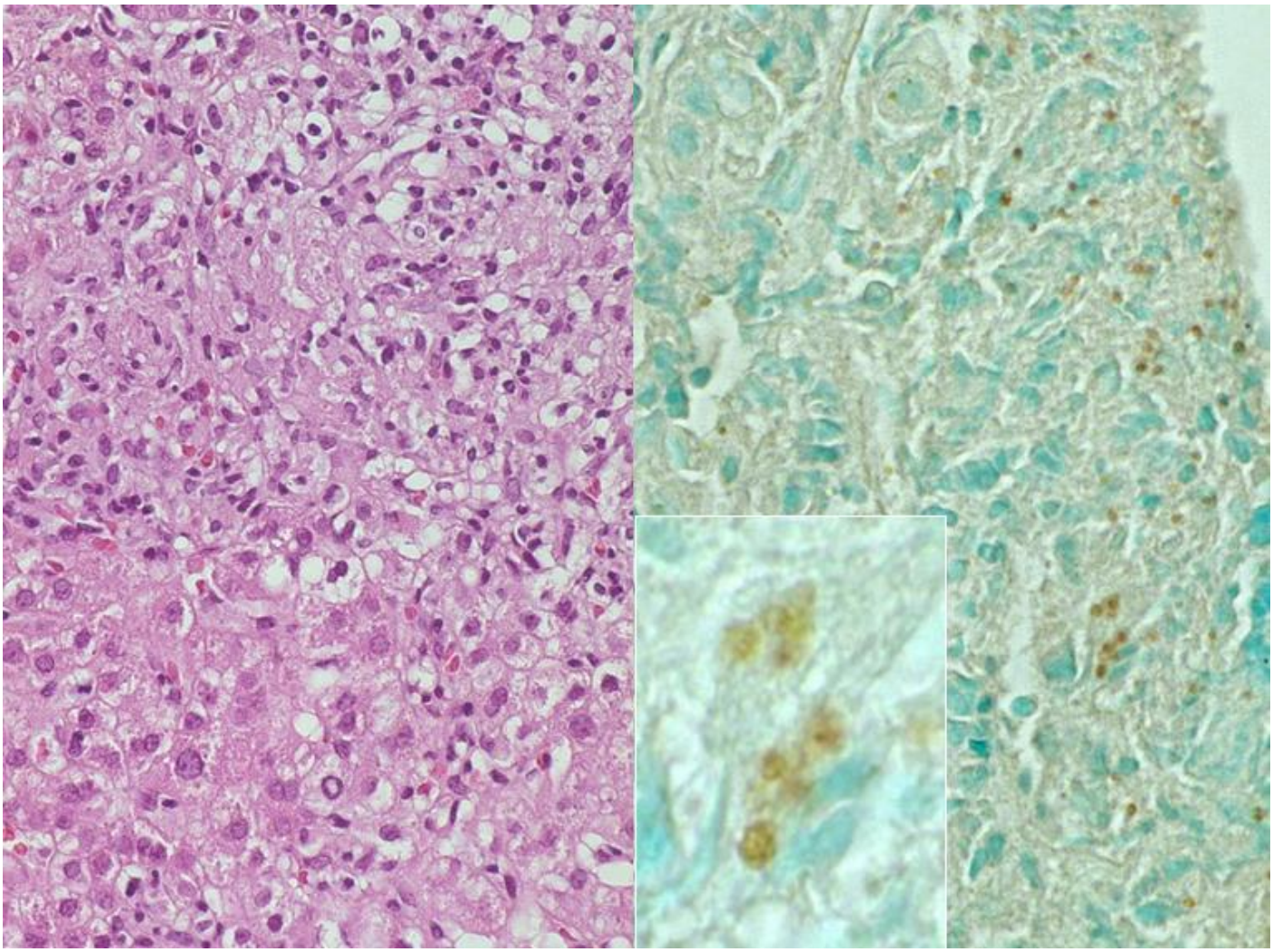

Figure 62. Immunostaining with patient's serum (I). Liver biopsy of visceral leishmaniasis (kala azar). **Left**: H&E, **Right**: 1:500 diluted patient's own serum (**inset**: high-powered view). Non-caseous epithelioid granulomas are dispersed in the liver parenchyma. Antibodies in patients' own serum identify red cell-sized positive signals in the cytoplasm of epithelioid cells and Kupffer cells. Although the specificity of the patient's serum is totally unknown in this case, it significantly contributed to suggest causative pathogens as protozoa.

Preprints (www.preprints.org) | NOT PEER-REVIEWED | Posted: 28 April 2021 doi:10.20944/preprints202104.0750.v1

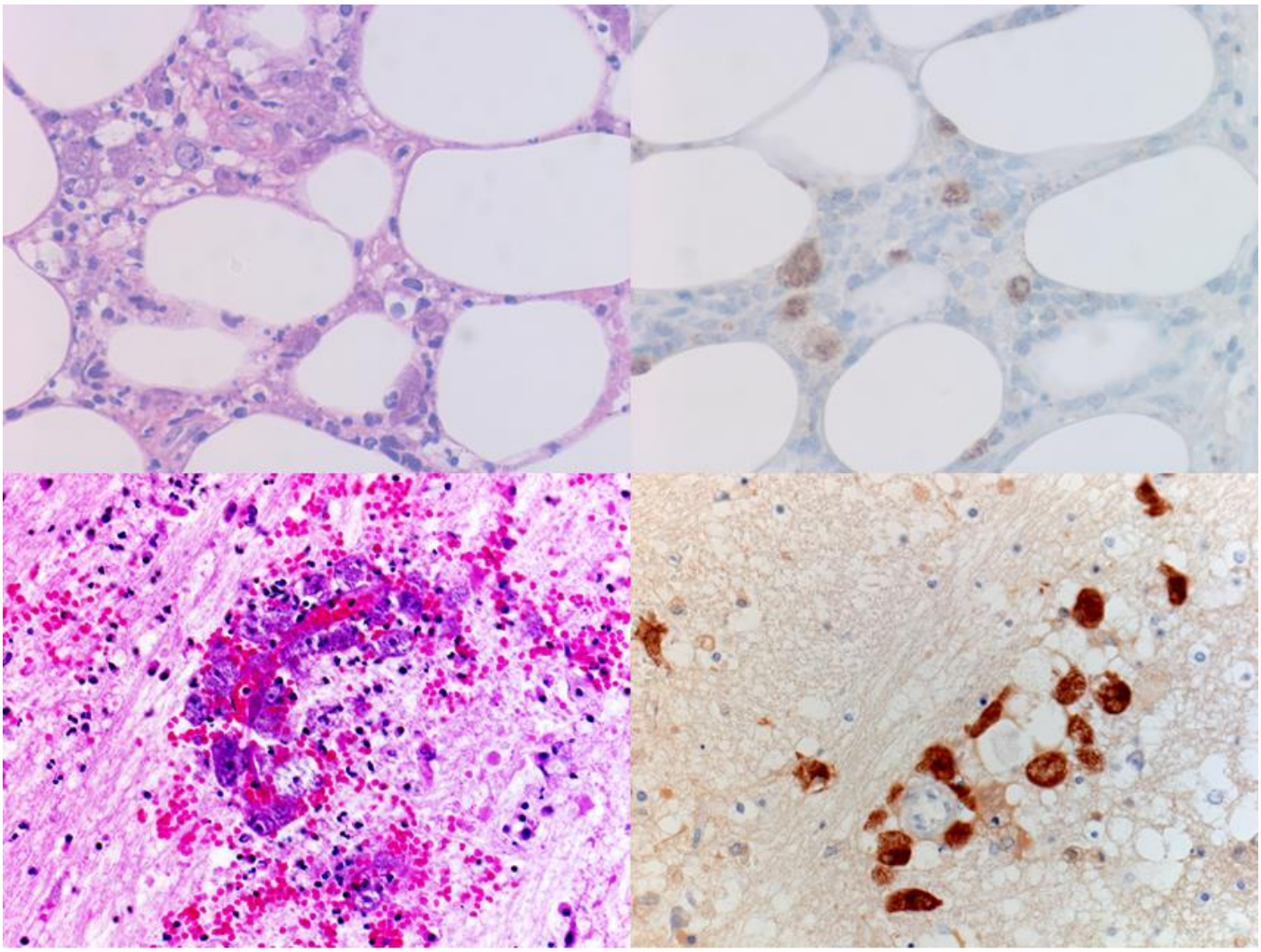

Figure 63. Immunostaining with patient's serum (II). **Left**: H&E, **Right**: immunostaining with 1:500 diluted serum from another case of balamuthiasis. *Balamuthia mandrillaris* infection in the skin (**top panels**) and brain (**bottom panels**) of the same patient. Trophozoites are visible in H&E-stained cutaneous panniculitis and chronic encephalitis, and they are strongly immunoreactive with the serum from another patient who suffered Balamuthia encephalitis.

Preprints (www.preprints.org) | NOT PEER-REVIEWED | Posted: 28 April 2021 doi:10.20944/preprints202104.0750.v1

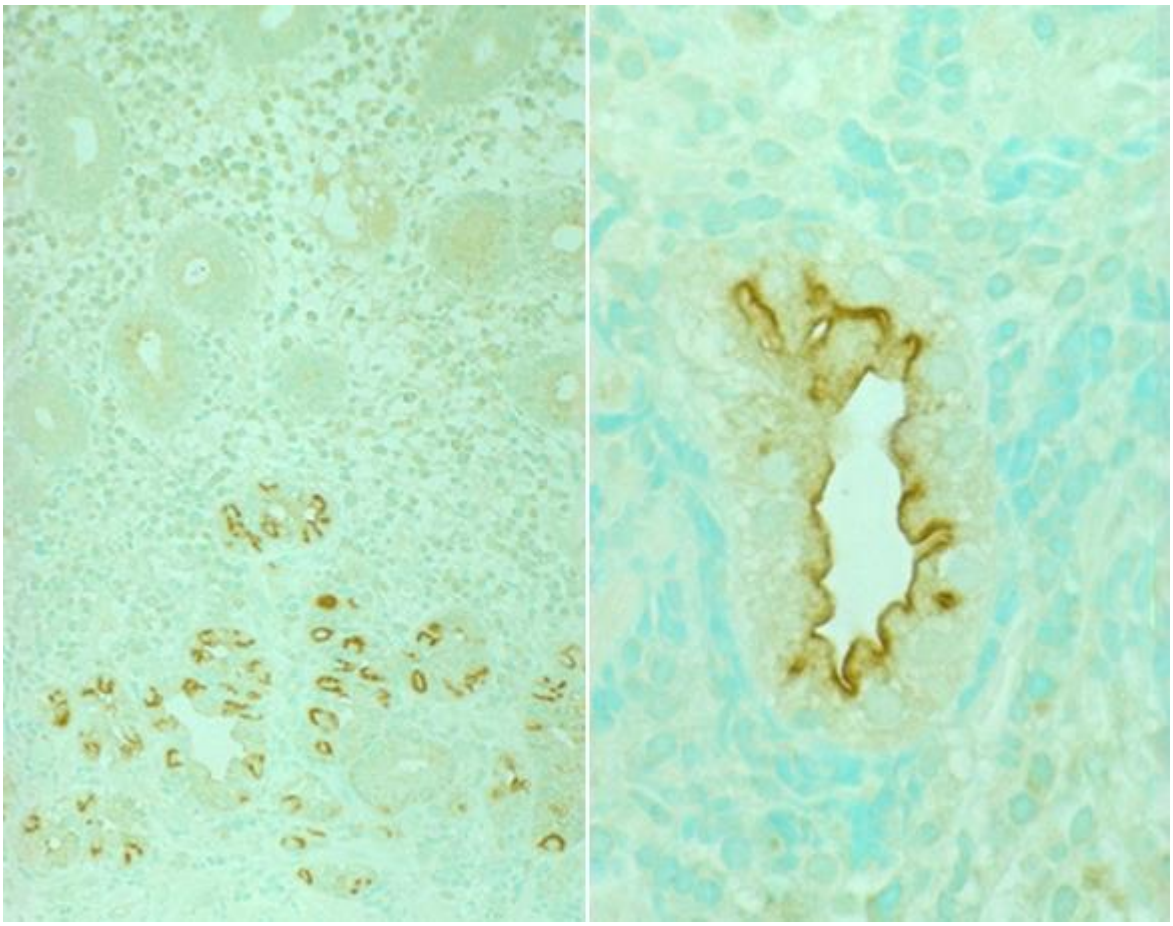

Figure 64. Demonstration of gastric parietal cells in FFPE sections with the serum of a patient with type A (autoimmune) gastritis (**Left**: low power, **Right**: high power). The 1:20 diluted patient's serum, containing autoantibodies against proton pump, decorates C-shaped intracytoplasmic structures (secretory canaliculi) in the acid-secreting parietal cells.

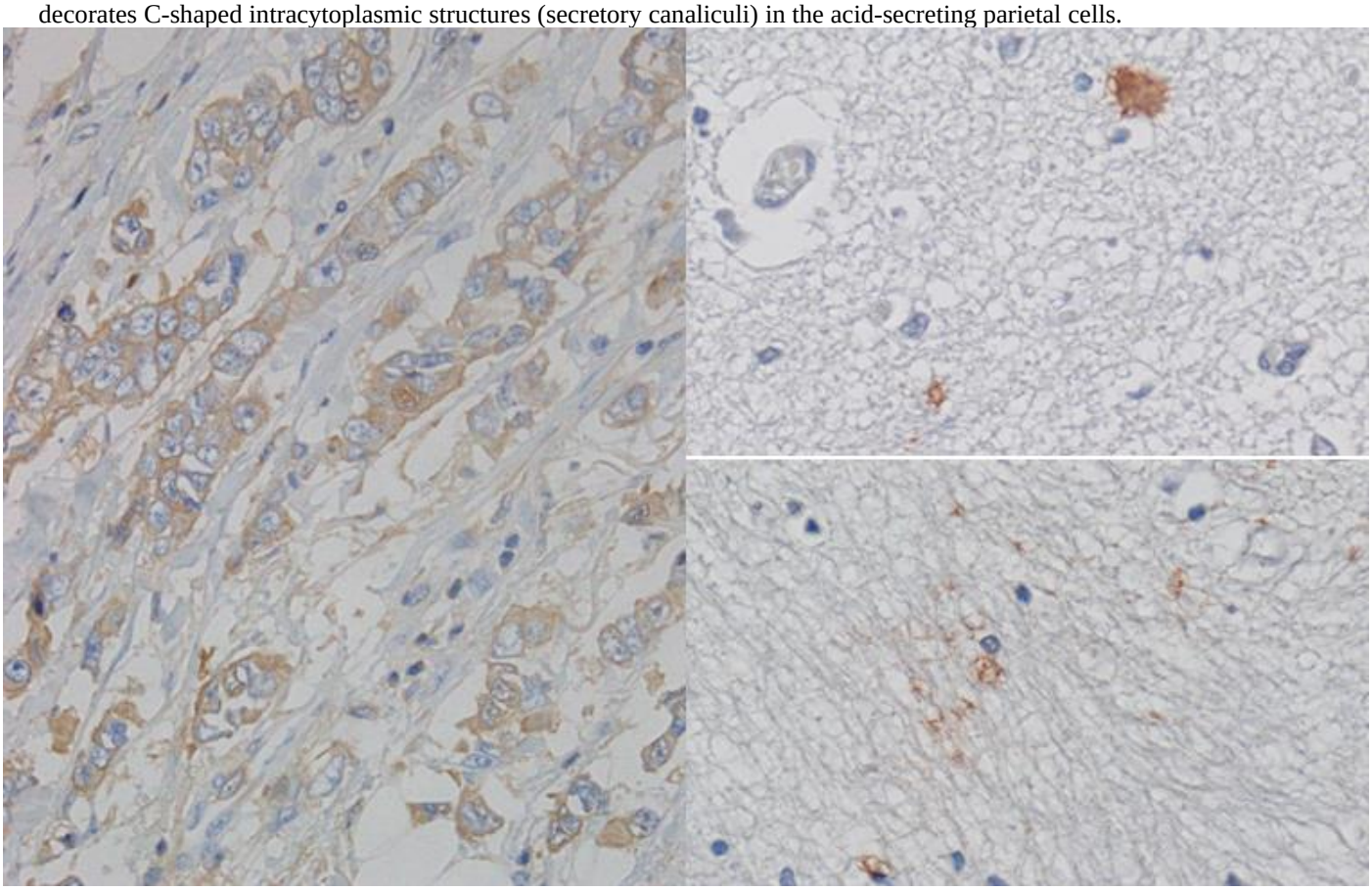

Preprints (www.preprints.org) | NOT PEER-REVIEWED | Posted: 28 April 2021 doi:10.20944/preprints202104.0750.v1

Figure 65. Immunostaining with the serum of two patients with autoimmune encephalitis. **Left**: paraneoplastic (breast cancer-associated) autoimmune encephalitis (Stiff-Man syndrome) with autoantibodies to amphiphysin, a 128 kDa presynaptic protein. **Right**: autoimmune limbic encephalitis. The 1:20 diluted patient's serum immunostains FFPE breast cancer cells of her own (left). The 1:20 diluted serum of limbic encephalitis decorates astroglia and their glial processes in normal basal ganglia of another autopsy case embedded in paraffin (right).